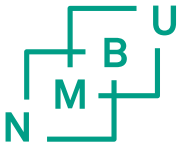
U
B
M
N

Acknowledgements

The work in this thesis was performed at Department for Medical Genetics, Oslo University Hospital, as a part of the master program in Biotechnology at the Norwegian University of Life Science (NMBU) from August 2013 to May 2014.

First of all, I would like to thank to my supervisor at the Department for Medical Genetics, Dr. Philos Nina Iversen for allowing me to join the research group and let me work with this exciting project. Your supervision and guidance have been excellent during this work. I also want to thank my co-supervisor Mari Tinholt for many good advices and constructive comments during the writing process. Big thanks to Dept. Engineer Marit Sletten for all the help and guidance in the laboratory. Your great knowledge and experience in the lab have helped me a lot. I would also like to thank my supervisor at NMBU, Prof. Tor Lea.

Next, I would like to thank Marte Kirkevold, my fellow master student, for a nice time together at Ullevål, sharing joys and frustrations. It would not have been the same without you. I would also like to thank Jørgen Syversen, my family and friends for all the support and encouragement.

Iselin Pollen

12.05.14

Sammendrag

Tissue factor pathway inhibitor (TFPI) er en plasma serine protease inhibitor som inneholder tre Kunitz-type protease inhibitor domener. TFPI kan transkriberes i to hovedformer; TFPIα og TFPIβ ved alternativ spleising. Hovedfunksjonen til TFPI er å inhibere tissue factor initiert blod koagulasjon, men økende bevis tilsier at TFPI også kan ha en rolle i kreftutvikling. Tidligere studier har rapportert at overuttrykk av både TFPIα og TFPIβ induserer programmert celledød i brystkreftceller, og at nedregulering av TFPI fremmer tumorvekst ved å stimulere cellebevegelighet. Effekten av nedregulert TFPIα i brystkreftceller har ikke tidligere blitt rapportert, og få har observert effekten av de to isoformene hver for seg i brystkreftceller. For å undersøke rollen til TFPI sine isoformer i kreftutvikling ytterligere, ble små interferende RNA molekyler (siRNA) spesifikke for TFPIα isoformen designet og en transient nedregulerings- og en overuttrykk modell av TFPIα og TFPIβ ble laget. Disse modellene ble videre brukt i funksjonelle eksperimenter for å undersøke hvordan de manipulerte TFPI nivåene påvirket vekst, adhesjon og migrasjon av brystkreftceller.

Resultatene i denne oppgaven viste en moderat reduksjon i adhesjon til collagen I sammen med reduserte nivåer av adhesjonsmolekylet integrin α2 ved oppregulering av TFPIα i MDA-MB-231 celler, og en reduksjon i migrasjon for både TFPIα og TFPIβ oppregulerte celler. Reduserte nivåer av fosforylert Src i TFPIα and TFPIβ oppregulerte celler ble også målt. Dette kan indikere en potensiell anti-tumor funksjon av begge TFPI isoformene hvor Src signalering muligens kan være involvert. Det ble også funnet en ny brystkreftcellelinje (MDA-MB-436) med samme karakteristikker som MDA-MB-231. I disse ble stabile cellelinjer med TFPIα og TFPIβ oppregulert laget. Disse cellene kan være en nyttig modell for videre studier av rollen til TFPI sine isoformer i kreftutvikling.

Abstract

Tissue factor pathway inhibitor (TFPI) is a plasma serine protease inhibitor which contains three Kunitz-type protease inhibitor domains. TFPI can be transcribed into two main isoforms; TFPIα and TFPIβ by alternative splicing. The main function of TFPI is to inhibit tissue factor initiated blood coagulation, however, increasing evidence has shown that TFPI may have an additional role in cancer development. Previous studies have reported that overexpression of both TFPIα and TFPIβ induces apoptosis in breast cancer cells, and that downregulation of TFPI increases tumor growth by stimulating cell motility. The effect of downregulated TFPIα in breast cancer cells has not been reported before, and only few have studied the effect of the separate isoforms in breast cancer cells. To further examine TFPI isoforms role in cancer development, siRNAs that exclusively knock down the TFPIα isoform were designed and a knockdown and an overexpression model of TFPIα and TFPIβ were made. These models were further used in functional studies to investigate how the manipulated TFPI levels affected growth, adhesion and migration of breast cancer cells.

The results provided in this thesis showed a slight decrease in adhesion to collagen I together with reduced levels of the adhesion molecule integrin α2 by upregulation of TFPIα, and a reduction in migration of both TFPIα and TFPIβ upregulated cells. A reduction of phosphorylated Src levels were also measured in the upregulated TFPIα and TFPIβ cells. This may indicate a possible anti-tumor function of both the TFPI isoforms where Src signaling may be involved. It was also identified a new breast cancer cell line (MDA-MB-436) with same characteristics as MDA-MB-231 where stable cell lines with TFPIα and TFPIβ upregulated were established. These cells may be useful in further studies of TFPI isoforms role in cancer development.

Abbreviations

aPC	Activated protein C
AT	Antitrombin
BSA	Bovine serum albumin
cDNA	Complementary DNA
COX-2	Cyclooxygenase-2
DISC	Death-inducing signaling complex
dsRNA	Doble stranded DNA
E.coli	*Escherichia coli*
EGFR	Epidermal growth factor receptor
ELISA	Enzyme-linked immunosorbent assay
FAK	Focal adhesion kinase
FBS	Fetal Bovine Serum
FV	Coagulation factor V
FVII	Coagulation factor VII
FVIII	Coagulation factor VIII
FIX	Coagulation factor IX
FX	Coagulation factor X
GPI	Glycosyl phosphatidylinositol
HRP	Horeradish peroxidase
h-rTFPI	Human recombinant TFPI
HUVEC	Human umbilical vein endothelial cells
LB	Luria Bertani
miRNA	Micro RNA
MMPs	Matrix metalloproteases
mRNA	Messenger RNA
PAI-1	Plasminogen activator inhibitor-1
PAR-1	Proteinase-activated receptor-1
PAR-2	Proteinase-activated receptor-2
PBS	Phosphate Buffered Saline
PI	Propidium iodide
PMM1	Phosphomannomutase 1
p-Src	Phosphorylated Src
qRT-PCR	Quantitative reverse transcription polymerase chain reaction
Rb	Retinoblastoma protein
RISK	RNA-Inducing Silencing Complex
RNAi	RNA interference
SDS-PAGE	Sodium dodecyl sulfate polyacrylamide gel electrophoresis
siRNA	Short interfering RNA
TBS	Tris-buffered saline
TBST	Tris-buffered saline with Tween 20
TF	Tissue factor
TFPI	Tissue factor pathway inhibitor
TNF	Tumor necrosis factor
VEGF	Vascular endothelial growth factor
VTE	Venous thromboembolism

Contents

1 Introduction

1.1 Cancer

Cancer is a disease affecting people all around the world. In 2012, 14.1 million new cases of cancer were diagnosed worldwide, and in 2035 the number is expected to be 24 million. The most common cancer today is lung cancer, followed by breast cancer which constitutes 11% of all cancer types (Ferlay *et al*. 2013).

Cancer develops when genes involved in maintenance of normal tissue are altered, leading to uncontrolled growth of cells. When an abnormal cell grows and divides uncontrolled, a benign tumor can occur. If the tumor invades the surrounding tissue, the tumor is called malignant (Alberts *et al*. 2008). The process in which a normal cell becomes malignant is multi-stepped. Six hallmarks/alterations have been suggested for malignant growth to take place, in addition to two emerging hallmarks (Hanahan & Weinberg 2000; Hanahan & Weinberg 2011) (Figure 1.1). These 8 hallmarks are described in brief below.

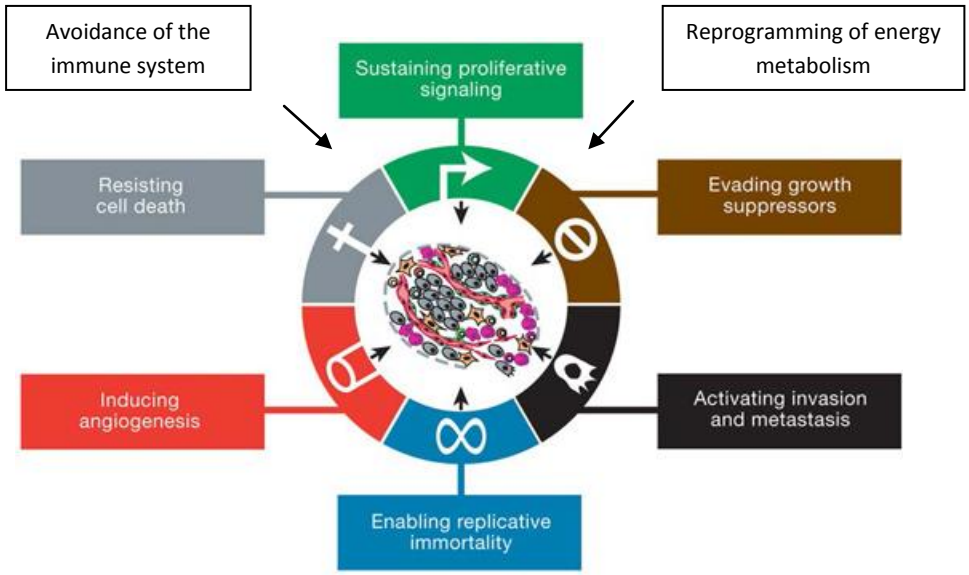

Figure 1.1: Hallmarks of cancer. Six hallmarks of cancer (sustaining proliferate signaling, evading growth suppressors, activating invasion and metastasis, enabling replicative immortality, inducing angiogenesis and resisting cell death) and two emerging hallmarks (avoidance of the immune system and reprogramming of energy metabolism) are suggested for malignant growth. Modified from Hanahan, D. & Weinberg, R., A. (2000). The hallmark of cancer. *Cell*, 100: 57-70.

Sustaining proliferative signaling

Cell division and proliferation of cells are normally strictly regulated by extracellular signaling molecules like growth factors, antigrowth signals and survival factors present in the body (Goustin *et al.* 1986). When more cells are needed, growth factors will bind to receptors located on the surface of a cell and activate intracellular signaling pathways that stimulate cell division and growth (Alberts *et al.* 2008). Cancer cells can produce their own growth signals and are therefore not dependent on exogenously derived signals, and thereby avoid the strict regulation (Hanahan & Weinberg 2000). Cancer cells also have the ability to switch the receptors on their surface to receptors involved in transmitting growth signals, and thereby activating more signaling pathway promoting growth (Lukashev & Werb 1998).

Evading growth suppressors

Growth-inhibitory signals are also a part of the strict growth regulation in cells. Anti-growth signals inhibit growth by arresting the cells in an inactive G_0 phase or to a post-mitotic phase (Hanahan & Weinberg 2000). The retinoblastoma protein (Rb) is an important protein in this process. The Rb protein can arrest cells in the G_1 phase by blocking the activity of the E2F transcription factors (Burkhart & Julien Sage 2008). The Rb protein is found inactive in many cancer types, which make the cancer cells insensitive to anti-growth signals and may thereby cause uncontrolled growth of cells (Hanahan & Weinberg 2000).

Resisting cell death

Apoptosis, also called programmed cell death, is a naturally occurring process that balances the cell number and removes damaged cells. When cells are damaged, ligands located on killer lymphocytes will bind to death receptors like FAS or TNF and activate the extrinsic pathway of apoptosis. Binding of ligands to FAS or TNF leads to recruitment of initiator procaspases (procaspase-8 and procaspase-10), and together they form the death-inducing signaling complex (DISC). When DISC is activated the procaspases will activate downstream executioner procaspases (caspase-3, caspase-6 and caspase-7) and induce apoptosis (Alberts *et al*. 2008; Igney & Krammer 2002). The cell will then shrink and break into apoptotic bodies which later will be engulfed by neighboring cells (Bortnera & Cidlowskia 1998; Kerr *et al.* 1994). Apoptosis is regulated by anti-apoptotic and pro-apoptotic signals. The *TP53* gene encodes the p53 protein, which is an important pro-apoptotic factor. p53 is frequently mutated in many cancer types (Olivier *et al.* 2010). Mutations in tumor-supressor genes, like

TP53, can prevent apoptosis in cells that should have been removed, and thereby promote abnormal cell growth (Hanahan & Weinberg 2000).

Enabling replicative immortality

Another hallmark of cancer is limitless replicative potential (Hanahan & Weinberg 2000). Normally, cells will only divide a specific number of times due to the chromosome ends, called the telomeres. Telomeres are crucial for the chromosome's integrity as it protects the chromosome for interactions with other chromosomes (Klug *et al.* 2007). Since the telomeres do not replicate during S phase, the telomeres become shorter for every successful cycle of replication. When the chromosome end is no longer protected, the affected cell will enter an irreversible growth arrest (Campisi 2001). Cancer cells avoid this by overexpressing the telomerase enzyme (Shay & Bacchetti 1997). The complex enzyme telomerase contain both a RNA component and a catalytic component. The RNA component will recognize the existing telomere DNA repeat, and the catalytic components will synthesize new telomeric DNA repeats (Yashima *et al.* 1998). Overexpression of this enzyme will therefore lead to an unlimited replicative potential (Sledge & Miller 2003).

Activating invasion and metastasis

Metastasis is the process when tumor cells invade the surrounding tissue, spread, and form secondary tumors at other sites in the body. This process is involved in approximately 90% of all cancer-associated deaths (Gupta & Massagué 2006), and is the main cause of death in breast cancer (Felding-Habermann *et al.* 2001). To form secondary tumors, the cells need to cross the vessel wall, enter the bloodstream and then leave the vessel to form new tumors at a distant site in the body. This is a complex multistep process (Spanoa *et al.* 2012).

Integrins, focal adhesion kinase (FAK) and the Src family plays important roles in tumor metastasis. Integrins are transmembrane adhesion molecules that can transmit signals in both directions across the cell membrane. There are many different types of integrins, but they all have similar composition. Two non-covalently linked subunits (α and β) that both have a large extracellular domain and a shorter intracellular tail constitutes an integrin molecule (Giancotti & Ruoslahti 1999; Luo & Springer 2006). In addition to signal transmission, the integrins are able to quickly change from an inactive to an active state and vice versa. This property is important in the migration process, when the cell needs to create and break attachments to the extracellular matrix rapidly in order to move (Alberts *et al.* 2008).

When an extracellular ligand binds to an integrin molecule, the α and β subunits of the integrin molecule will cluster and form a strong intracellular binding site for anchor proteins like talin or paxillin (Mitra & Schlaepfer 2006). The intracellular anchor proteins will then recruit the tyrosine kinase FAK, which becomes phosphorylated on specific tyrosine residues upon binding to the intracellular anchor proteins (Moschos *et al.* 2007). Autophosphorylated FAK creates a docking site for Src family proteins (Giancotti & Ruoslahti 1999), including Src, Yes, Fgr, Fyn, Lck, Lyn, Hck and Blk, which are all protein kinases containing SH2 and SH3 domains involved in protein-protein interactions (Sánchez-Bailón *et al.* 2012). Furthermore, Src can trans-phosphorylate FAK, and the FAK-Src complex can activate different signaling pathways that regulate migration (Figure 1.2) (Moschos & Kirkwood 2007).

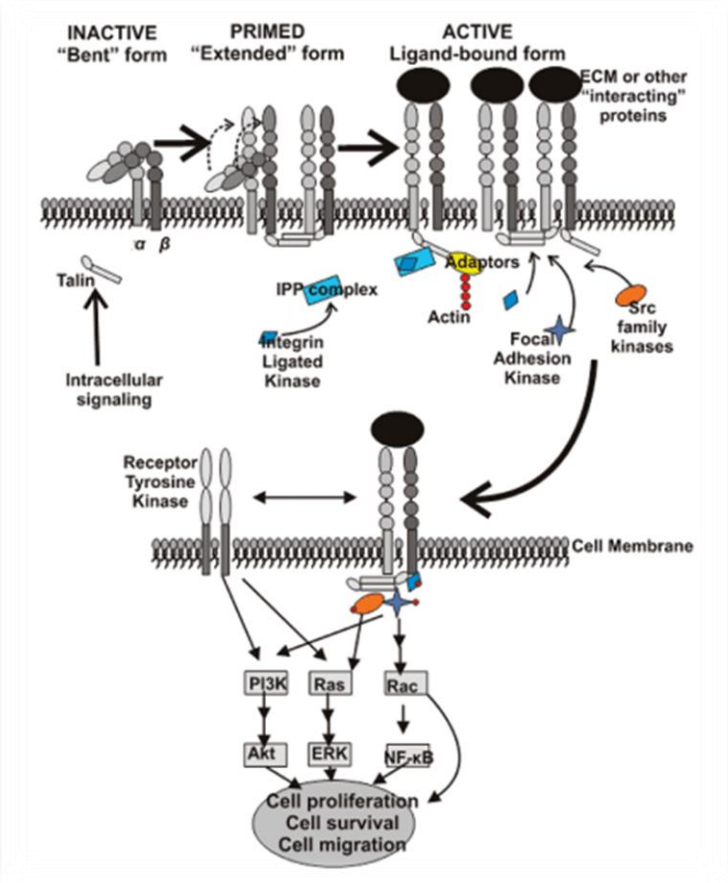

Figure 1.2: Integrin signaling. Integrins can exist in both an inactive form and an active form. When an integrin is activated, a signal protein can bind to the integrin, creating a binding site at the integrin tail that will recruit different anchor proteins. FAK will then bind to the anchor proteins and become phosphorylated at different tyrosine residues. Src family proteins can bind to FAK and the FAK-Src complex will activate different signaling pathways that induce cell survival, proliferation and migration. From Moschos, S. J., Drogowski, L. M., Reppert, S. L. & Kirkwood, J. M. (2007). Integrins and cancer. *Oncology*, 21 (9): 13-20.
.

The cell-cell adhesion molecules cadherins and matrix metalloproteases (MMPs) are also involved in tissue invasion and metastasis. Cadherins mediate cell-cell attachment, thus assisting to maintain the cell shape (Breier *et al.* 2014). MMPs, on the other hand, are enzymes with the ability to degrade matrix proteins like collagen, laminin and fibronectin in the extracellular matrix (Stetler-Stevensona & Yub 2001). Activation of these MMPs or alterations in binding specificity of cadherins and integrins may result in tissue invasion and metastasis of cancer cells, and is therefore considered as a hallmark of cancer (Hanahan & Weinberg 2000).

Inducing angiogenesis

Angiogenesis is the process where new blood vessels are formed from pre-excisting vessels. When a tumor grows, it will eventually reach a size where it needs additional vasculature to be supplied with enough oxygen and nutrients to sustain growth (Carmeliet & Jain 2000). To achieve this, tumor cells secrete proteins including vascular endothelial growth factor (VEGF) to stimulate blood vessel growth. VEGF will bind to VEGF receptors located on the endothelial cells and stimulate them to proliferate and to produce proteases and other blood vessel promoting proteins. The proteases will degrade the extracellular membrane and cells will migrate and differentiate into new blood vessels, thus providing the tumor with nutrients that facilitate more tumor growth (Cross & Claesson-Welsh 2001).

Two emerging hallmarks

Two emerging hallmarks of cancer were suggested by Hanahan and Weinberg in 2011. These were reprogramming of energy metabolism and avoidance of the immune system. Cancer cells have the ability to reprogram their energy metabolism, and thus go into a state termed aerobic glycolysis. In such a state the cancer cells can limit their metabolism to glycolysis even though oxygen is present. Increased glycolysis gives glycolytic intermediates which can go into various biosynthetic pathways, including pathways which generate nucleosides and amino acids. From nucleosides and amino acids, macromolecules and organelles can be made, which again can give rise to new cells (DeBerardinis *et al.* 2008). Increased glycolysis has been observed in many tumors, suggesting a new hallmark of cancer (Hanahan & Weinberg 2011). The second emerging hallmark of cancer is avoidance of the immune system. The immune system is a defense mechanism that protects the body against invaders. Tumor cells, however, seem to avoid this mechanism and can thereby form tumors in the body without disruption of the immune system. Experiments performed with mice lacking various

components of the immune system, like T-cells and natural killer cells have been reported to show higher frequency of tumor growth (Smyth *et al*. 2001; Teng *et al.* 2008).

1.2 The cell-based model of TF initiated blood coagulation

Blood coagulation is the process when bleeding from a damaged blood vessel is prevented by forming a clot at the damaged site. The tissue factor (TF) initiated blood coagulation is initiated when TF forms a complex with the circulating coagulation factor VII (FVII). TF is a constitutively expressed transmembrane glycoprotein receptor present on extravascular cells, including mucosal epithelium, epidermis, alveolar macrophages and vascular adventitia, which enable a quick initiation of coagulation upon vessel injury. Monocytes can also express TF upon cytokine stimulation (Kasthuri *et al*. 2010; Ueno *et al*. 2000). TF is organized in three domains; an extracellular domain, a transmembrane segment and a cytoplasmic domain (Gomez & McVey 2006). When TF binds to FVII, FVII will be activated to FVIIa. The TF-FVIIa complex will then cleave coagulation factor IX (FIX) and coagulation factor X (FX) and activate them to FIXa and FXa. FXa will thereafter activate prothombin to thrombin. The trace amount of thrombin can then activate platelets and coagulation factor V (FV), a cofactor of FXa, and FVII, a cofactor of FIXa which will enhance the thrombin formation. Thrombin will cleave fibrinogen to fibrin, which, together with activated platelets forms a clot that terminates the bleeding at the damaged site (Figure 1.3) (Gomez & McVey 2006). Phospholipids on the surface of the activated platelets constitute a structural platform for the coagulation, and the phospholipids will enhance the activation of the different coagulation factors (Zwaal *et al.* 1998).

The coagulation process is regulated by coagulation activators and inhibitors. This is important in order to avoid disturbances in the blood flow. An excessive activation of the coagulation process may lead to thrombosis, while incapacity to activate the coagulation cascade may result in bleeding. One of the inhibitors of blood coagulation is tissue factor pathway inhibitor (TFPI). TFPI inhibits blood coagulation by binding to TF-FVIIa or FXa (Lindahl 1996). The FXa inhibition has recently reported to be enhanced by protein S (PS) (Wood *et al.* 2014). Two other coagulation inhibitors are the activated protein C (aPC) and antithrombin (AT). aPC together with PS inhibits coagulation by binding FVa and FVIIIa, while AT inactivates thrombin, FIXa and FXa (Gomez & McVey 2006).

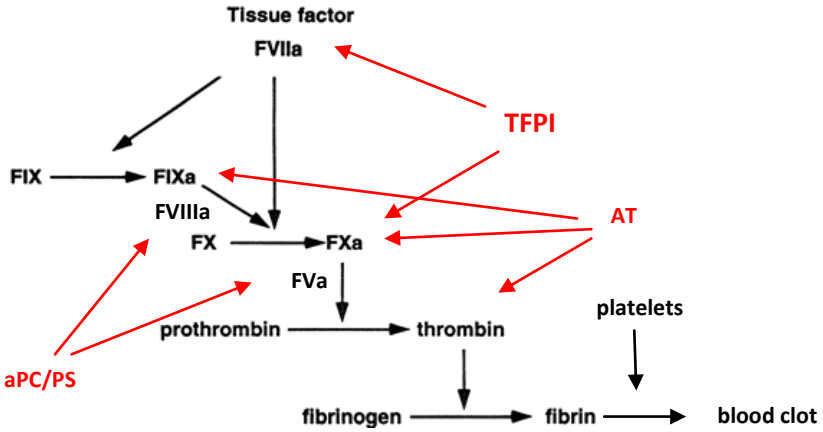

Figure 1.3: Tissue factor initiated blood coagulation. Blood coagulation is initiated when TF forms a complex with FVII. The TF-FVIIa complex will then activate FIX and FX to FIXa and FXa. FXa will thereafter activate prothrombin to thrombin, and thrombin will activate fibrinogen to fibrin. FVIIa and FVa, cofactors of FIXa and FXa, respectively, will enhance the thrombin formation. Fibrin monomers, together with platelets will form a blood clot. TFPI can inhibit blood coagulation by binding to TF-FVIIa or FXa, while aPC/PC can inhibit FVIIIa and FVa. AT may inhibit blood coagulation by binding to FIXa, FXa or thrombin. Modified from: Lindahl, A. K. (1996). Tissue factor pathway inhibitor: from unknown coagulation inhibitor to major antithrombotic principle. *Cardiovascular Research*, 33 (286–291)

1.3 Blood coagulation and cancer

If the blood coagulation is out of balance, a blood clot in the vein can arise and cause venous thromboembolism (VTE), which is one of the leading cause of death in cancer patients (Furie & Furie 2006). The association between thromboembolism and cancer were first described in 1823 by Bouilland, and was later confirmed by Trousseau in 1865 (Lillicrap 2013). In 2005 Blom *et al.* reported that patients with malignancy had a 7-fold higher risk of developing VTE compared to patients without malignancy. The risk was even higher in the five first months after the diagnosis of cancer, or for patients with distant metastases, or carriers of the factor V Leiden variant (Blom *et al.* 2005). The cancer types with the highest risk of developing VTE during the first year of follow-up are reported to be pancreas, stomach, bladder, uterus, kidney and lung cancer (Chew *et al.* 2006). The association between cancer and VTE might be explained by the fact that tumor cells can activate blood coagulation in a number of ways. Increased levels of TF in tumor cells compared to normal cells have been reported (Kasthuri *et al.* 2010). This can lead to excessive activation of coagulation which might explain why cancer patients have a higher risk of developing VTE. Cell-adhesion molecules at the surface of cancer cells can also promote clotting by directly binding to a healthy cell and induce localized clotting and thrombus formation (Prandoni *et al.* 2005).

Not only have patients diagnosed with cancer an increased risk of developing VTE, but patients with activated coagulation also have an increased risk of developing cancer (Sørensen *et al.* 1998). Evidence exist that blood coagulation processes may accelerate cancer progression, and the effects may be both dependent- and independent of the clotting activity (Falanga *et al.* 2013). A clotting-dependent effect is when thrombin activate platelets to bind to circulating tumor cells, as thrombin is the most potent activator of platelets (Gomez & McVey 2006; Nasha *et al.* 2001). When platelets bind to tumor cells, the platelets may release coagulation factors and proangiogenic factors including VEGF (Nasha *et al.* 2002). VEGF can further stimulate angiogenesis which supplies the tumor cells with more oxygen and nutrients, and the tumor cells can continue growing. VEGF may also stimulate endothelial cells to express more TF (Mechtcheriakova *et al.* 1999), which provide a positive feedback as more platelets become activated. In addition, activated platelets may contribute to enhanced cancer progression by protecting the tumor cells from lysis by natural killer cells (Nieswandt *et al*. 1999). Furthermore, fibrin may also contribute to the cancer progression by providing a scaffold for the angiogenesis process and stabilizing tumor cell adhesion (Falanga *et al*. 2013). Elevated thrombin levels can promote cancer development independently of the clotting activity by binding to proteinase-activated receptor 1 (PAR-1), which lead to transactivation of epidermal growth factor receptor (EGFR) and induced Src phosphorylation which may result in enhanced cell proliferation (Darmoul *et al.* 2004). Another clotting-independent effect that activate angiogenesis and thereby enhanced cancer progression is when TF together with FVII cleave proteinase-activated receptor-2 (PAR-2) (Schaffner & Ruf 2009).

A relationship between cancer and blood coagulation is also seen by MET signaling. The MET encodes the tyrosine kinase receptor for hepatocyte growth factor/scatter factor that controls invasive growth (Boccaccio & Comoglio 2005; Boccaccio *et al.* 2005). This oncogene becomes activated when oxygen levels are low, known as hypoxia, which is often a condition observed in the area around tumor cells (Pennacchietti *et al.* 2003). Activated MET oncogene will further induce the transcription of the hemostasis genes; plasminogen activator inhibitor-1 (PAI-1) and cyclooxygenase-2 (COX-2), which leads to fibrin polymerization around the tumor cells, providing the cells a scaffold that promotes angiogenesis (Boccaccio & Comoglio 2005). Activated MET oncogene, and induced PAI-1 and COX-2 may also lead to thrombohaemorrhagic syndrome (Boccaccio *et al.* 2005).

1.4 Tissue Factor Pathway Inhibitor (TFPI)

1.4.1 TFPI structure and function

Tissue factor pathway inhibitor (TFPI) is a plasma serine protease inhibitor located on chromosome 2, where it spans about 70 kb (van der Logt *et al.* 1991). Three of the ten exons, encode for Kunitz-type protease inhibitor domains (exon 4, 6 and 9) (Broze & Girard 2013). Human TFPI can be transcribed into three isoforms by alternative splicing, TFPIα, TFPIβ and TFPIδ. These isoforms differ in structure and size. The full length TFPIα isoform consists of 276 amino acids, and includes an acidic N-terminal domain, three Kunitz-type protease inhibitory domains, and a positively charged C-terminal domain (Broze & Girard 2013). The third Kunitz domain and the C-terminal domain contain heparin binding sites (Enjyoji *et al.* 1995; Novotny *et al.* 1991). Injection of heparin will thus result in increased levels of TFPIα in plasma (Sandset *et al.* 1988). The alternatively TFPIβ isoform is shorter then TFPIα, and consists of 223 amino acids where amino acids 1-181 are identical to TFPIα. TFPIβ lacks the third Kunitz domain and has a different C-terminal end that directs the binding of a glycosyl phosphatidyl inositol (GPI) anchor (Zhang *et al.* 2003). The TFPIδ isoform has not been characterized yet, but its sequence is available in the NCBI GeneBank (AB209866.1) and encode for Kunitz domain 1 and 2 (Broze & Girard 2013). The TFPIδ isoform has also a different C-terminal end which constitutes 12 amino acids (Maroney *et al.* 2010). Figure 1.4 illustrates the structure of TFPIα and TFPIβ.

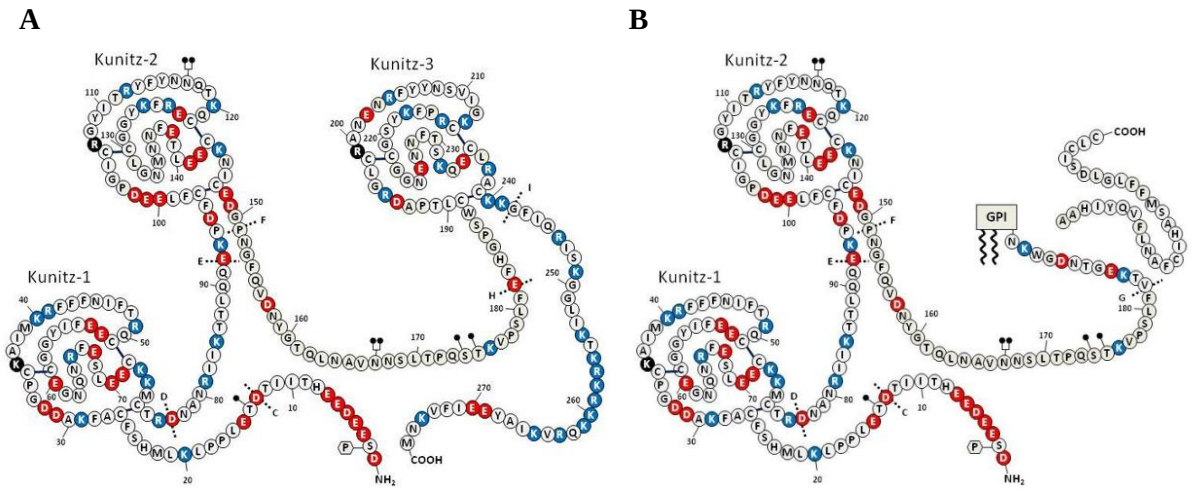

Figure 1.4: The structure of TFPIα and TFPIβ. The amino acids are shown in a single letter code, positively charged amino acids in red and negatively charged amino acids in blue. A) TFPIα consists of an acidic N-terminal domain, three Kunitz-type protease inhibitory domains, and a C-terminal domain, while B) TFPIβ consists of an acidic N-terminal domain, two Kunitz-type protease domains and a positively charged C-terminal domain that directs attachment to the cell membrane through a GPI anchor. From: Broze, G. J. J. & Girard, T. J. (2013). Tissue Factor Pathway Inhibitor: Structure-Function. *Front Biosci*, 17: 262-280.

The TFPIα- and TFPIβ isoforms differ in location and cell surface binding properties. After TFPI (α and β) mRNA are translated by ribosomes, and translocated into the endoplasmatic reticulum lumen, TFPI is transported to the cell membrane in vesicles through the Golgi apparatus. TFPIα either stays soluble in a full-length form or as a C-terminally truncated form that associates with plasma lipoproteins (Wood *et al.* 2014). TFPIα may also remain attached to the cell membrane through a yet unknown GPI anchored co-receptor. TFPIβ on the other hand, is exclusively found on the cell surface where it is directly bound to the cell membrane through a GPI anchor encoded by its unique C-terminal domain (Zhang *et al*. 2003).

The main function of TFPI is to regulate tissue factor initiated blood coagulation by binding to FXa or the TF-FVIIa complex. It is the second Kunitz-domain that binds to FXa and thus function as a direct protease inhibitor of FXa (Gomez & McVey 2006), however, experiments have shown that involvement of the C-terminal domain results in a more efficient FXa inhibition (Wesselschmidt *et al.* 1992). In the presence of phospholipids and calcium ions, proteins S will enhance the inhibition by binding TFPIα to the surface membrane. This effect requires Kunitz-3 and the C-terminal domain (Broze & Girard 2013; Ndonwi *et al*. 2010; Wood *et al.* 2014). TFPI can also inhibit blood coagulation by binding to TF-FVIIa. This can either take place in a one-step process where Kunitz domain 1 binds to TF-FVIIa-FXa or in a two-step process where the Kunitz domain 1 first binds to FXa and then, the TFPI-Xa complex binds to TF-FVIIa, forming a quaternary inhibitory complex (Broze & Girard 2013).

1.4.2 Non-hemostatic properties of TFPI

Although TFPI's main function is to inhibit blood coagulation, non-hemostatic properties of TFPI, including effects on cancer biology, have also been reported. An experiment performed by Kamikubo and colleagues in 1997, demonstrated that human recombinant TFPI (h-rTFPI) inhibited proliferation of cultured human aortic smooth muscle cells, and the effect was mediated by the C-terminal end (Kamikubo *et al*. 1997). A similar effect was observed in human umbilical vein endothelial cells (HUVEC), but in these cells the effect was associated with very low density lipoprotein receptor (Hembrough *et al*. 2001). It has also been reported that h-rTFPI inhibits growth in both HUVEC (Hamuro *et al*. 1998) and in rat mesengial cells by inducing apoptosis. This effect likely involved the PI3-Kinase-Akt signaling pathway (Lin *et al*. 2007). Moreover, h-rTFPI has been reported to also inhibit adhesion, migration and angiogenesis in HUVECs (Provencal *et al.* 2008).

Several experiments have shown that TFPI plays a role in cancer. In 1989, increased levels of TFPI were found in patients with progressing gastrointestinal carcinoma. The levels of TFPI seemed to increase as the cancer progressed, while the other coagulation inhibitors including antitrombin, protein C and heparin cofactor II, decreased (Lindahl *et al.* 1989). A similar effect was also seen in patients with pancreatic cancer (Lindahl *et al.* 1992). In 1998, Iversen *et al.* measured high levels of TFPI in patients with solid tumors, in accordance with the study by Lindahl and colleagues. The effect seemed to be unrelated to the degree of activated coagulation (Iversen *et al.* 1998). Considering that anticoagulant therapy have shown to reduce metastasis in mice and rats (Agostino *et al*. 1966; Lee *et al*. 1990), Amirkhosravi *et al.* (2002) investigated the effect of TFPI on metastasis in B16 melanoma. They found that TFPI reduced lung metastasis by 83%, and fewer lung nodules were developed when mice received TFPI intravenously. A similar effect was found by Hembrough and colleagues in 2003 when they reported that TFPI inhibited growth of both primary and secondary tumors, and blocked angiogenesis through a non-hemostatic mechanism (Hembrough *et al*. 2003).

To further investigate the effect of TFPI in cancer, Stavik *et al.* (2010) studied overexpression and downregulation of TFPI in breast cancer cells. TFPIα and TFPIβ cDNA inserts were cloned into expression vectors and stably transfected into the breast cancer cell line SK-BR-3. Overexpression of either TFPI isoforms in SK-BR-3 cells resulted in increased apoptosis showed by increased caspase-3 activity and fragmented DNA, while the opposite effect was observed in stable Sum102 cell lines with TFPI downregulated. Induced death receptor ligand TNF-α was measured when TFPIα and TFPIβ were overexpressed, indicating that the apoptosis was mediated through the death receptor pathway. TFPI's effect on self-sufficient growth and motility in breast cancer cells was also investigated in an another study by the same authors (Stavik *et al.* 2011). Increased cell adhesion to collagen 1, together with elevated integrin α2 levels were measured in total TFPI (α+β) or in TFPIβ downregulated MDA-MB-231 cells. An increased ability to migrate was also observed in the total TFPI (α+β) or TFPIβ downregulated cells. This effect was possibly mediated through tyrosine phophorylation signaling (Stavik *et al.* 2011). To find the molecular mechanisms responsible for the effects of TFPI, gene expression studies were further performed by Stavik *et al.* (2012). It was revealed that overexpression of TFPI affected several genes involved in cell development, and that the EGFR pathway possibly was involved. Furthermore, it has been reported that tumors in mice injected with cells with high endogenous TFPI levels (control)

were significant smaller than in mice injected with TFPI knockdown cells (Tinholt *et al.* 2012).

1.5 Overexpression and knockdown cell models

1.5.1 RNA interference

RNA interference (RNAi) is a biological process that either destroys or inhibits the translation of the mRNA (Watson *et al.* 2008). RNAi occurs in many different organisms as a cell defense mechanism, and the same mechanism is used in knockdown studies to study functions of a specific protein (Downward 2004). The RNAi process starts when the endonuclease Dicer cleaves double stranded RNA into fragments of 21-30 nucleotides, called short interfering RNA (siRNA). After the cleaving, siRNA will bind to Argonaute and form RNA-Induced Silencing Complex (RISK). siRNA will then guide RISK to the complementary mRNA where Argonaute cleaves, and degrades the mRNA (Jinek & Doudna 2009).

In knockdown studies, this process can be used to observe functions of a specific protein. By introducing siRNA complementary to the mRNA of the protein of interest, the specific mRNA will be degraded and a loss-of-function phenotype can be observed (Cullen 2006a). Since this method is quite simple and inexpensive, this tool is widely used in gene function studies, including cancer studies. Today there are several companies that provide pre-designed siRNA that target the gene of interest. siRNA exist both in 21mer and 27mer siRNA, where 27mer siRNAs have been reported to be more efficient (Kim *et al.* 2005).

1.5.2 Overexpression

Overexpression of a specific gene can be studied by introducing a plasmid into the cell by transfection. Plasmids are circular, double-stranded DNA molecules (Klug *et al.* 2007). cDNA for a specific gene of interest can be cloned into a plasmid, and by transfecting the plasmid into cells, an overexpression of the specific gene can be observed. The overexpression can either be studied in transiently transfected cells or in stably transfected cells. When performing a transient transfection, the plasmid will be introduced to the nucleus, but will not integrate into the chromosome. Since the plasmids often contain a constitutive eukaryote promoter, high levels of protein is being produced. The overexpression can then be observed for a limited period of time, before the plasmid is lost due to continuous cell division. The

time interval where the effect of the transfection may be observed is dependent of the cell type used in the transfection. The transfection can be observed in longer periods in cells that divide slowly compared to cells that have a short doubling time. In stable transfections, on the other hand, the plasmid will become integrated into the chromosomal DNA. The plasmids contain an antibiotic-resistance gene, which can be used for selection of the cells with integrated plasmid. By adding the appropriate antibiotics to the transfected cells for several weeks, only the cells with integrated plasmid will survive, and results in a homogenous cell population that continuously overexpress the specific gene of interest (Qiagen 2014). Stable transfection may also provide a cell population that continuously silences the gene of interest by using plasmid containing shRNA.

In this thesis a plasmid with TFPIα or TFPIβ insert was used for overexpression experiments. TFPIα and TFPIβ cDNA inserts have previously been cloned into a eukaryote expression vector (pcDNA 3.1/V5-His TOPO vector, shown in Figure 1.5) by the research group (Stavik *et al.* 2011). The plasmid with TFPIα cDNA insert was called TFPIα plasmid, and the plasmid with the TFPIβ cDNA insert was called TFPIβ plasmid. The pcDNA 3.1/V5-His TOPO vector used for making these plasmids contains different restriction sites, a constitutive eukaryote promoter (PCMV), an ampicillin resistance gene for selection of transformed prokaryotic cells and a neomycin resistance gene for selection of stably transfected eukaryotic cells (Invitrogen 2009).

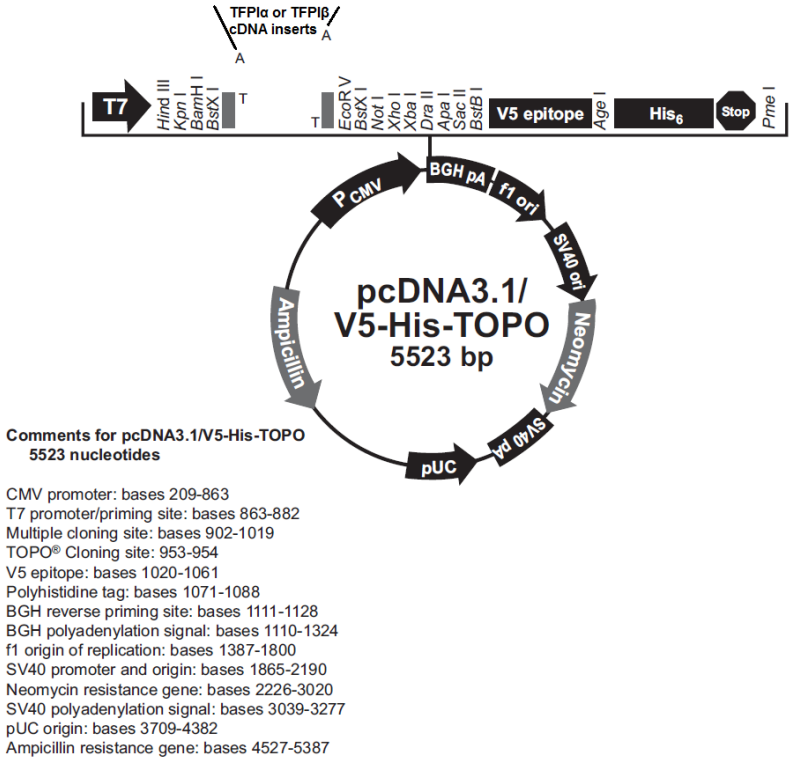

Figure 1.5: Schematic map of pcDNA 3.1/V5-His-TOPO vector. TFPIα and TFPIβ cDNA are inserted as shown in the figure. Modified from Invitrogen (2009). *pcDNA™3.1/V5-His TOPO® TA Expression Kit - User Manual.*

1.6 Breast cancer cell lines

Breast cancer is the second most common cancer after lung cancer, however, it is the most frequently diagnosed cancer in women (Ferlay *et al*. 2013). Breast cancer tumors constitute a very heterogeneous group, affecting their behavior and response to different treatments. Based on gene-expression profiles, breast cancer tumors may be divided into 5 subtypes; luminal A, luminal B, luminal C, ERBB2+, and basal-like. These subtypes have different survival rates where the luminal A subtype patients have been associated with the highest survival rate, while patients with basal-like tumors have shown the lowest survival rate (Sørlie *et al*. 2001). Most of the triple negative cancer cells are found within the basal-like subtype. Cells that are triple negative lack the estrogen receptor, the progesterone receptor, and the human epidermal growth factor receptor 2 (HER2), and are associated with poor prognosis of cancer since they do not respond to endocrine therapy that target the hormone receptors, or trastuzumab that prevents downstream signaling pathway activated by HER2 receptor (Foulkes *et al*. 2010; Hudis 2007).

In this thesis, breast cancer cell lines were used to study TFPI's function in cancer. Other cancer cells could also have been used, but since the research group already had access to a clinical material from breast cancer patients, the functional studies were also conducted in breast cancer cells. Breast cancer cell lines may serve as a good model for investigating the possible non-hemostatic effects of TFPI since breast cancer is among the cancer types with low risk of developing VTE (Chew *et al*. 2006). The TFPIα and TFPIβ expression have been reported to vary between different breast cancer cell lines. Stavik *et al*. (2013) have recently reported that invasive basal-like breast cancer cells have higher TFPIα and TFPIβ expression compared to non-invasive luminal-like breast cancer cells and the TF expression followed the TFPI expression. The research group has also observed a correlation between TFPI expression and p53 mutation, and this is currently under investigation.

The breast cancer cell lines used in this thesis are called MDA-MB-231 and MDA-MB-436. Both are triple negative (Lehmann *et al.* 2011) and have a mutation in the *TP53* gene (International Agency for Research on Cancer 2014). These cells were chosen because of the different TFPI level. MDA-MB-231 has a high TFPI expression compared to MDA-MB-436 which has a low TFPI expression (Figure 1.6) (Lund University 2012). This made the MDA-MB-436 cells a good candidate for TFPI overexpression studies, while downregulation of TFPI was performed in the MDA-MB-231 cells.

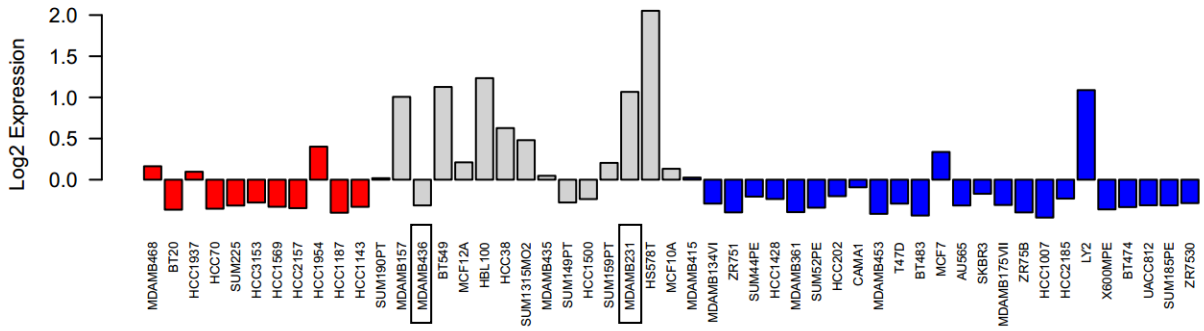

Figure 1.6: Expression of TFPI in different cell lines. The diagram show low TFPI expression in the MDA-MB-436 cells, compared to high expression in the MDA-MB-231 cells. From the GOBO database: Lund University. (2012). *GOBO - Gene set analysis - Cell lines*. Available at: http://co.bmc.lu.se/gobo/gsa_cellines.pl (accessed: 14.04.14

1.7 Aims of the study

TFPI is a plasma serine protease inhibitor which is transcribed into two isoforms; TFPIα and TFPIβ, by alternative splicing. TFPI has its main task in the coagulation system where it inhibits TF-FVIIa and FXa to prevent blood coagulation, but several studies have suggested an anti-tumor role for TFPI in cancer. Finding the molecular mechanisms behinds these effects of TFPI could potentially provide new therapeutic strategies against cancer and cancer associated thrombosis.

The research group has previously conducted experiments where TFPI was downregulated to evaluate TFPI's effect on adhesion and migration of breast cancer cells. They have successfully managed to knock down TFPIα and TFPIβ isoform together (total TFPI), and the TFPIβ isoform alone, but they have not succeeded to knock down only the TFPIα isoform. They have also created a stable cell line in MDA-MB-231 cells where total TFPI (α+β) or TFPIβ was knocked down, but have not managed to make a stable cell line in MDA-MB-231 where TFPIα or TFPIβ is upregulated. The specific aims of this study were:

1. To find siRNA oligonucleotides that could exclusively knock down the TFPIα isoform in breast cancer cell lines
2. To find a breast cancer cell line with similar characteristics as MDA-MB-231, in order to establish a stable cell line with TFPIα or TFPIβ upregulated
3. To study the effect of TFPIα and TFPIβ on growth, migration and adhesion by transient up- and downregulation in MDA-MB-231 cells

2 Materials

2.1 Reagents and chemicals

Reagents and chemicals	Supplier	Catalog number
Albumin from bovine serum	Sigma-Aldrich, St. Louis, USA	A7906
Amersham™ ECL Prime Western Blotting Detection Reagents	GE Healthcare, Buckinghamshire, UK	RPN2209
Aprotinin from bovine lung	Sigma-Aldrich, St. Louis, USA	A6279
Bromphenol blue	Sigma-Aldrich, St. Louis, USA	B0126
Collagen 1, Rat tail	Gibco by Life Technologies, UK	A10483-01
DMEM	Lonza, Verviers, Belgium	BE12-604F
Dithiotreitol (DTT)	Thermo Scientific, Rockford, USA	#R0861
Fetal Bovine Serum Gold	GE Healthcare, Pasching, Austria	A15-151
G 418 disulphate solution	Sigma-Aldrich, St. Louis, USA	G8168
GelRed Nucleic Acid Gel Stain	VWR, Oslo, Norway	730-2958
Generuler 1KB DNA ladder	Fermentas, Vilnius, Lithuania	SM0311
Glycine	BioRad, CA, USA	#161-0718
Glycerol	Sigma-Aldrich, St. Louis, USA	G5516
HCl	Merck, Darmstadt, Germany	K36971017
Isopropanol	Merck, Darmstadt, Germany	1.09634.2500
Lipofectamine®2000 Transfection Reagent	Invitrogen, Carlsbad, CA, USA	11668-019
Magermilchpulver	Appchem GmbH, Darmstadt, Germany	A0830
Methanol	Merck, Darmstadt, Germany	I677909313
OPTI-MEM® (1X)	Gibco by Life Technologies, UK	31985-062
Phenylmethanesulfonylfluoride	Sigma-Aldrich, St. Louis, USA	78830
Phosphatase inhibitor cocktail 2	Sigma-Aldrich, St. Louis, USA	P5726
Phosphate Buffered Saline (PBS)	Gibco by Life Technologies	14190-094
Precision Plus Protein™ Dual Color Standards	BioRad, CA, USA	161-0374
Reagent A100 Lysis buffer	Chemometec, Allerød, Denmark	910-0003
Reagent B Stabilizing buffer	Chemometec, Allerød, Denmark	910-0002
Restriction enzyme *BstX 1*	Fermentas, Vilnius, Lithuania	FD1024
RIPA buffer	Sigma-Aldrich, St. Louis, USA	R0278
Seakem ® LE Agarose	Lonza, Rockland, USA	50004
S.O.C medium	Invitrogen, Carlsbad, CA, USA	15544-034
Sodium Cloride (NaCl)	Merck, Darmstadt, Germany	1.06404.5060
Sodium Dodecyl Sulfate	BioRad, CA, USA	147268A
TaqMan ® Gene Expression Master Mix	Applied Biosystems, Foster City, USA	4369016
TBE Electrophoresis buffer (10X)	Fermentas, Vilnius, Lithuania	#5B2
TransIT®2020 Transfection Reagent	Mirus, Madison Wisconsin, USA	#MIR5410s
Trizma ® base	Sigma-Aldrich, St. Louis, USA	T1503
Trypan blue stain (0,4%)	Invitrogen, Carlsbad, CA, USA	T10282
Trypsin EDTA	Lonza, Viviers, Belgium	3B17-16IE
Tween ® 20	Sigma-Aldrich, St. Louis, USA,	P1379
Versene EDTA	Lonza, Viviers, Belgium	BE17-711E
WST-1 Cell Proliferation Reagent	Abcam, UK	ab155902
10X BlueJuice™ Gel Loading Buffer	Invitrogen, Carlsbad, CA, USA	10816015
10X Fast Digest Buffer	Fermentas, Vilnius, Lithuania	B64

2.2 siRNA oligonucleotides

siRNA	Producer	mRNA target position*	Sequence (5´→ 3´)
siRNA α1	Eurogentec	693-712	CAGAUUCUACUACAAUUCATT (21)
siRNA α2	Eurogentec	808-825	AUAUUCUUUGGAUGAAACCTC (21)
siRNA α3	Eurofins	688-714	GAGAACAGAUUCUACUACAAUUCAGUC (27)
siRNA α4	Eurofins	689-715	AGAACAGAUUCUACUACAAUUCAGUCA (27)
siRNA α5	Eurofins	693-719	CAGAUUCUACUACAAUUCAGUCAUUGG (27)
siRNA α6	Eurofins	683-709	CCAAUGAGAACAGAUUCUACUACAAUU (27)
siRNA β7	Dharmacon	655-675	GGAAGAAUGCGGCUCAUAUUU (21)
siRNA β9	Dharmacon	656-676	GAAGAAUGCGGCUCAUAUUUU (21)
Silencer® NegativeControl siRNA#5	Ambion		Cat.no: AM4642

* mRNA target position (counted from start codon), accession nr: NM_006287.4 for TFPIα and NM_001032281 for TFPIβ

2.3 qRT-PCR assays

Assay	Name	Sequence (5´→ 3´)
PMM1	PMM1-80 Forward Primer	CCGGCTCGCCAGAAAATT
	PMM1-149 Reverse Primer	CGATCTGCACTCTACTTCGTAGCT
	PMM1-99 Probe	ACCCTGAGGTGGCCGCCTTCC
TFPIα	TFPI-8/9 Forward Primer	AAGAATGTCTGAGGGCATGTAAA
	TFPI-8/9 Reverse Primer	CTGCTTCTTTCTTTTTCTTTTGGTTT
	TFPI-8/9 Probe	AGGGTTTCATCCAAAGAATATCAAAAGGAGGCC
TFPIβ	TFPI-β Forward	CAAGGTTCCCAGCCTTTTGT
	TFPI-β Reverse	CAAAGGCATCACGTATACATATA
	TFPI-β Probe	TCCAACCATCATTTGTTCCTTCTTTTGT

All the assays were synthesized/produced by Eurogentec

2.4 Kits

Kit	Supplier	Catalog number
Asserachrom ® TOTAL TFPI kit	Diagnostica Stago, Asnieres, France	00261
BigDye® Terminator v3.1 Cycle Sequencing Kit	Applied Biosystems, Foster City, USA	4337455
Endofree ® Plasmid Giga Kit	Qiagen, Hilden, Germany	12391
High Capacity cDNA Reverse Trancription	Applied Biosystems, Foster City, USA	4368813
Pierce ® BCA Protein Assay Kit	Thermo Scientific, Rockford, USA	23225
RNAqueous ® PhenolFree Total Isolation Kit	Ambion, USA	AM1912

2.5 Antibodies

Antibody	Supplier	Catalog nr
Purified Mouse Anti-Human CD49b	BD Biosciences	611016
Phospho-Src Family (Tyr 416) Antibody	Cell Signaling Technology	#2101
GAPDH (D16H11) XP®Rabbit mAb	Cell Signaling Technology	#5174
Polyclonal Goat Anti- Rabbit Immunoglobin /HRP	DAKO	P0448
Polyclonal Goat Anti-Mouse Immunoglobin /HRP	DAKO	P0447

2.6 Primers

Primer	Supplier	Sequence (5´→ 3´)
T7 forward primer	Invitrogen, Carlsbad, CA, USA	TAATACGACTCACTATAGGG
BGH reverse primer	Invitrogen, Carlsbad, CA, USA	TAGAAGGCACAGTCGAGG

2.7 Cells

Cell type	Supplier	Catalog number
MDA-MB-231	American Type Culture Collection, Manassas, USA	ATCC® HTB-26™
MDA-MB-436	American Type Culture Collection, Manassas, USA	ATCC® HTB-130™
HEK293T cells	American Type Culture Collection, Manassas, USA	ATCC® CRL-11268™
One Shot® TOP10 Chemically Competent cells	Invitrogen, Carlsbad, CA, USA	C4040-10

2.8 Equipment

Equipment	Supplier
Countess® chamber slide	Invitrogen
Nucleocounter Casette	Chemometec
Nunc cell flask (25cm^2, 80cm^2, 175cm^2)	Thermo Scientific
Nunc™ Cell-Culture Treated Multidishes (6-, 12- and 96-well)	Thermo Scientific
Mini-PROTEAN®TGX™ Gels 10%	BioRad
Whatman®PROTRAN Nitrocellulose Transfer Membrane	Sigma-Aldrich
10% Precise ™ Tris-Glycine gel	Thermo Scientific
0,2ml non-skirted 96-well PCR plate	Thermo Scientific
384-well clear optical reaction plate	Thermo Scientific

2.9 Instruments

Instrument	Supplier
ABI PRISM 7900HT Sequence Detection System	Applied Biosystems
ABI 3730 DNA Analyzer	Applied Biosystems
Benchmark Microplate Reader	BIO-RAD, Hercules, CA
Countess® Automated Cell Counter	Invitrogen
ImageQuant LAS 4000 imaging system	GE Healthcare
NanoDrop® ND-1000 Spectrophotometer	NanoDrop Technologies
Nikon Eclipse TE300 microscope	Nikon Instruments
Nucleocounter ® NC-100™	Chemometec
Omega Lum G imaging system	Aplegen
Steri-Cycle CO_2 Incubator	Thermo Electron Corporation

2.10 Solutions

Primary antibody solution

- 1 ml 5% BSA
- 4 ml TBST
- Antibody (1:1000-1:2000)

Secondary antibody solution

- 4.8 ml TBST 1X
- 0.2 ml 5% Magermilchpulver
- Antibody (1:1000-1:2000)

TBS 10X

- 24.23 g Trizma ® base
- 80.06 g NaCl
- H_2O to 1L (pH 7.6)

5% BSA

- 5 g Albumin from bovine serum
- 100 ml TBS 1X

TBST 1X

- 100 ml TBS 10X
- 900 ml H_2O
- 1 ml Tween ® 20

Running buffer 10X (Western blotting):

- 30 g Trizma® base
- 144 g Glycine
- 10 g Sodium Dodecyl Sulfate (SDS)
- H_2O to 1L (pH 8.3)

Blotting Buffer

- 3 g Trizma ® base
- 14.4 g Glycine
- 800 ml H_2O
- 200 ml Methanol

LB-medium

- 10 g tryptone
- 5 g yeast extract
- 10 g NaCl
- H_2O to 1L (pH 7.0)

Loading buffer (Western blotting)

- 1.5 ml 1M Trizma® base
- 6.0 ml 10% SDS
- 1.0 ml 2% Bromphenol blue
- 1.5 ml 99% Glycerol
- 1/10 1M Dithiotreitol (DTT)

RIPA buffer with inhibitor cocktail

- 1 ml RIPA buffer
- 2 µl Aprotinin from bovine lung
- 10 µl Phosphatase inhibitor cocktail 2
- 6 µl Phenylmethanesulfonylfluoride (100 µM)

1,5% agarose gel

- 0.75 g Seakem ® LE Agarose
- 50 ml 1X TBE Electrophoresis buffer

Boil for 30 sec, and then add 5 µl GelRed Nucleic Acid Gel Stain.

3 Methods

3.1 Microbiological techniques

3.1.1 Transformation of chemically competent *Escherichia coli* cells

OneShot® TOP10 Chemically Competent *E.coli* cells were transformed with TFPIα and TFPIβ plasmids in order to produce enough plasmid for TFPI overexpression experiments. Plasmids without cDNA insert were made as a control. The *E.coli* cells used for this transformation were already made chemically competent by Invitrogen with calcium chloride treatment.

Chemically competent *E.coli* cells were transformed according to Invitrogen OneShot® TOP10 Chemical Transformation protocol. In brief, 1 µg of each plasmid was added to chemically competent *E.coli* cells. Cells without plasmid were used as a negative control. The cells were heat-shocked at 42 °C for 30 sec, and placed on ice. S.O.C medium was added to the tubes, before incubation at 37 °C with constant shaking. After one hour, 10 µl of each transformed cell suspension was spread on pre-warmed LB agar plates with 100 µg/ml ampicillin for selection, and incubated overnight at 37°C. The next day, a single colony of each plasmid transformation was picked from plate, and transferred to vials with selection medium (LB-medium with 100 µg/ml ampicillin). To grow a sufficient number of bacteria for plasmid isolation, the vials were pre-cultured for 8 hours at 37°C and constant shaking, before they were transferred to conical flasks with LB-medium with ampicillin, and incubated for another 16 hours at 37 °C.

3.2 DNA and RNA techniques

3.2.1 Nucleic acid isolation and quantification

Isolation of plasmid DNA from transformed E.coli cultures

To isolate plasmids from *E.coli* cultures, Endofree ® Plasmid Giga Kit was used according to the manufacturer's protocol. In brief, transformed bacteria (described in section 3.1.1) were harvested by centrifugation. The supernatant was decanted, and the bacterial cell pellets were resuspended in buffer P1 and lysed in buffer P2. To remove proteins, cell debris and genomic DNA, the lysates were filtered through a QIA filter using a vacuum pump. The filtered lysates were added to a DNA binding Qiagen-tip and eluted after washing. The eluate was stored overnight at 4 °C. The next day, isopropanol was added to precipitate the plasmid DNA. After centrifugation, the pellet was washed with 70% ethanol, and then air-dried before it was resuspended in endotoxin-free TE buffer. The isolated plasmids were stored at -20 °C.

Isolation of RNA from cells lysed in RNA lysis buffer

For isolation of RNA from cells, RNAqueous ® PhenolFree Total Isolation Kit was used according to the manufacturer's protocol. First, an equal volume of 64% ethanol was added to the lysate(s), and mixed by inverting the tube several times. The lysate/ethanol mixture was drawn through a filter cartridge by centrifugation at 12 000 rpm for 30 sec. The flow-through was removed and to get RNA without contamination like phenols and proteins, three washing steps were performed. After the last wash step, the samples were centrifuged again to remove all remaining wash solution. Pre-heated elution buffer (75 °C) was added to the filter and the samples were centrifuged at 12 000 rpm for 30 sec to elute RNA. The elution step was performed twice. The isolated RNA was stored at -75 °C.

Quantification of DNA and RNA

To determine the concentration of DNA and RNA, NanoDrop® ND-1000 Spectrophotometer was used. Since nucleic acids absorb UV light at 260 nm, and protein at 280 nm, UV absorbance spectrophotometry can be used to measure the concentration and the purity of DNA and RNA samples (Sambrook & Russell 2001). An OD_{260} measurement of 1 corresponds to ~50 µg/ml for double-stranded DNA and 40 µg/ml for single-stranded DNA and RNA. The $^{OD260}/_{OD280}$ ratio gives an estimate for the purity of the DNA and RNA

samples. $^{OD260}/_{OD280}$ ratios of 1.8 and 2.0, indicates pure DNA and RNA, respectively. Lower ratios indicate protein or phenol contamination (Sambrook & Russell 2001).

3.2.2 Restriction enzyme digestion

To verify the presence of the TFPIα and TFPIβ cDNA inserts in the pcDNA 3.1/V5-His TOPO vector (described in introduction, section 1.5.2), the plasmids were cut by restriction enzymes before agarose gel electrophoresis was applied to separate the DNA. The restriction enzyme *BstX 1* was chosen since *BstX 1* cuts on both sides of the cDNA insert (PCR product) as shown in Figure 1.5. The reagents shown in Table 3.1 was mixed and then incubated for 15 min at 37 °C. The mixtures were stored on ice before the agarose gel was run.

Table 3.1: Reagents and volumes used in the restriction enzyme digestion

Reagents	**Volume**
Plasmid	x µl (1 µg)
10X Fast Digest Buffer	2 µl
BstX 1 enzyme	1 µl
Nuclease-free water	x µl
Total	20 µl

3.2.3 Agarose gel electrophoresis

An agarose gel electrophoresis was performed to estimate the sizes of the resulting fragments of the restriction digested plasmids. An agarose gel electrophoresis separates negatively charged macromolecules by size using an electric field. Separation occurs since smaller molecules move faster through the gel pores than larger molecules. The fragments can be visualized since the gel contains GelRed. GelRed bound to DNA emits light when exposed to ultraviolet light. When performing agarose gel electrophoresis, 10X BlueJuice™ Gel Loading Buffer (3 µl) was added to the DNA samples prior to gel loading, and the samples were electrophoresed for 1 hour with 80 Volts in a 1,5% agarose gel (described in section 2.10). The gel was photographed using the Omega Lum G imaging system, and the fragments were compared with a Generuler 1KB DNA ladder to estimate the sizes.

3.2.4 DNA Sequencing

Sanger sequencing of the isolated TFPIα and TFPIβ plasmids (described in section 3.2.1) was performed to confirm the correct sequences. In Sanger sequencing DNA polymerase will incorporate nucleotides, but the nucleotide mix also contains nucleotides lacking the 3´hydroxyl group (ddNTP), adding one of these ddNTPs will terminate the extension randomly. This results in many fragments with different lengths which are separated by size in capillary columns. The nucleotide analogues are labeled with different fluorescent dyes which make it possible to determine the sequence. Table 3.2 shows the reagents used in one sequencing reaction. For each sample one reaction with T7 forward primer, and one reaction with BGH reverse primer were run. The products from the reactions were sequenced in the ABI 3730 DNA Analyser. For alignment with the TFPIα and TFPIβ sequences in NCBI GeneBank, BLASTn was used.

Table 3.2: Reagents and volume used in one sequencing reaction

Reagents	**Volume**
Plasmid	750 ng
Primer	3.2 pmol
BigDye® Terminator v3.1 Ready Reaction Mix	0.25 µl
5X Sequencing Buffer	2 µl
H_2O	x µl
Total	10 µl

3.2.5 Complementary DNA synthesis

Complementary DNA (cDNA) was synthesized from RNA with the High Capacity cDNA Reverse Transcription Kit. The kit includes Multiscribe Reverse Transcriptase that transcribes the RNA to cDNA from different random hexamer primers that prime at different sites along the RNA. When performing cDNA synthesis, the reagents shown in Table 3.3 were mixed in a 96-well plate. All RNA samples were diluted to the same concentration using nuclease-free water, to a final volume of 25 µl. RNA input ranged from 500-5000 ng between the different experiments.

Table 3.3: Reagents used for one cDNA reaction

Reagent	Volume
10X RT Buffer	5 µl
25X dNTP Mix (100nM)	2 µl
10X RT Random Primers	5 µl
MultiScribe™ Reverse Transcriptase	2.5 µl
Nuclease-free H_2O	10.5 µl
RNA input	25 µl (500-5000 ng)
Total volume per reaction	50 µl

After the plate was sealed and centrifuged, the plate was ready for the thermal cycler program described in Table 3.4.

Table 3.4: The thermal cycler program optimized for the High Capacity cDNA Reverse Transcription Kit.

	Step 1	Step 2	Step 3	Step 4
Temperature	25 °C	37 °C	85 °C	4 °C
Time	10 min	120 min	5 min	∞

3.2.6 qRT-PCR

To compare gene expression levels, real time quantitative reverse transcription polymerase chain reaction (qRT-PCR) was used. TaqMan qRT-PCR is a type of PCR, in which a probe with two fluorescent dyes, a 5´reporter (R) and a 3´quencher (Q), anneals to the cDNA target sequence between a forward and a reverse primer as shown in Figure 3.1B. When the probe is intact, the reporter and the quencher are close to each other and there is no fluorescent signal, since light emitted by the reporter is absorbed by the quencher. In each cycle, Taq polymerase with its 5´nuclease activity will cleave the probe, so that the reporter will no longer be quenched and a fluorescent signal can be detected. During the first cycles, the fluorescent signal is weak, but as the amount of PCR products accumulate, the signal increases exponentially, before the signal reaches a plateau phase in lack of critical components in the PCR (Kubista *et al.* 2006). The fluorescent signal is proportional to the amount of PCR product, (which is a measurement of gene expression) and is shown in real time in an amplification plot (Figure 3.1A) during the PCR.

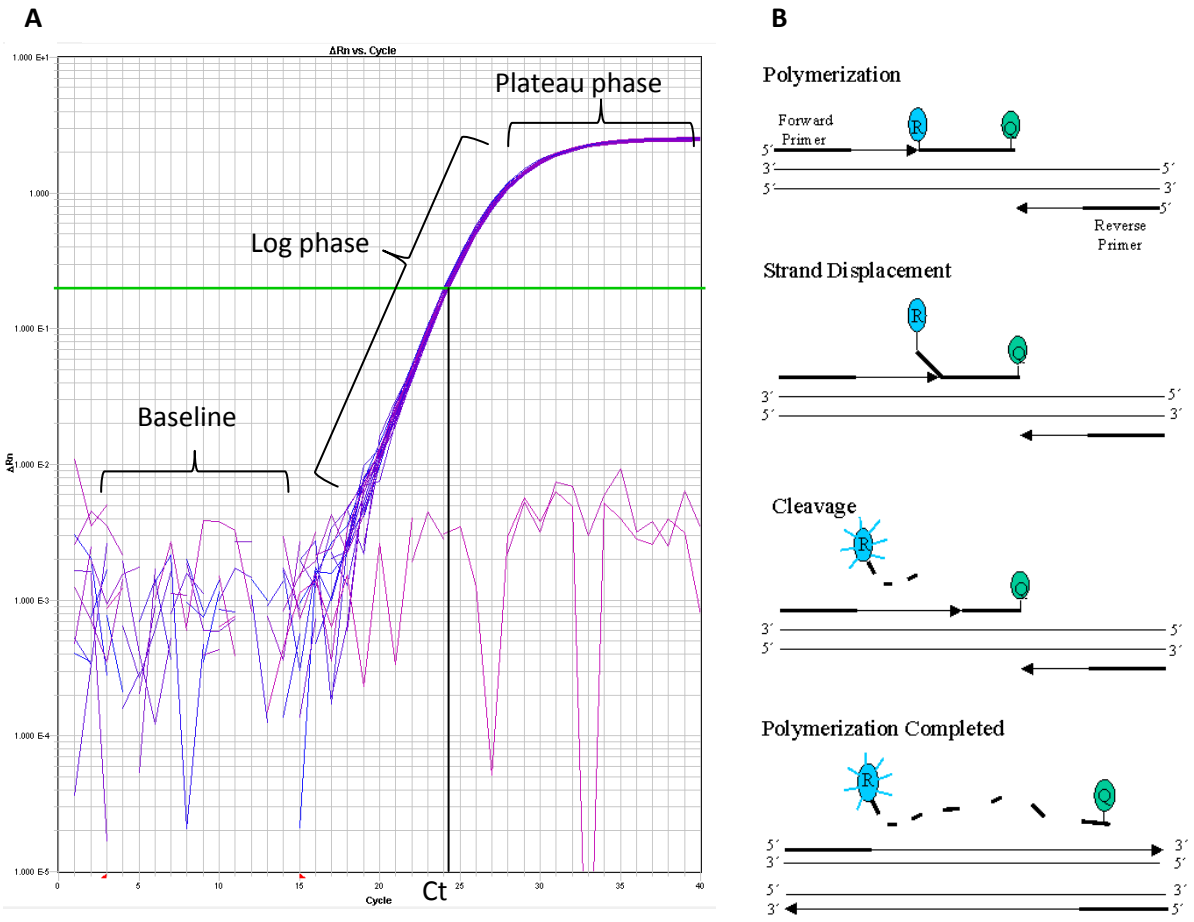

Figure 3.1: A) Amplification plot for an endogenous control (PMM1). Baseline, from cycle 3 to 15 is the area where the fluorescent signal is approximately constant and is used as background. The threshold (green line) is a point set in the log phase where the precision of the reaction is optimal. The cycle threshold (Ct) value is the number of cycles needed to reach the threshold. **B)** Principles of qRT-PCR. When the florescent probe is intact, the light emitted by the reporter (R) is absorbed by the quencher (Q). When Taq polymerase cleaves the probe, the quenching ceases since R and Q are no longer close, and a fluorescent signal can be detected from the reporter.

The comparative Ct method was used to analyze the qRT-PCR data. In each qRT-PCR set-up, an endogenous control was included to normalize the results for sample to sample variations in RNA input and reverse transcriptase efficiency. The endogenous control should have a constant expression level in all the samples, such as a housekeeping gene and should not be affected by different stimuli. In this study, phosphomannomutase 1 (PMM1) was used as an endogenous control since PMM1 was not affected by up or down regulation of TFPI, previously tested by the research group. The relative target gene expression level was calculated by using the formulas below:

ΔCt = Ct value (target) – Ct value (endogenous control)

$\Delta\Delta Ct$ = ΔCt (test sample) – ΔCt (calibrator, the reference in the experiment)

$RQ = 2^{-\Delta\Delta Ct}$

RQ gives the relative quantity of the samples compared to the calibrator. Values < 1 means that the target gene is downregulated, and values >1 means that the target gene is upregulated compared to the reference. In this study, three TaqMan assays, (listed in Table 2.3 under Materials), were used for qRT-PCR. The assays are self-designed and the final reaction contains 900 nM of each primer (forward and reverse) and 250 nM probe. The qRT-PCR components were mixed in a 96-well plate and added in triplicates (10 µl) in a 384-well reaction plate. Table 3.5 show volume and components for one qRT-PCR reaction. The cDNA samples were diluted before adding them to the qRT-PCR reaction, the amount varied from 40-100 ng between the qRT-PCR setups.

Table 3.5: Volume and components for one qRT-PCR reaction

Component	Volume
Assay (20x)	0.5µl
Taqman ® Gene Expression Master Mix (2x)	5 µl
cDNA and H_2O	4.5 µl (40-100 ng)
Total	10 µl

After the plate was sealed and centrifuged at 1500 rpm for 2 min, the plate was placed in the ABI PRISM 7900HT Sequence Detection System and was run according to the thermal cycling program in Table 3.6.

Table 3.6: The ABI PRISM 7900HT Sequence Detection System Program

Step	Time	Temperature	Cycles
AmpErase®UNG Activation	2 min	50 °C	1
DNApolymerase activation	10 min	95 °C	1
Denaturation	15 sec	95 °C	40
Annealing/extending	1 min	60 °C	

To confirm equal PCR efficiency for the four assays, which is a requirement for calculating ΔΔCt, standard curves were made by running a dilution series of one cDNA sample.

3.3 Cell techniques

3.3.1 Cell lines

Two breast cancer cell lines; MDA-MB-231 and MDA-MB-436, and one epithelial cell line HEK293T were used in this study. All the cell lines were obtained from the American Type Culture Collection (Table 2.7). HEK293T cells were used for siRNA-screening experiments, since this cell line is easy to transfect. MDA-MB-231 cells were used for the functional studies and MDA-MB-436 cells for establishment of stable cell lines.

3.3.2 Culturing and storage

MDA-MB-231, MDA-MB-436 and HEK293T cells were all grown in DMEM with 10% Fetal Bovine Serum Gold (FBS). The cells were passaged into new cell flasks when the cells reached 80-90% confluence, observed visually by microscopy. This was done by removing the medium, washing the cells with Phosphate Buffered Saline (PBS), and then detaching the cells by incubating with trypsin EDTA for 5 min at 37 °C. After incubation, DMEM with 10% FBS was added. The Fetal Bovine serum inactivates trypsin EDTA. The cells were cultured in a Steri-Cycle CO_2 Incubator at 37 °C with 5% CO_2. For long time storage, 1.0 - 2.0x10^6 cells in medium with 5%-10% DMSO were stored in liquid nitrogen.

3.3.3 Cell counting

Cell counting was performed using Nucleocounter ® NC-100™. Cells were first lysed with Reagent A, before the pH was raised by adding Reagent B to stabilize the cell nuclei and to optimize the fluorescence of propidium iodide (PI). The mixture was loaded into a Nucleocounter cassette coated with PI. PI stains cell nuclei and the Nucleocounter estimates the stained nuclei, which is an indication of cell number (cell/ml).

3.3.4 Transient transfection

Screening of TFPIα knockdown with siRNA oligonucleotides in HEK293T cells

Before performing TFPI knockdown in MDA-MB-231 cells, the siRNA oligonucleotides that target TFPIα (siRNA α1-α6) were tested in HEK293T cells. Silencer ® NegativeControl siRNA#5 served as control. Transient transfection was performed using Lipofectamine®2000 Transfection reagent protocol. Lipofectamine®2000 contains cationic lipid molecules with neutral co-lipids, which form liposomes in aqueous environments. The liposomes enclose

siRNA, and due to the positive charge, the liposome fuses with the negatively charge cell membrane and siRNA can be transferred in to the cells cytoplasm.

In brief, cells ($2.0x10^5$) were seeded in 12-well plates the day before transfection. On the day of transfection, 200 pmol siRNA and 2.0 µl Lipofectamine were diluted in 200 µl OptiMEM. After 5 min of incubation, medium from the seeded cells was removed, and the siRNA/Lipofectamine mix (200µl) was added to each well before DMEM with 10% FBS was added. Since Lipofectamine can be toxic to the cells, the medium with Lipofectamine was replaced by fresh media 4-6 hours after transfection to prevent cell death. Cells were harvested after 24 hours as described in section 3.3.5.

Optimization of TFPIα knockdown with siRNA oligonucleotides in MDA-MB-231

siRNA α3, α5 and α6 were further used to optimize the transfection in MDA-MB-231 cells. Different siRNA concentrations (50 nM - 200 nM), Lipofectamine volume (2.5 µl - 5 µl) and siRNA:Lipofectamine ratios (20:1 and 10:1) were tested in MDA-MB-231, in the same way as described above.

TFPIα and TFPIβ knockdown with siRNA oligonucleotides in MDA-MB-231

After optimization, TFPIα and TFPIβ knockdown were performed in MDA-MB-231 cells. Cells ($2.25x10^5$ – $2.5x10^5$) were transfected with 75 pmol siRNA and 7.5 µl Lipofectamine®2000 as described above, 6-well plates was used instead of 12-well plates. The cells were harvested 24 – 120 hours after transfection as described in section 3.3.5.

TFPIα and TFPIβ overexpression with plasmids in MDA-MB-231

TFPI overexpression with TFPIα and TFPIβ plasmids in MDA-MB-231 was performed using Lipofectamine®2000 according to the manufacturer's protocol. Plasmid without cDNA insert served as control. In brief, cells ($3.0x10^5$) were seeded in 6-well plates the day before transfection. On the day of transfection, medium was removed and 200 µl OptiMEM containing 2.5 µg plasmid and 7.5µl Lipofectamine®2000 were added to each well, before 1.5 ml DMEM with 10% FBS was added. The plasmid/Lipofectamine mix was replaced with fresh media 4-6 hours after transfection. The RNA and protein lysates were prepared as described in section 3.3.5.

TFPIα and TFPIβ overexpression with plasmids in MDA-MB-436

Both Lipofectamine®2000 Transfection reagent and TransIT®2020 were tested in MDA-MB-436 cells. Since TransIT®2020 gave higher transfection efficiency and caused less cell death, TransIT®2020 was preferred as transfection reagent for MDA-MB-436 cells. Transient transfection using TransIT®2020 were performed according to the manufacturer's protocol. In brief, cells ($4.5x10^5$) were seeded in 6-well plates the day before transfection. The following day, 2.5 µg plasmid and 8 µl TransIT®2020 diluted in 200 µl Opti-MEM were added to each well, before 1.5 ml DMEM with 10% FBS was added. The media was replaced with fresh media 4-6 hours later. RNA and protein lysates were prepared as described in section 3.3.5.

3.3.5 Cell harvesting for RNA isolation and for total protein

Cells harvested for RNA isolation were washed with cold PBS after removing the media, before 300-600µl RNAqueous lysis/binding buffer were added to each well. The cells were scraped, resuspended, and transferred to eppendorf tubes. The samples were stored at -75 °C until RNA isolation. Cells harvested for total protein were lysed in 200-300 µl RIPA buffer with an inhibitor cocktail (described in section 2.10). Media were removed and the cells were washed 3 times with cold PBS. RIPA buffer with inhibitor cocktail was added and incubated on ice for 5 minutes before the cells were scraped and transferred to eppendorf tubes. The protein lysates were stored at -20 °C.

3.3.6 Stable cell lines

To create stable cell lines, MDA-MB-231 and MDA-MB-436 were transfected as described in section 3.3.4. Since the plasmids (described in section 1.5.2 in introduction) contain a neomycin resistance gene, cells with incorporated plasmid were selected by culturing the cells in the presence of 500-750 µg/ml geneticin G418 for 3 weeks. The selected cells were frozen for later use.

3.4 Protein techniques

3.4.1 Total protein quantification

Total protein in cell lysates was quantified using Pierce ® BCA Protein Assay Kit. Proteins will reduce Cu^{+2} to Cu^{+1}, and Cu^{+1} which produces a purple color reaction in the presence of bicinchoinic acid can be measured optically. Protein standards were made from albumin (2 mg/ml) in a 2-fold dilution series, with RIPA buffer with inhibitors. 5 µl of standards, protein lysates and a blank sample were added in triplicate to a 96-well plate. WR solution (200 µl of a 50:1 solution of reagent A and B) was added to each well, and the plate was incubated for 30 min at 37 °C. The absorbance was measured at 570 nm in Benchmark plate reader, and total protein concentrations were determined by comparing the OD-values to the standard curve with known protein concentrations by using MicroplateManager software.

3.4.2 Western blotting

Western blotting is a semi quantitative immunoassay method used to identify proteins. The procedure includes several steps as described below.

SDS-PAGE

The first step is separation of the proteins by sodium dodecyl sulfate polyacrylamide gel electrophoresis (SDS-PAGE) according to size. This step was performed by boiling the lysates (10-15 µg total protein) containing loading buffer (10 µl) for 5 min at 97 °C. Precision Plus Protein ™ Dual Color Standard and the samples were loaded into separate lanes in a 10% Tris-Glycine gel. The proteins were separated according to size by electrophoresis in 1X running buffer at 185 Volts for 40-45 min.

Blotting

The proteins in the gel were transferred to a membrane by wet blotting. A Whatman®PROTRAN Nitrocellulose Transfer Membrane was soaked in Tris Glycine buffer, before the membrane was placed on top of the gel and a sandwich consisting of cardboard, membrane and gel, was made. The proteins were electro transferred to the membrane in cold blotting buffer at 110V for 20 min.

Blocking and antibody exposure

The membrane was blocked in 5% bovine serum albumin (BSA) for one hour to prevent nonspecific binding of proteins to unbound membrane sites. The membrane was thereafter washed 3x10 min with Tris-buffered saline with Tween 20 (TBST) and incubated with a target specific primary antibody overnight at 4°C or for 1 hour at room temperature. The primary antibody will bind to the specific protein of interest. After the incubation, the membrane was washed (3x10 min) in TBST to remove unbound antibody. The membrane was then incubated with a species-specific secondary antibody labeled with horseradish peroxidase (HRP). The secondary antibody will bind to primary antibody. To remove unbound secondary antibody, the membrane was washed 3x10 min with TBST.

Visualization

For visualization, Amersham™ ECL Prime Western Blotting Detection Reagents was used according to the manufacturer's protocol. The reagents contain luminol, which become oxidized in presence of HRP. The oxidized product emits light in proportion to the amount of protein on the membrane. The membrane was photographed using ImageQuant LAS 4000 imaging system. For storage, the membrane was washed and wrapped in plastic and stored at -20 ºC. ImageQuant TL was used to quantify the bands.

3.4.3 Enzyme-linked immunosorbent assay (ELISA) for total TFPI quantification

For total TFPI protein quantification, Asserachrom ® TOTAL TFPI kit, which is a quantitative immunoassay, was used according to manufacturer's protocol. The kit contains plates which are precoated with a TFPI monoclonal antibody. Total TFPI in samples will bind to this antibody and a second TFPI monoclonal antibody labeled with peroxidase, added at the same time as the samples will bind to TFPI. The antibody-TFPI-antibody sandwich is made in a one-step reaction. Peroxidase will give a colored product in the presence of ura peroxide. The reaction stops by adding H_2SO_4, and the color produced is measured at 492 nm. The OD values are compared to a TFPI standard curve and total TFPI protein concentration is determined.

3.5 Functional studies

3.5.1 Cell counting

Cells were counted at four different time points after transfection as a measurement of growth. First the transfected cells were detached from the wells using trypsin EDTA, then an equal volume of trypan blue and cell suspension were loaded in to a Countess® chamber slide, and counted in Countess® Automated Cell Counter. Trypan blue will pass through the cell membrane of dead cells and stain the cells blue, while living cells will appear white since trypan blue cannot pass through the cell membrane of living cells. Countess® Automated Cell Counter uses an algorithm to count living and dead cells based on their size and color.

3.5.2 Cell adhesion to collagen I

Adhesion studies were performed to observe TFPI's effect on the cells adhesion to collagen I. Transfected cells were starved overnight in DMEM with 1% FBS. The next day, wells were coated with collagen I (10 µg/ml). The coating was performed by adding 50 µl of collagen I (10 µg/ml) to each well in a 96-well plate. After one hour incubation at room temperature, the wells were washed twice with medium, and the plate was ready for seeding. The cells were detached by incubating the cells with 500 µl versene EDTA for 15 min at 37 °C. Versene EDTA detaches the cells without cleaving the cell binding receptors. Versene EDTA was removed after the cells were centrifuged and the cells were resuspended carefully in DMEM with 10% FBS. Cells ($2.5x10^4$) were then seeded in a 96-well plate precoated with collagen I. After 10 min incubation, the plate was washed gently once with medium and then 100 µl medium and 10 µl WST-1 was added. WST-1 is a tetrazolium salt which gets cleaved to formazan by the succinate-tetrazolium reductase system in metabolically active cells, so the amount of produced formazan correlates with the amount of living cells. Adhered cells were counted indirectly at wavelength 450 nm in a Benchmark plate reader after 60 min incubation with WST-1. A wavelength of 745 nm were used as a reference wavelength.

3.5.3 Scratch-wound assay

To study TFPI's effect on migration a scratch-wound assay was performed. At 80-90% cell confluence transfected cells seeded in 6-well plates were starved overnight and then a scratch was made using a sterile pipette tip. Images were taken after 0, 6, 24 and 48 hours using Nikon Eclipse TE300 microscope with an attached Nikon DS-5M-L1 Camera system. The

width of the wound was measured manually and % wound closure between 0 and 6, 24 and 48 hours were calculated by subtracting the width for 6, 24 or 48 hours from the width measured after 0 hours. The difference is given in % wound closure.

3.5.4 FBS stimulation experiment

To evaluate the involvement of Src in the experiments, the phosphorylation status of Src in cell lysates of transfected cells after FBS stimulation were measured. Transfected cells were starved for 5 hours before $1x10^6$ cells were stimulated with DMEM with 10% FBS for 0, 5 and 10 min. After the indicating time points the cells were washed twice with PBS, and then lysed in RIPA buffer with inhibitor cocktail. The samples were stored at -20 °C until Western blotting was performed.

3.6 Statistics

To test whether there was a difference in effect of the up- and downregulated cell compared to the control, a two-sample T-test assuming equal variance were performed. This t-test can be used to test if the average value from a normally distributed dataset is significantly different from the average of another normally distributed dataset. Probability values less than 0.05 were considered statistically significant and was marked with *, and p-value less than 0.005 was marked with **.

4 Results

4.1 Validation of TaqMan assays

4.1.1 PCR efficiency

qRT-PCR and the comparative Ct method was used to study relative mRNA expression of TFPIα and TFPIβ in this thesis. In order to use this method, the PCR efficiency of the target gene assay and the endogenous control assay needs to be approximately the same. The efficiency for the assays was determined by analyzing a 5-fold dilution series of a cDNA sample in the ABI PRISM 7900HT Sequence Detection System. An assay is 100% efficient when the value of the slope is -3.32. The endogenous control assay (PMM1) had a slope value of -3.39 (Figure 4.1A), while the TFPIα assay and TFPIβ assay had slope values of -3.46 (Figure 4.1B) and -3.37 (Figure 4.1C), respectively. The efficiency was calculated by the formula $(10^{(-1/slope)}-1)x100\%$. All the assays passed the requirement of < 0.1 difference in slope between the endogenous control assay and the target gene assay (Table 4.1) and could thus be used to calculate mRNA expression by the comparative Ct method in this thesis.

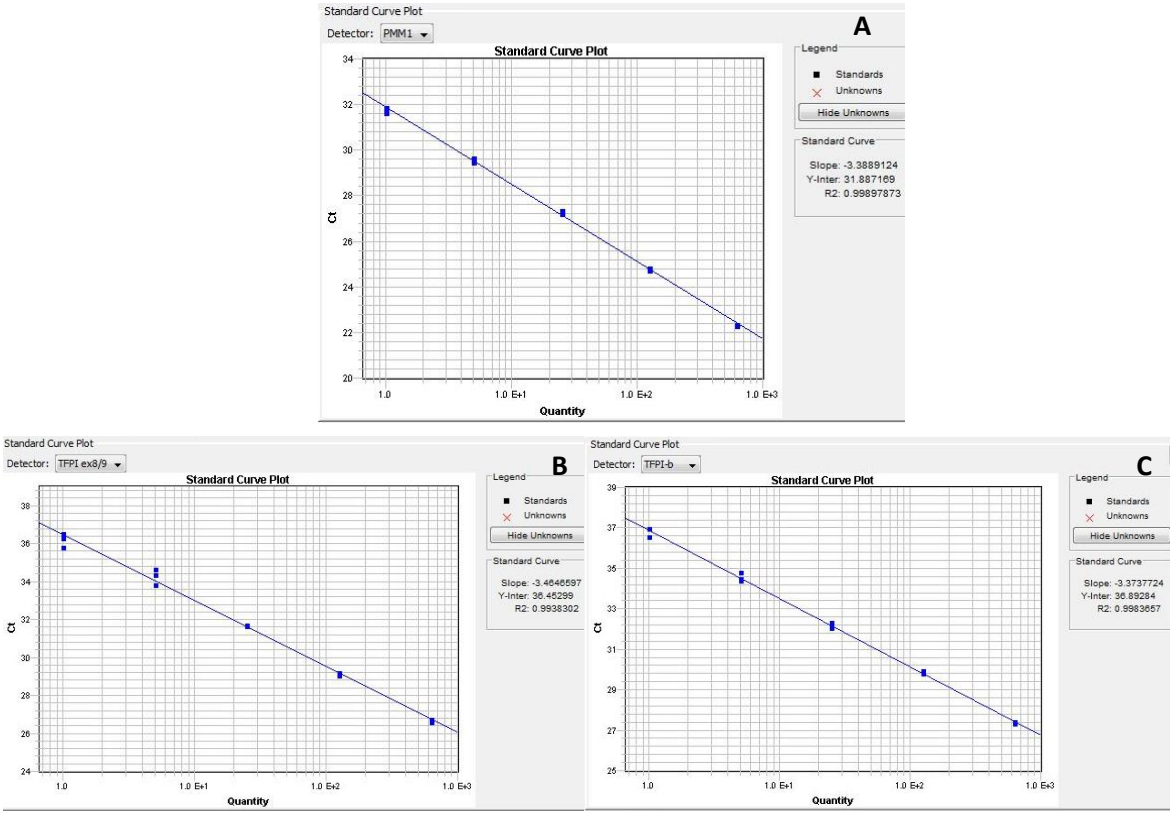

Figure 4.1: Standard curve plots of the Taqman assays. Standard curve plot for A) the endogenous control assay (PMM1) B) the TFPIα assay and C) the TFPIβ assay.

Table 4.1: Slope, ΔSlope and the efficiency of the qRT-PCR assays. The slope value, Δ Slope and efficiency of the three assays PMM1 (endogenous control), TFPIα and TFPIβ.

Assay	Slope	Δ Slope*	Efficiency
PMM1	-3.39	-	97.2%
TFPIα	-3.46	0,07	94.5%
TFPIβ	-3.37	0,02	98,0%

*Δ Slope were calculated by subtracting the slope value for the target assay from the slope value for the endogenous control

4.1.2 Assay specificity

The specificity of the assays used in this thesis was validated by analyzing cDNA from a TFPIβ upregulated cell sample on the TFPIα assay, and cDNA from a TFPIα upregulated cell sample using the TFPIβ assay. No overexpression was detected when the TFPIβ upregulated cDNA sample was analyzed using the TFPIα assay (Figure 4.2A), or when the TFPIα upregulated cDNA sample was analyzed using the TFPIβ assay (Figure 4.2B). This demonstrated that the TFPIα assay and the TFPIβ assay were specific and could therefore be used in further experiments.

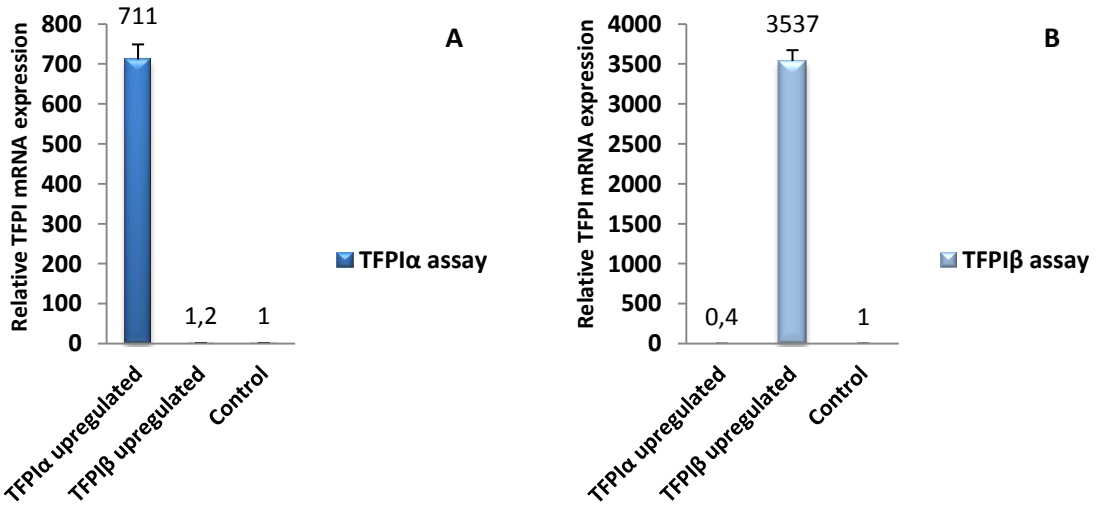

Figure 4.2: Specificity for the qRT-PCR assays. Relative TFPI mRNA expression was measured in TFPIα and TFPIβ upregulated MDA-MB-231 cells and analyzed using qRT-PCR with A) TFPIα assay and B) TFPIβ assay. Cells transfected with Negative siRNA#5 served as control and were set to 1.0. Normalized mean values (n = 2 biological parallels run in triplicates) + SD of one independent qRT-PCR measurement are presented.

4.2 TFPIα and TFPIβ knockdown with siRNA oligonucleotides

4.2.1 Selection of siRNA oligonucleotides against TFPI

siRNA oligonucleotides that could exclusively knock down the TFPIα isoform were found by comparing the TFPIα and TFPIβ mRNA sequences to locate the region specific for TFPIα. TFPIα differ from TFPIβ from nucleotide 628 (counted from start codon), so siRNA complementary to a region from that position, will theoretically knock down TFPIα, and not TFPIβ. Eurofins MWG Operon provided a program for self-design of siRNAs. The accession number for TFPIα (NM_006287.4) and the TFPIα specific region were fed to the program. Eurofins algorithm (unknown to users) came up with five alternative siRNAs, of which we ordered the four siRNAs with the highest score. The siRNAs were ordered as 27mers, since 27mer siRNAs have previously proven more efficient than the until now standard 21mer siRNAs (Kim *et al.* 2005). Two siRNAs against TFPIα (siRNA α1 and siRNA α2) were already in house. The new 27mer siRNAs were called siRNA α3 – α6. In house siRNAs that target TFPIβ (siRNA β7 and siRNA β9) were already optimized by the research group. The siRNA sequences and TFPI mRNA target positions are listed in Table 2.2 under Materials. For all the transfection experiments performed with siRNAs in this thesis, Silencer ® Negative Control siRNA#5 served as a control. This control siRNA is an unspecific sequence which will not bind to any known sequences.

4.2.2 Screening of TFPIα siRNA oligonucleotides in HEK293T cells

The selected siRNAs against TFPIα (α1 – α6) were screened in HEK293T cells. siRNA α3, α5, and α6 showed the most efficient TFPIα knockdown; 76%, 65% and 80% respectively (Figure 4.3), and were therefore selected to use in further experiments. Relative TFPIβ mRNA expression was also measured to verify that the TFPIα siRNA candidates were isoform specific. Except for siRNA α4 that showed a small effect on TFPIβ mRNA expression (24% knockdown), no other siRNAs had any effect on the TFPIβ mRNA expression (Figure 4.3).

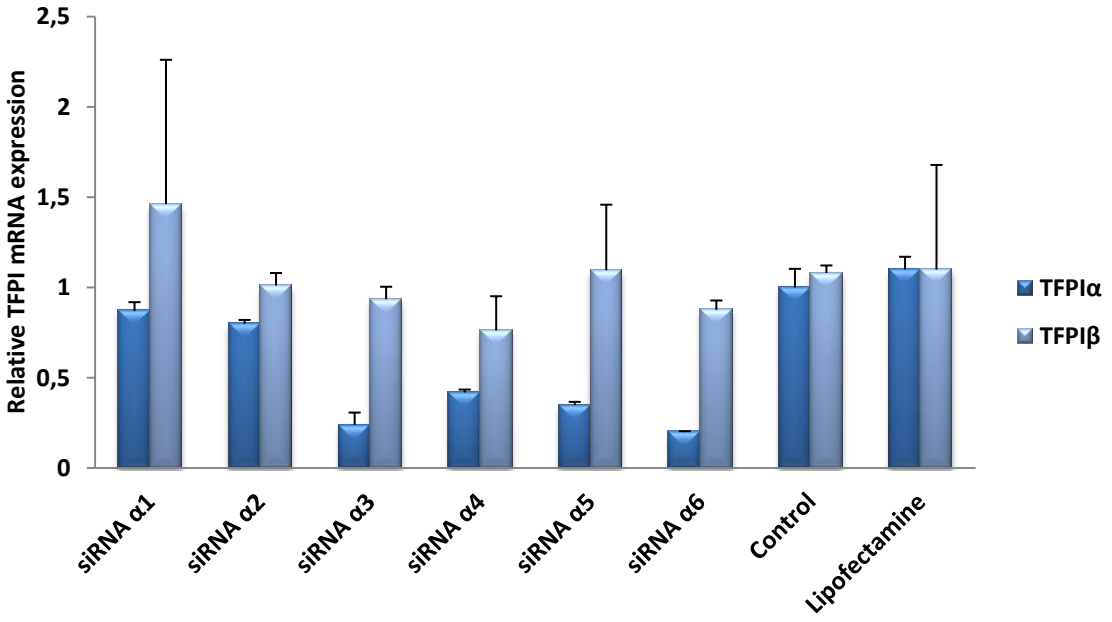

Figure 4.3: Screening of TFPIα siRNA oligonucleotides in HEK293T cells. Relative TFPI mRNA expression measured in HEK293T cells transfected with TFPIα specific siRNAs (siRNA α1- α6) using qRT-PCR. The cells were harvested 24 hours after transfection. Cells transfected with Negative siRNA#5 served as control and were set to 1.0. Normalized mean values (n = 2 biological parallels run in triplicates) + SD of one independent qRT-PCR measurement are presented.

4.2.3 Optimization of TFPIα knockdown in MDA-MB-231 cells

The siRNAs with the most efficient TFPIα knockdown from the screening experiment in HEK293T cells (siRNA α3, α5, and α6) were used to optimize the TFPIα knockdown in the MDA-MB-231 breast cancer cells. Different siRNA concentrations, Lipofectamine volumes and siRNA:Lipofectamine ratios were tested. A dose-response effect was observed when both the different siRNA concentrations and Lipofectamine volumes was tested in MDA-MB-231 cells (data not known). When two different siRNA:Lipofectamine ratios (10:1 and 20:1) were tested using siRNA α6, it was the 10:1 ratio that showed the highest knockdown efficiency (80%), compared to a knockdown of 50% for the 20:1 ratio (Figure 4.4). Based on these measurements it was the 10:1 ratio using 75 pmol siRNA and 7.5 µl Lipofectamine that was chosen for further experiments.

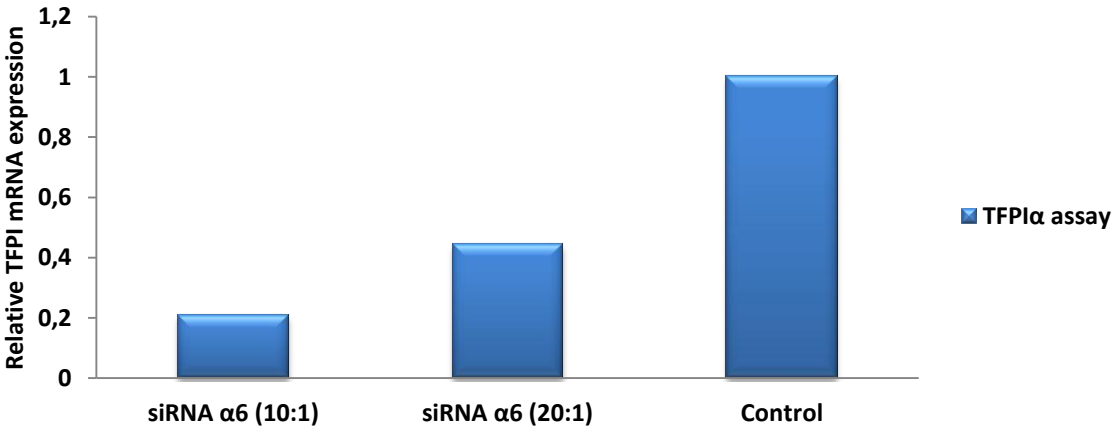

Figure 4.4: Optimization of different siRNA:Lipofectamine ratios in MDA-MB-231 cells. Relative TFPI mRNA expression in MDA-MB-231 cells transfected with two different siRNA:Lipofectamine ratios (the 10:1 ratio: 75 pmol siRNA: 7,5µl Lipofectamine, and the 20:1 ratio: 100pmol siRNA: 5µl Lipofectamine). Normalized values (n = 1 biological sample run in triplicates) of one independent qRT-PCR measurement are presented.

4.2.4 Time dependent TFPIα and TFPIβ knockdown in MDA-MB-231 cells

TFPI mRNA expression

TFPIα and TFPIβ mRNA expression in TFPIα and TFPIβ downregulated cells was measured at five different time points after transfection to find the time point with the highest knockdown efficiency. Cells transfected with siRNA α3 or siRNA α5 showed a TFPIα knockdown of 70-80% after 24 hours and the knockdown remained stable up to 120 hours (Figure 4.5). There were only small differences in knockdown efficiency between the different time points, but it was at 96 hours after transfection the highest knockdown efficiency for both siRNA α3 and siRNA α5 was measured.

The MDA-MB-231 cells were in addition transfected with siRNAs that target the TFPIβ isoform (Figure 4.6). Cells transfected with siRNA β7 and β9 resulted in a knockdown of 60-80% from 24 to 120 hours. The highest knockdown efficiency using siRNA β7 or β9 was measured at 24 and 72 hours after transfection, respectively.

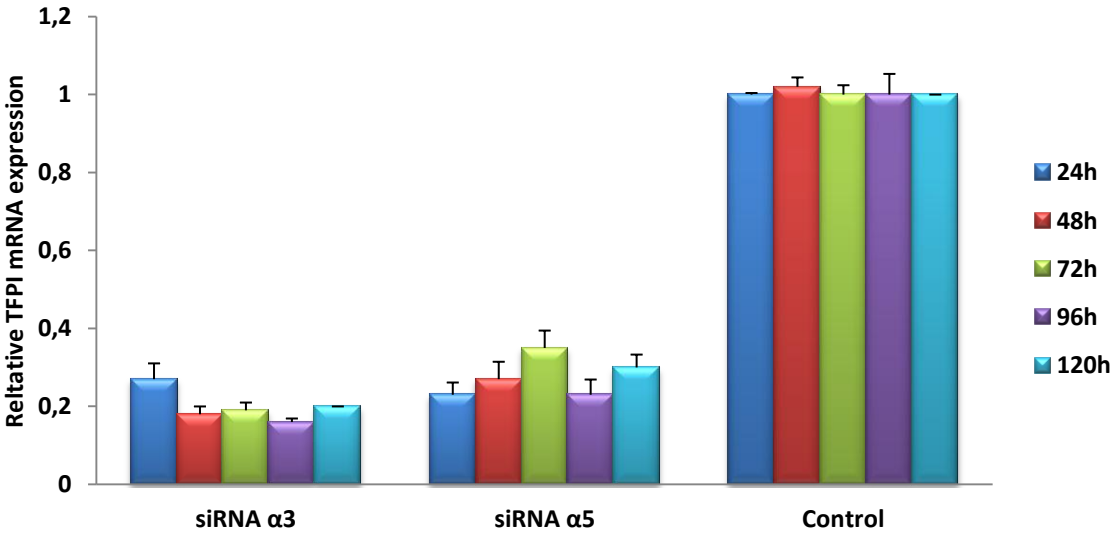

Figure 4.5: Time dependent TFPIα mRNA expression in downregulated MDA-MB-231 cells. Relative TFPIα mRNA expression was measured in MDA-MB-231 cells transfected with siRNA α3 and siRNA α5 that target TFPIα and analyzed using quantitative qRT-PCR. Normalized mean values (n = 2 biological parallels run in triplicates) + SD of one independent qRT-PCR measurement are presented.

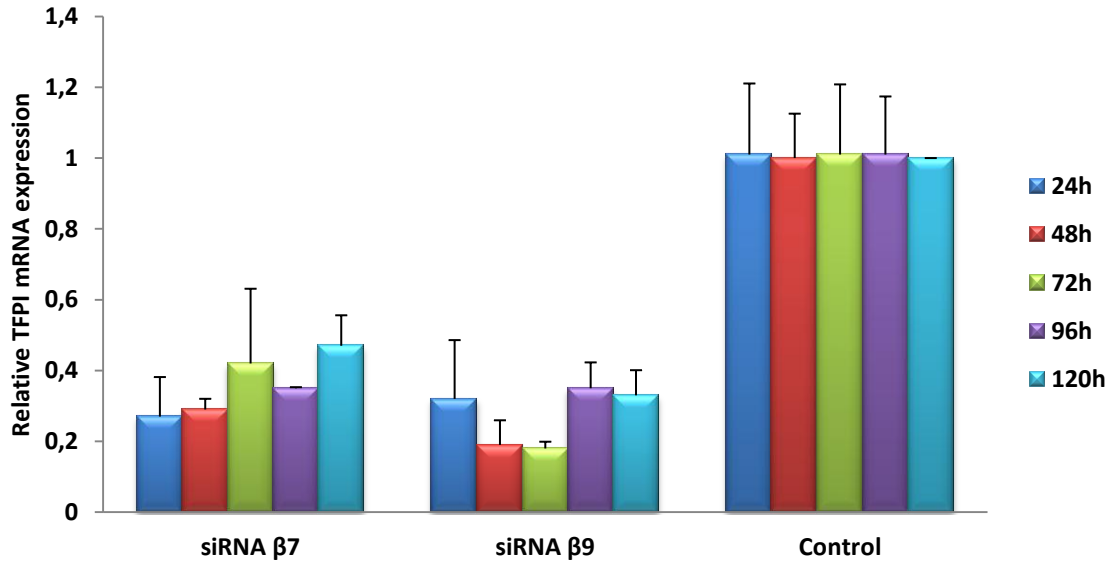

Figure 4.6: Time dependent TFPIβ mRNA expression in downregulated MDA-MB-231 cells. Relative TFPIβ mRNA expression was measured in MDA-MB-231 cells transfected with siRNA β7 and siRNA β9 that target TFPIβ and analyzed using qRT-PCR. Normalized mean values (n = 2 biological parallels run in triplicates) + SD of one independent qRT-PCR measurement are presented.

Total TFPI protein quantification

The total TFPI protein levels in cell media and lysates were measured in TFPIα and TFPIβ downregulated MDA-MB-231 cells using an enzyme-linked immunosorbent assay (ELISA). TFPIα protein levels were measured in medium since this isoform is released to the extracellular environment, while both isoforms may be detected in the cell lysate. The downregulation of TFPIα showed no effect before after 48 hours when a 2-fold decrease in total TFPI protein was measured for both siRNA α3 and siRNA α5 compared to the control (Figure 4.7). From 48 hours and up to 120 hours a gradually decrease in total TFPI protein was measured. The downregulation effect was greatest after 96 hours where a 6.8- and 3.9-fold decrease in total TFPI protein compared to control cells was measured for both siRNA α3 and siRNA α5. There was no change in TFPI protein levels in the cell media of TFPIβ downregulated cells, as expected (data not shown).

The downregulation of TFPIβ showed no effect after 24 or 48 hours when total TFPI protein was measured in lysate from cells transfected with siRNA β7, but a 1.4-fold decrease was observed in cells transfected with siRNA β9 after 48 hours (Figure 4.8). After 72 hours and up to 120 hours, a gradually decrease of total TFPI protein compared to the control was measured, except for the measurement at 96 hours. The greatest difference in TFPI levels was observed after 120 hours, where a 2.2-fold and 1.7-fold decrease in total TFPI protein compared to the control was measured. When total TFPI was measured in lysate from cells transfected with siRNA α3, a 3-fold decrease was observed after 96 hours (data not shown).

Since siRNA α3 seemed to have a greater downregulation effect compared to siRNA α5, and siRNA β9 showed a more stable effect than siRNA β7, siRNA α3 and siRNA β9 were chosen to use in further experiments. It was also decided to perform the functional studies at 96 hours after transfection for the TFPI downregulated cells.

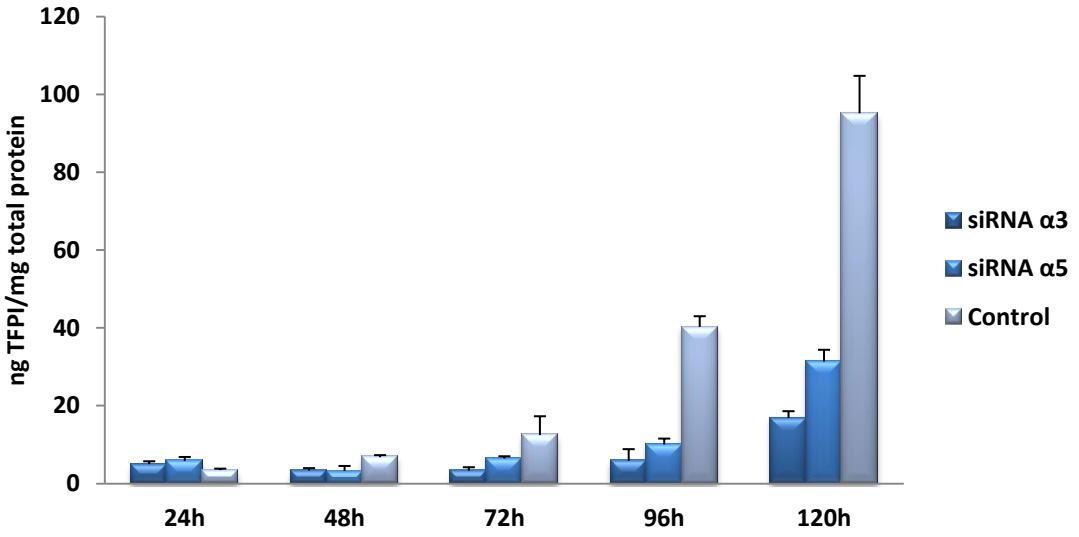

Figure 4.7: Total TFPI protein in cell medium from TFPIα downregulated MDA-MB-231 cells. Total TFPI protein was measured in cell medium from cells transfected with siRNA α5 and siRNA α3 using total TFPI ELISA kit. Cells transfected with Negative control#5 served as control. The total TFPI protein levels were corrected against cellular total protein and presented as ng TFPI/mg total protein. Mean values (n=2 biological parallels) + SD of one experiment are presented.

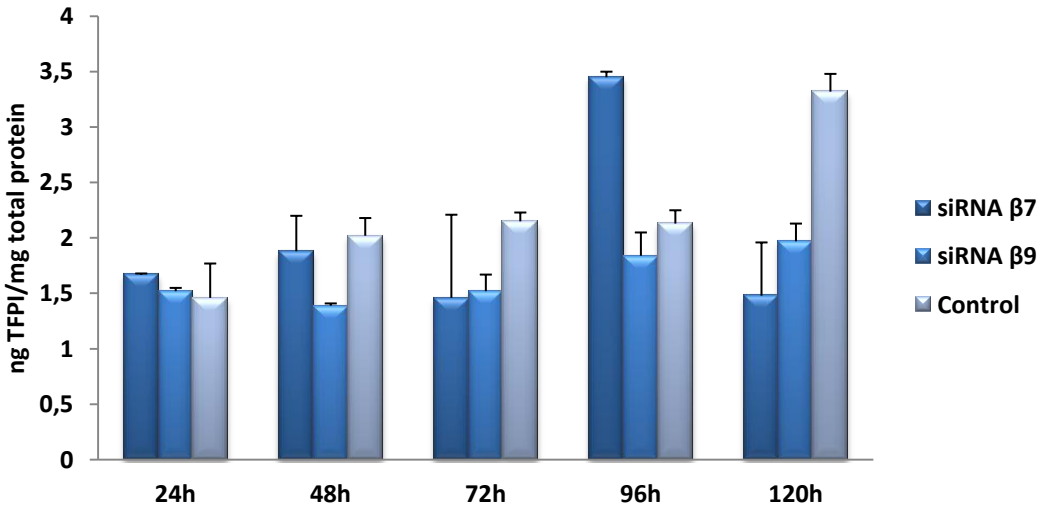

Figure 4.8: Total TFPI protein in cell lysates from TFPIβ downregulated MDA-MB-231 cells. Total TFPI protein was measured in cell lysates from cells transfected with siRNA β7 and siRNA β9 using total TFPI ELISA kit. Cells transfected with Negative control#5 served as control. The total TFPI protein levels were corrected against cellular total protein and presented as ng TFPI/mg total protein. Mean values (n=2 biological parallels) + SD of one experiment are presented.

4.3 TFPIα and TFPIβ overexpression with plasmids

4.3.1 Characterization of the TFPIα and TFPIβ plasmid

An agarose gel electrophoresis was performed to verify the presence of the TFPIα and TFPIβ cDNA inserts in the TFPIα and TFPIβ plasmids (Figure 4.9). A fragment of 956 kb was observed for the digested TFPIα plasmid, and a fragment of 846 kb for the digested TFPIβ plasmid. These fragments corresponded to the expected sizes of the cDNA inserts.

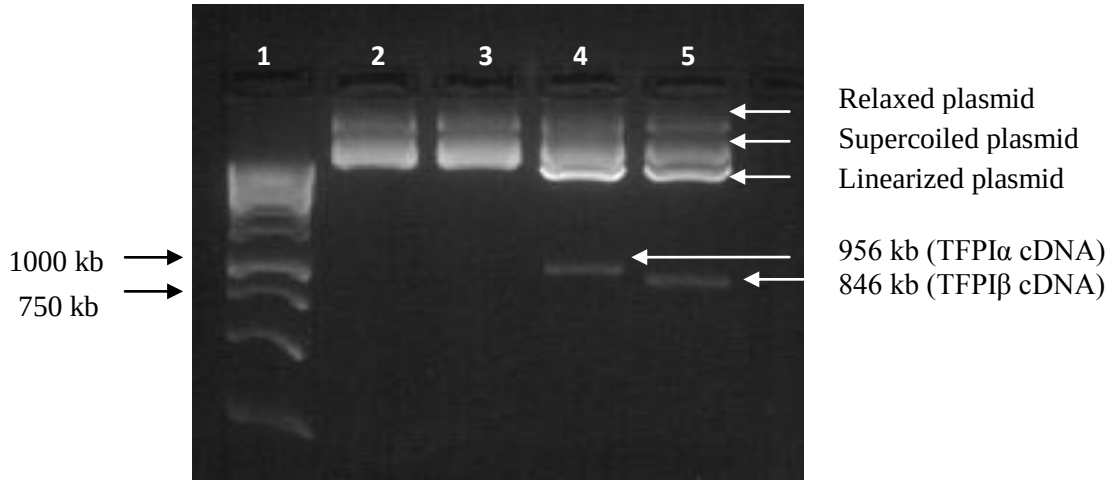

Figure 4.9: Agarose gel electrophoresis of undigested and digested TFPI plasmid. Undigested TFPIα plasmid (lane 2), undigested TFPIβ plasmid (lane 3), digested TFPIα plasmid (lane 4), digested TFPIβ plasmid (lane 5). Lane 1 = ladder.

4.3.2 Sanger sequencing of the TFPIα and TFPIβ plasmid

The isolated TFPIα and TFPIβ plasmids were also Sanger sequenced to confirm correct sequences. The sequences were aligned to the sequences in NCBI GeneBank (TFPIα: NM_006287.4, TFPIβ: NM_001032281), and no sequence dissimilarities were observed (data not shown).

4.3.3 Time dependent TFPIα and TFPIβ overexpression in MDA-MB-231 cells

TFPI mRNA expression

Relative TFPI mRNA expression was measured in MDA-MB-231 cells transfected with TFPIα and TFPIβ plasmid at four different time points after transfection to observe the overexpression over time, and to find the optimal time point to conduct functional experiments. After only 6 hours, a 600-fold relative increase in TFPIα mRNA expression was

observed as compared to control. At 24 hours, the overexpression reached its maximum with a 700-fold increased TFPIα mRNA expression (Figure 4.10). From 48 hours the TFPIα mRNA expression decreased. Cells transfected with the TFPIβ plasmid showed the highest overexpression after 6 hours (4436-fold increase), which thereafter decreased to 3265-fold at 72 hours (Figure 4.11).

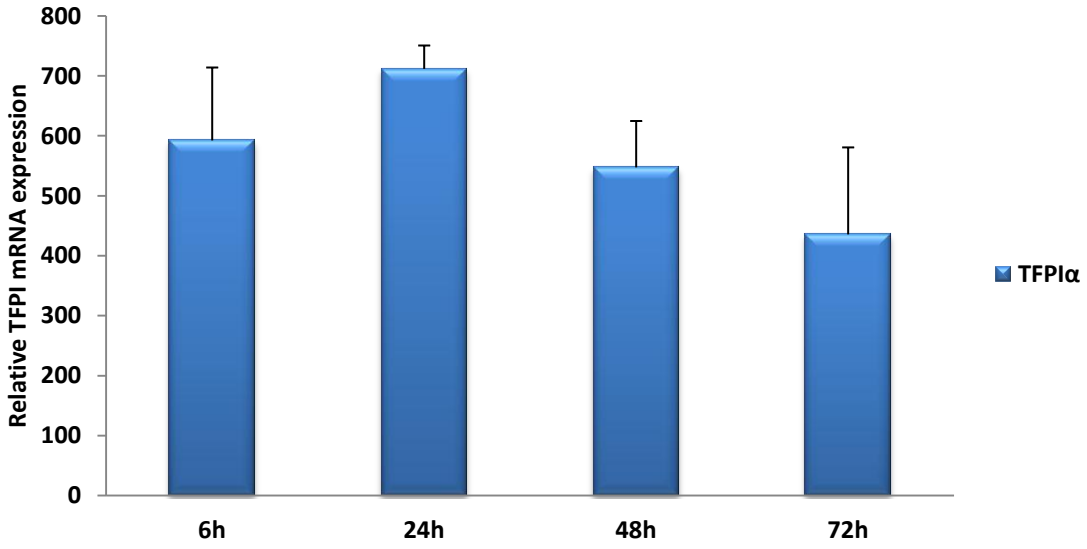

Figure 4.10: Relative TFPIα mRNA expression in TFPIα upregulated MDA-MB-231 cells. TFPIα mRNA expression in TFPIα upregulated MDA-MB-231 cells relative to TFPIα mRNA expression in cells transfected with empty vector, which was set to 1.0. Normalized mean values (n=2 biological parallels run in triplicate) + SD from one experiment are presented.

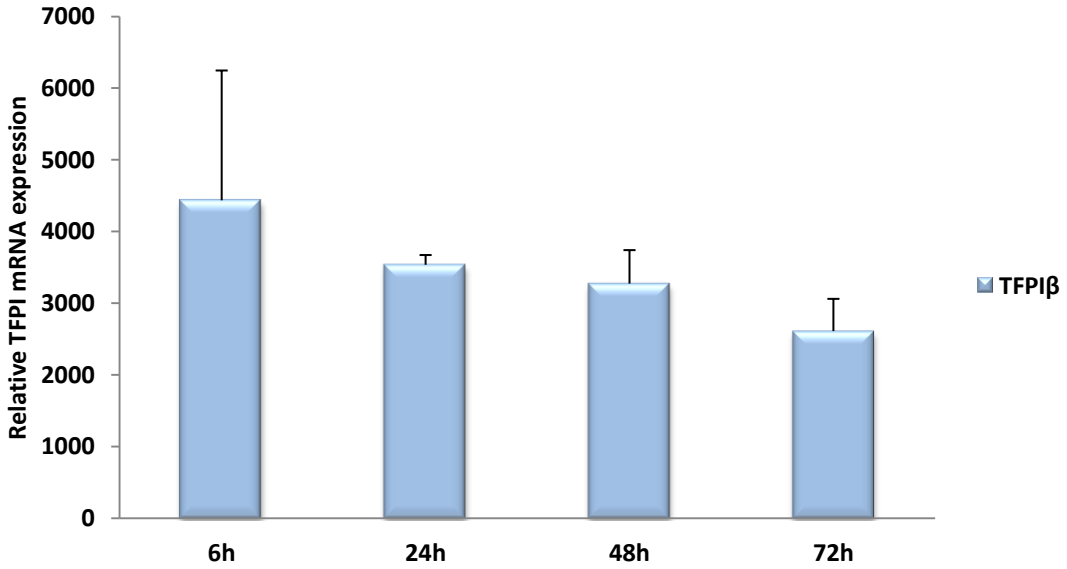

Figure 4.11: Relative TFPIβ mRNA expression in TFPIβ upregulated MDA-MB-231 cells. TFPIβ mRNA expression in TFPIβ upregulated MDA-MB-231 cells relative to TFPIβ mRNA expression in cells transfected with empty vector, which was set to 1.0. Normalized mean values (n=2 biological parallels run in triplicate) + SD from one experiment are presented.

Total TFPI protein quantification

Levels of total TFPI protein in cell media and lysates were measured in TFPIα and TFPIβ upregulated MDA-MB-231 cells using total TFPI ELISA. Total TFPI in cell medium from cells transfected with the TFPIα plasmid, measured after 72 hours, showed a 53-fold increase in total TFPI compared to the control (Figure 4.12A). Total TFPI in lysate from cells transfected with the TFPIβ plasmid were measured 24, 48 and 72 hours after transfection (Figure 4.12B) After 24 hours, a 33-fold increase in total TFPI compared to the control was measured, and after 48 and 72 hours, an 106-fold and 25-fold increase was observed, respectively.

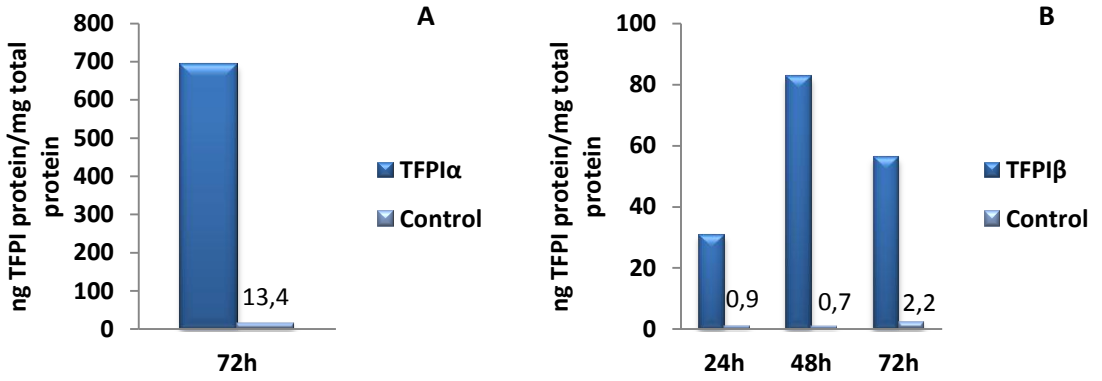

Figure 4.12: Total TFPI protein in medium and cell lysates from TFPIα and TFPIβ upregulated MDA-MB-231 cells. Total TFPI protein was measured in A) medium from TFPIα upregulated cells and in B) lysates from TFPIβ upregulated cells using total TFPI ELISA kit. Empty vector served as control. The total TFPI protein levels were corrected against cellular total protein and presented as ng TFPI/mg total protein. Values (n=1) from one experiment are presented.

4.3.4 Time dependent TFPIα and TFPIβ overexpression in MDA-MB-436 cells

Relative mRNA expression was measured at three different time points after transfection in TFPIα and TFPIβ upregulated MDA-MB-436 cells (Figure 4.13). Cells transfected with TFPIα plasmid showed a 111-fold relative increase in mRNA expression after 24 hours, and after 48 and 72 hours a 225- and 238-fold increase, respectively, was observed (Figure 4.13A). For cells transfected with TFPIβ plasmid, a 22 196-fold relative increase in TFPIβ mRNA expression compared to the control was measured after 24 hours, while at 48 and 72 hours the mRNA expression was somehow lower (10 518- and 8268-fold increased, respectively) (Figure 4.13B).

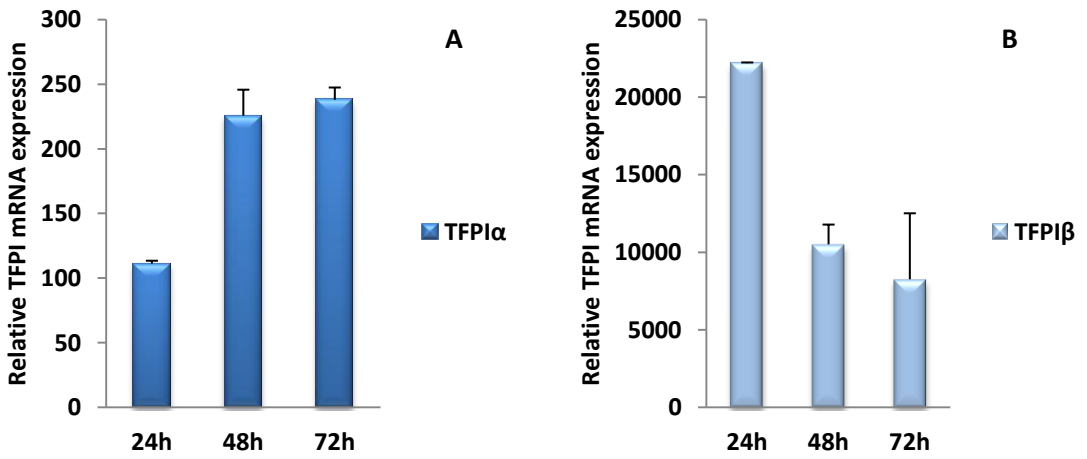

Figure 4.13: Relative TFPI mRNA expression in TFPIα and TFPIβ upregulated MDA-MB-436 cells. A) TFPIα mRNA expression in TFPIα upregulated MDA-MB-436 cells and B) TFPIβ mRNA expression in TFPIβ upregulated MDA-MB-436 cells relative to TFPIα or TFPIβ mRNA expression in cells transfected with empty vector, which was set to 1.0. Normalized mean values (n=2 biological parallels run in triplicate) + SD from one experiment are presented.

4.3.5 Stable cell lines with TFPIα and TFPIβ upregulated in MDA-MB-436 cells

Stable cell lines with TFPIα and TFPIβ upregulated were created in MDA-MB-436 cells. The TFPI overexpression was verified in the cells both at the mRNA and the protein level. A 65-fold increase in TFPIα mRNA expression (Figure 4.14A), and a 3.5-fold increase in total TFPI protein, compared to the control, was measured in the stable cell lines with TFPIα upregulated (Figure 4.14B). For the stable cell lines with TFPIβ upregulated, a 190-fold increase in TFPIβ mRNA expression (Figure 4.14C), and a 5.8-fold increase in total TFPI protein levels compared to the control was measured (Figure 4.14D).

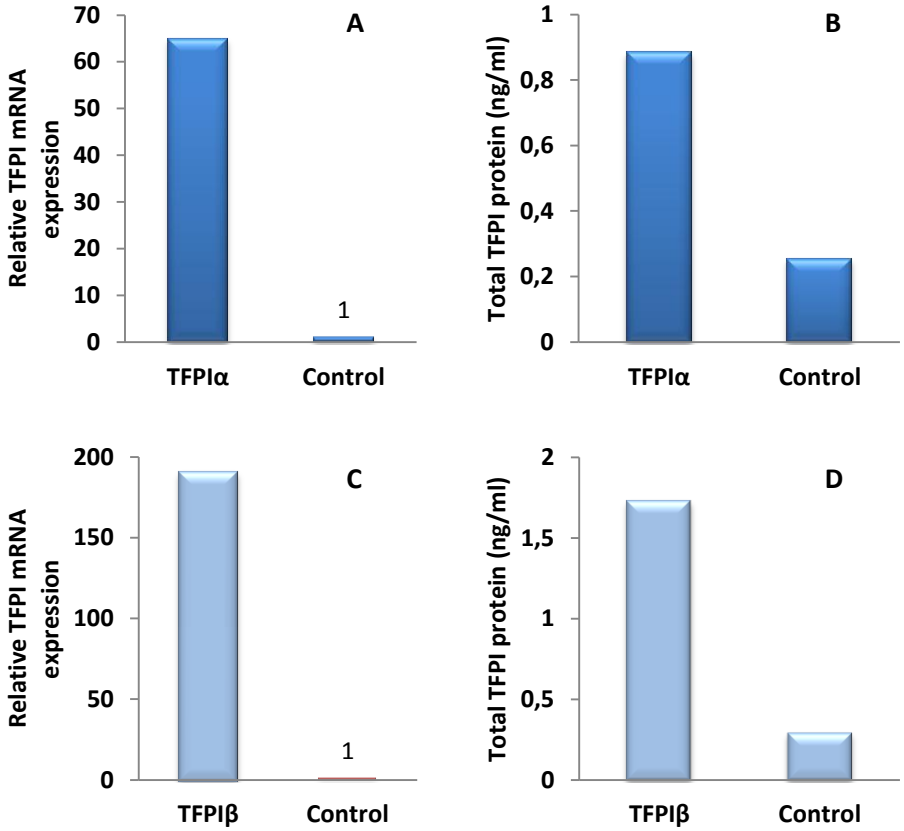

Figure 4.14: Relative mRNA expression and total TFPI protein in stable cell lines with TFPIα and TFPIβ upregulated. Relative TFPI mRNA expression and total TFPI levels were measured in stable cell lines with TFPIα and TFPIβ upregulated using qRT-PCR and total TFPI ELISA kit, respectively. Cells transfected with empty vector served as control. A) Relative mRNA expression in stable cell lines with TFPIα upregulated B) Total TFPI protein levels in stable cell lines with TFPIα upregulated C) Relative mRNA expression in stable cell lines with TFPIβ upregulated D) Total TFPI protein levels in stable cell lines with TFPIβ upregulated. Values (n=1) from one experiment are presented.

4.4 Functional studies

4.4.1 Effect of TFPI isoforms on growth

Total protein quantification of TFPIα and TFPIβ downregulated cells

To evaluate the TFPI isoforms effect on growth, total protein was measured in cell lysate from TFPIα and TFPIβ downregulated MDA-MB-231 cells at four different time points after transfection (Figure 4.15). The result indicated that both the TFPIα and TFPIβ downregulated cells grew slower than the control cells since lower total protein levels was measured in the TFPI downregulated cells compared to the control cells. However, a significant difference in total protein levels was only observed for TFPIα downregulated cells at 48 and 72 hours ($P<0.05$), and for TFPIβ downregulated cells after 72 hours ($P<0.05$).

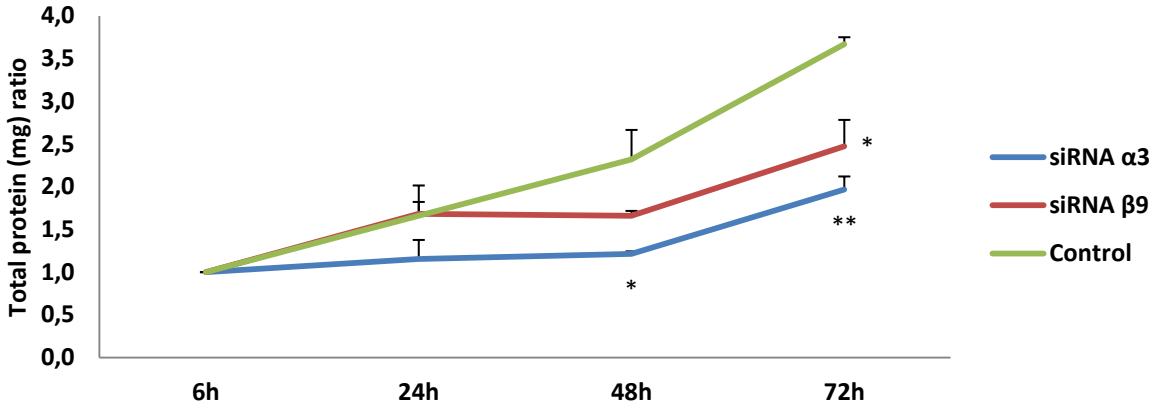

Figure 4.15: Total protein quantification of TFPI downregulated MDA-MB-231 cells. Total protein in cell lysates from cells downregulated with siRNA α3 and β9 harvested after 6, 24, 48 and 72 hours were measured by Pierce ® BCA Protein Assay Kit. Mean values (n=2 biological parallels run in triplicates) + SD of one experiment are presented.

Cell counting of TFPIα and TFPIβ downregulated cells

The effect of TFPI isoforms on growth were also determined by counting living cells at four different time points after transfection (Figure 4.16). MDA-MB-231 cells transfected with siRNA α3 and β9 showed the same growth pattern as for the control cells up to approximately 48 hours after transfection. After 72 hours, a slightly lower number of cells were counted for the TFPIα and TFPIβ downregulated cells compared to the control cells, but the difference was not significant (*P>0.05*).

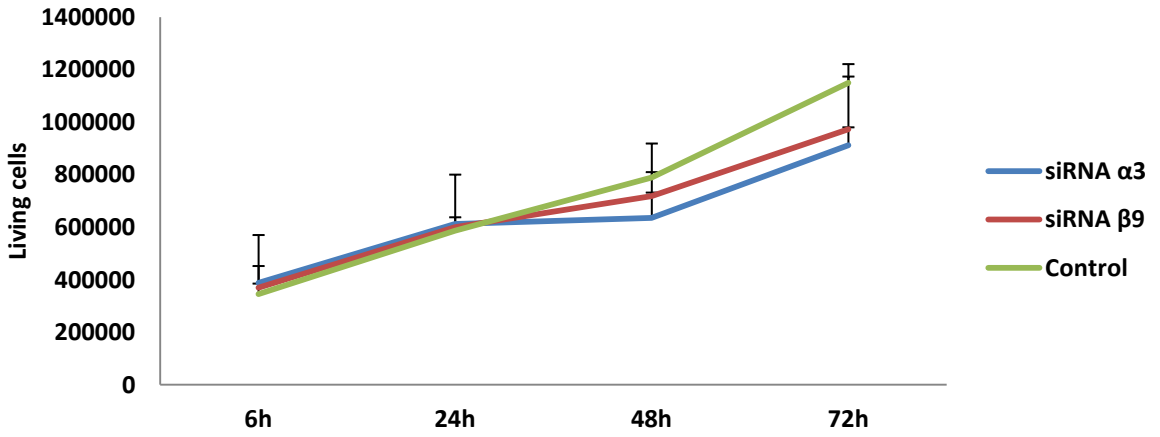

Figure 4.16: Cell counting of TFPIα and TFPIβ downregulated MDA-MB-231 cells. Living MDA-MB-231 cells with downregulated TFPIα or TFPIβ, and control cells were counted between 6-72 hours after transfection. Mean values (n=2 biological parallels counted in triplicates) + SD of one experiment are presented.

Total protein quantification of TFPIα and TFPIβ upregulated cells

Total protein in lysates from cells with TFPIα and TFPIβ upregulated was measured to evaluate the TFPI isoforms effect on growth (Figure 4.17). No growth was observed, except from a slight increase in total protein levels after 24 hours for the TFPIβ upregulated cells. There was no significant difference between TFPIα or TFPIβ downregulated cells compared to the control cells at any time point ($P > 0.05$).

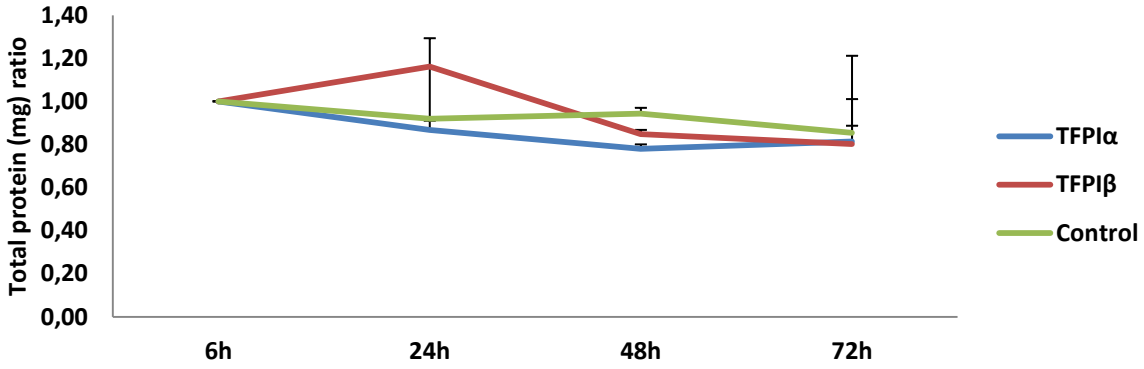

Figure 4.17: Total protein quantification of TFPIα and TFPIβ upregulated MDA-MB-231 cells. Total protein in cell lysate from cells upregulated with TFPIα and TFPIβ plasmids harvested for 72 hours were measured by Pierce ® BCA Protein Assay Kit. Mean values (n=2) + SD of one experiment are presented.

Cell counting of TFPIα and TFPIβ upregulated cells

Growth of TFPIα and TFPIβ upregulated MDA-MB-231 cells was also measured by counting cells at four different time points after transfection. As for the total protein quantification, no growth was measured between 6-72 hours, and there were no significant differences between TFPIα and TFPIβ upregulated compared to the control at any time point ($P > 0.05$) (Figure 4.17).

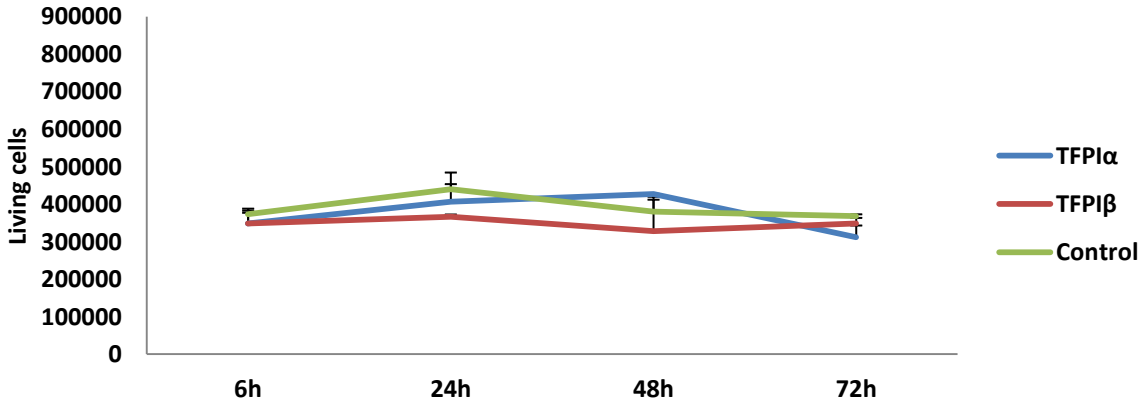

Figure 4.18: Cell counting of TFPIα and TFPIβ upregulated MDA-MB-231 cells. Living MDA-MB-231 cells with upregulated TFPIα and TFPIβ, and control cells were counted between 6-72 hours after transfection. Mean values (n=2) + SD of one experiment are presented.

4.4.2 Effect of TFPI isoforms on adhesion to collagen I

Adhesion to collagen I with TFPIα and TFPIβ up- and downregulated cells

The research group has previously observed increased adhesion to collagen I with total TFPI or TFPIβ downregulated stable cell lines (Stavik *et al.* 2011). To study the effect when only the TFPIα isoform were downregulated, experiments with adhesion to collagen I with downregulated TFPIα and TFPIβ MDA-MB-231 cells were conducted. A significant decrease of 55% and 33% in adhesion to collagen I compared to the control was observed in both TFPIα and TFPIβ downregulated cells, respectively ($P<0.05$) (Figure 4.19A). Experiments with adhesion to collagen I were also conducted with TFPIα and TFPIβ upregulated cells. Although no significant differences were observed between the TFPI upregulated cells and the control cells, a slight decrease of 20% in adhesion to collagen I was observed for TFPIα (Figure 4.19B). And in one of the three experiments conducted, a decrease of 40% was measured for the TFPIα upregulated cells (data not shown). The knockdown and overexpression in the cells was confirmed by analyzing the TFPI mRNA expression. A mean knockdown of 80% and 72% was measured in TFPIα and TFPIβ downregulated cells, while a 300- and 850-fold mean increase in TFPI mRNA expression were measured for TFPIα and TFPIβ upregulated cells, respectively (data not shown).

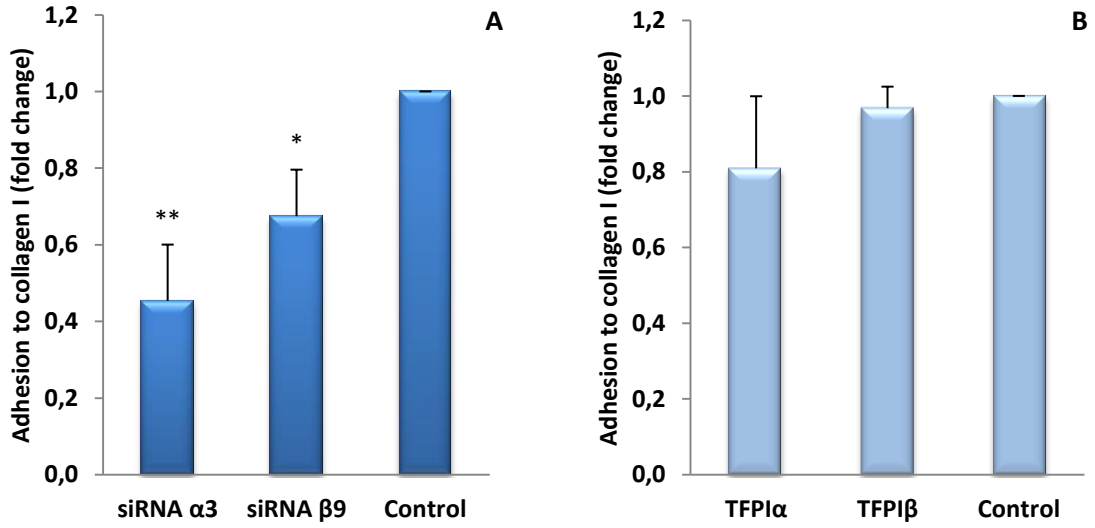

Figure 4.19: Adhesion to collagen 1 with TFPI up- or downregualted MDA-MB-231 cells. Transfected cells were seeded in collagen 1 coated 96-well trays and incubated for 10 min before the amount of attached cells were analyzed using WST-1. Mean values of fold change (n=3) + SD of three independent experiments with 6 replicates are presented. A) Cells transfected with siRNA α3 and β9, and Negative control#5 (control). The adhesion experiment was performed 96 hours after transfection. B) Cells transfected with TFPIα or TFPIβ plasmid and empty vector (control). The adhesion experiment was performed 48 hours after transfection.

Integrin α2 levels in TFPI up- and downregulated cells

Western blotting with integrin α2 were performed in lysates from both TFPIα and TFPIβ up- and downregulated cells since the research group have former experienced increased level of integrin α2 in lysate when total TFPI or TFPIβ were downregulated (Stavik *et al.* 2011). TFPIα and TFPIβ downregulated cells showed higher integrin α2 levels compared to the control (Figure 4.20A), although not statistically significant (*P>0.05*). For the TFPIα upregulated cells, a significant decrease in integrin α2 levels compared to the control were observed (*P<0.05*), while no difference in integrin α2 level was measured between the TFPIβ upregulated cells and the control cells (*P>0.05*) (Figure 4.20B).

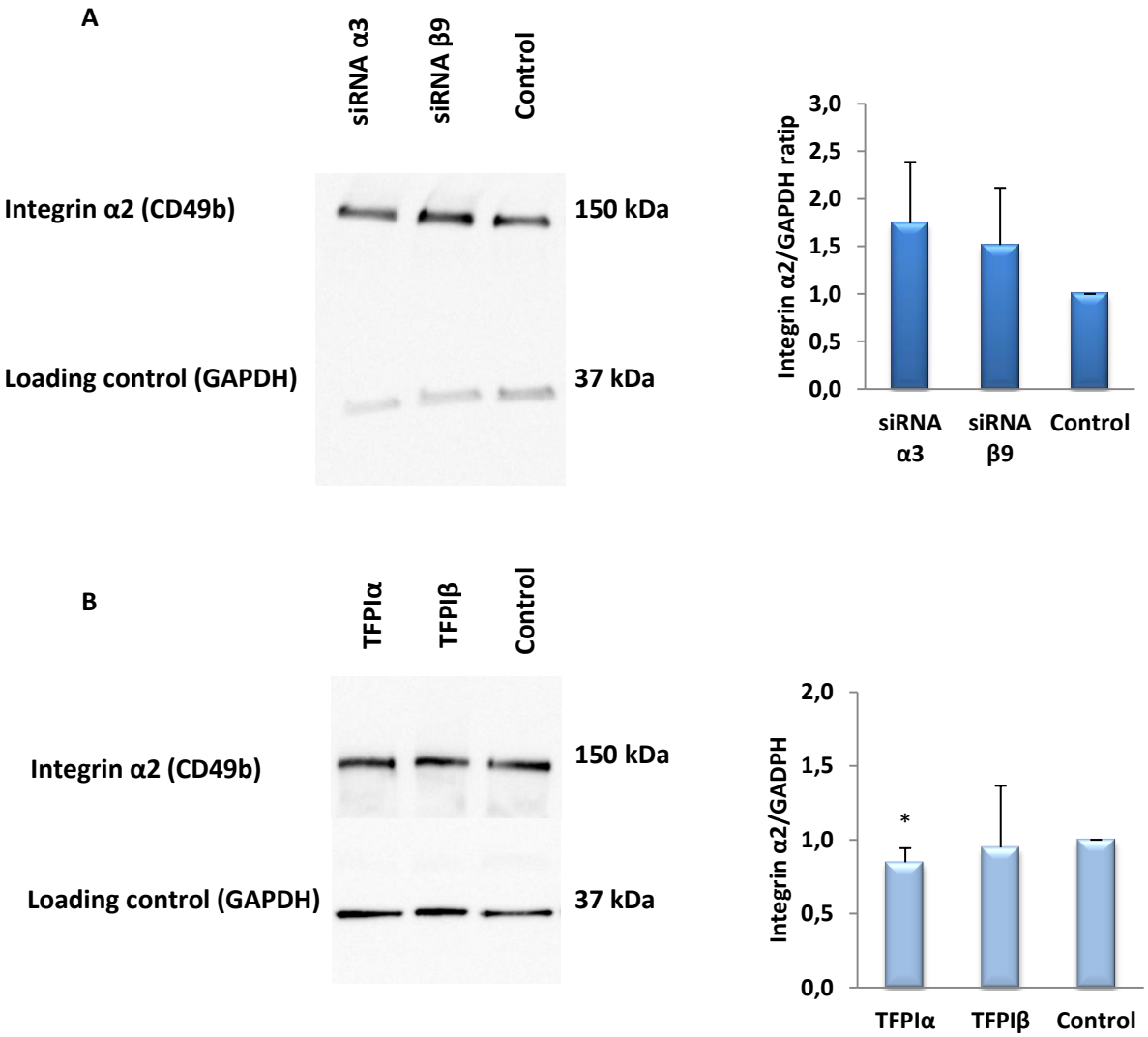

Figure 4.20: Integrin α2 levels in up- and downregulated MDA-MB-231 cells. Integrin α2 levels in A) TFPIα and TFPIβ downregulated cells and control cells shown by Western blotting (left) and in a diagram where integrin α2 levels were corrected with GADPH. B) TFPIα and TFPIβ upregulated cells and control cells shown by Western blotting (left) and in a diagram where integrin α2 levels were corrected with GADPH. Mean values (n=3) + SD of three experiments is presented in the diagram.

4.4.3 Effects of TFPI isoforms on migration

Scratch-wound assay in TFPI downregulated cells

Migration experiments were performed using a scratch-wound assay. Mean values of four experiments showed that after 6 hours were 11% and 15% of the wound closed in TFPIα and TFPIβ downregulated cells respectively, compared to 14% in the control cells (Figure 4.21). After 24 hours the wound was 63% closed in TFPIα downregulated cells, and 71% closed in TFPIβ downregulated cells, while a closure of 75% was observed for the control cells. The four experiments showed that there were no significant difference in migration of TFPIα or TFPIβ downregulated cells compared to the control cells after 6 or 24 hours (*P>0.05*) (Figure 4.22). The downregulation of TFPIα and TFPIβ was confirmed by analyzing the mRNA expression, and a knockdown of 76% and 66% was observed for TFPIα and TFPIβ downregulated cells, respectively (data not shown).

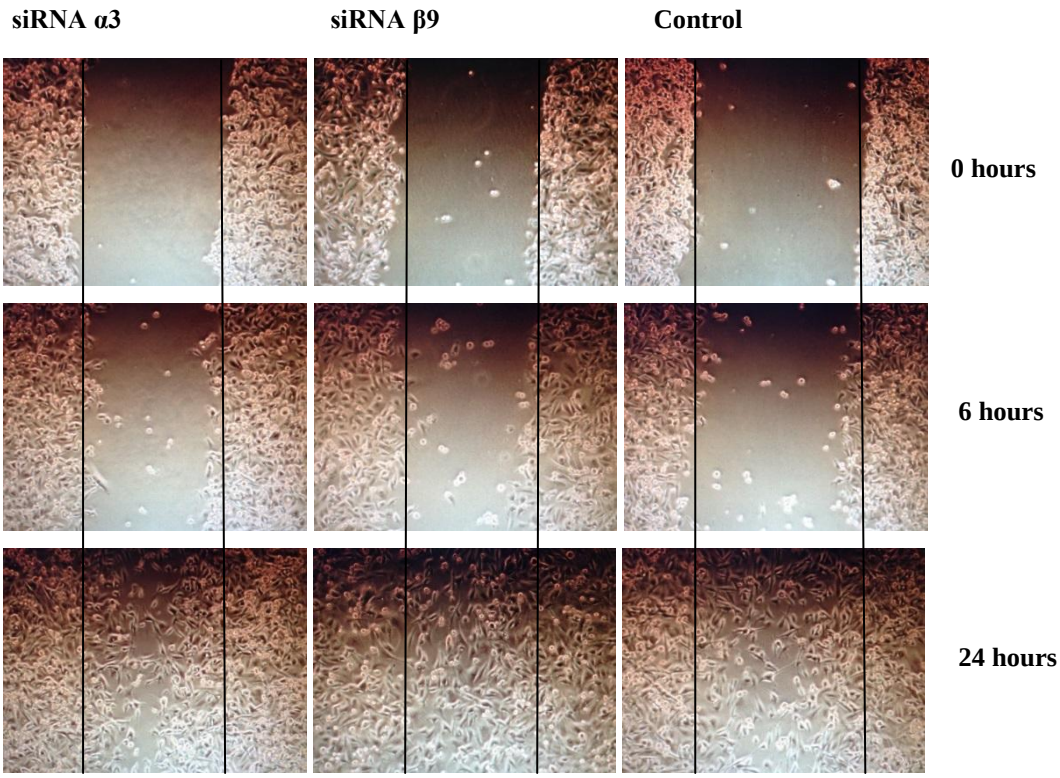

Figure 4.21: Scratch-wound assay in TFPIα or TFPIβ downregulated MDA-MB-231 cells. Scratch-wound migration of TFPIα and TFPIβ downregulated cells, and control cells. Cells were transfected with siRNA α3 that target TFPIα, siRNA β9 that target TFPIβ and cells transfected with Negative control#5 served a control. At 80-90% cell confluence a wound was made. Images were taken after 0, 6 and 24 hours. One representative experiment of four is presented.

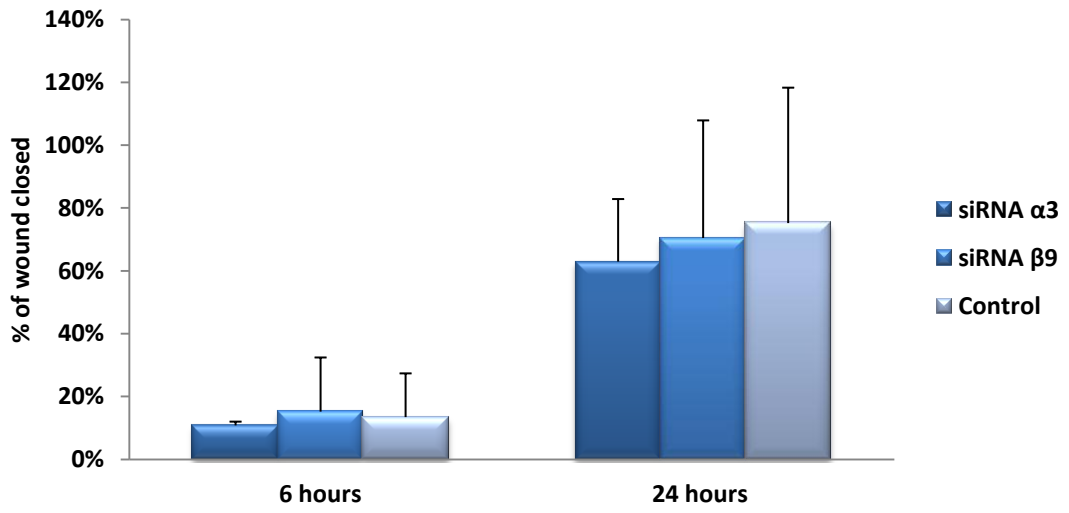

Figure 4.22: Closure (%) from scratch-wound assays performed with TFPI downregulated cells. Four scratch wound assays were performed, the width of the wound was measured manually and mean and SD was calculated and plotted in a diagram.

Scratch-wound assay in TFPI upregulated cells

The scratch wound assay was also performed with TFPIα and TFPIβ upregulated cells. Mean values from four experiments showed a 22% and 16% wound closure for TFPIα and TFPIβ upregulated cells after 24 hours, compared to 34% in the control cells. After 48 hours, a closure of 44% and 50% were observed for TFPIα and TFPIβ upregulated cells, respectively, compared to 80% closure in the control cells, which is a 30-36% reduction in migration for the TFPIα and TFPIβ upregulated cell compared to the migration in the control cells (Figure 4.23). The difference in migration measured between the TFPIα upregulated cells and the control cells after 48 hours was significant ($P<0.05$), and for the TFPIβ upregulated cell, the difference was borderline significant (Figure 4.23). The upregulation of TFPIα and TFPIβ was confirmed by analyzing the mRNA expression, a 600-fold and 400-fold increase was measured for TFPIα and TFPIβ upregulated cells, respectively (data not shown).

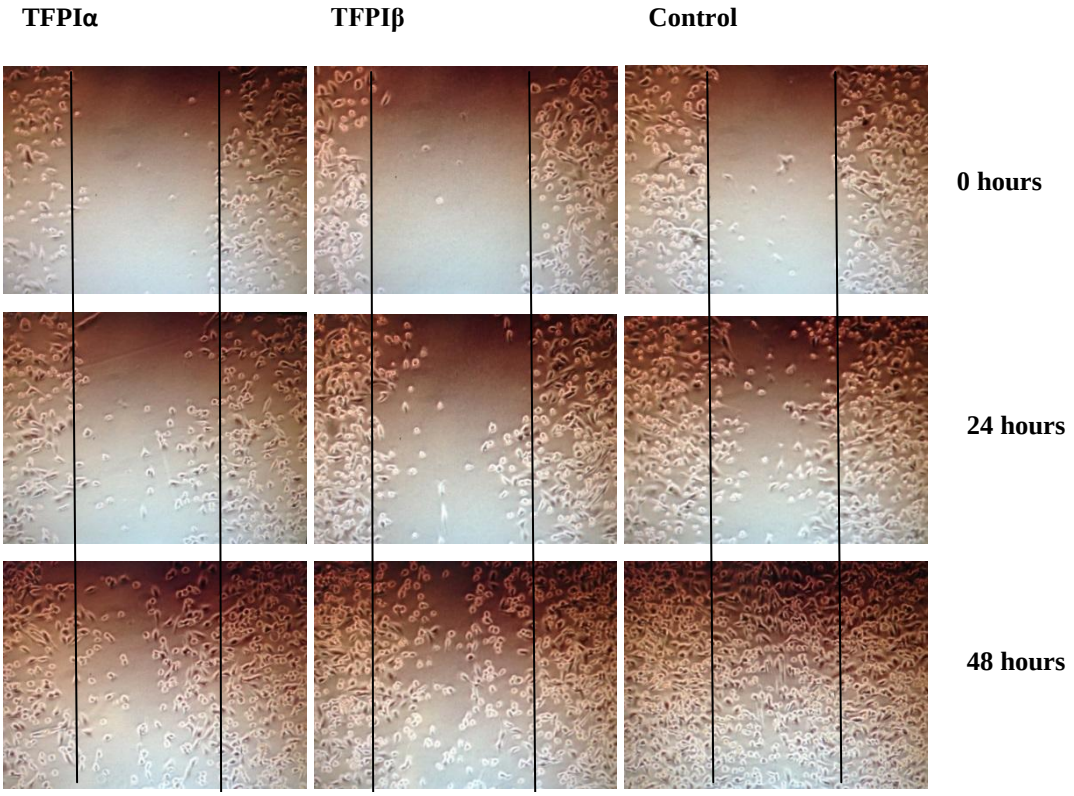

Figure 4.23: Scratch-wound assay with TFPI upregulated MDA-MB-231 cells. Scratch-wound migration of TFPIα and TFPIβ upregulated cells, and control cells. Cells were transfected with TFPIα plasmid, TFPIβ plasmid and empty vector served as control, and at 80-90% cell confluence a wound was made. Images were taken after 0, 24 and 48 hours. One representative experiment of four is presented.

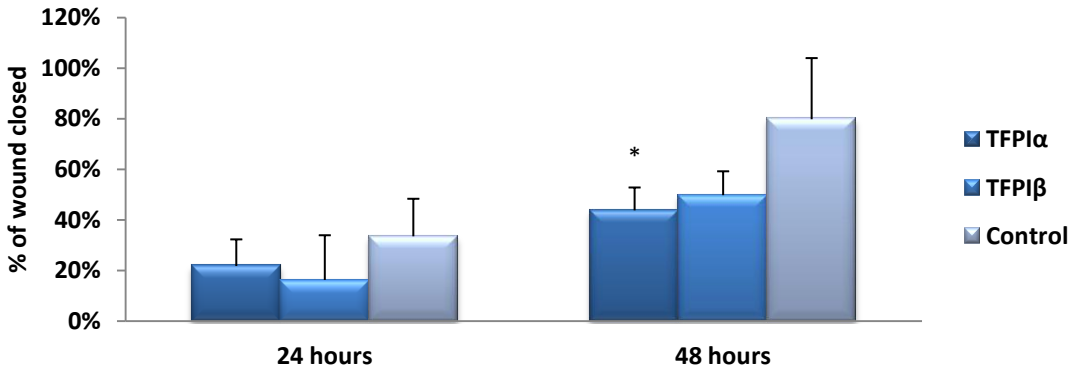

Figure 4.24: Closure (%) from scratch-wound assays performed with TFPI upregulated cells. Four scratch wound assays were performed, the width of the wound was measured manually and average and SD was calculated and plotted in a diagram.

Scratch-wound assay in TFPIα or TFPIβ upregulated cells with Src inhibitor

To evaluate a possible involvement of Src in TFPI's effect on cell migration, a Src inhibitor was incubated with the TFPIα or the TFPIβ upregulated cells and the control cells 30 min before the wound was made. After 24 hours there was no difference between the cells incubated with the Src inhibitor and the control cells (Figure 4.25). After 48 hours the wound

made in the TFPIα upregulated control cells was slightly more closed than for the cells incubated with Src inhibitor, while the opposite was observed for the TFPIβ upregulated cells.

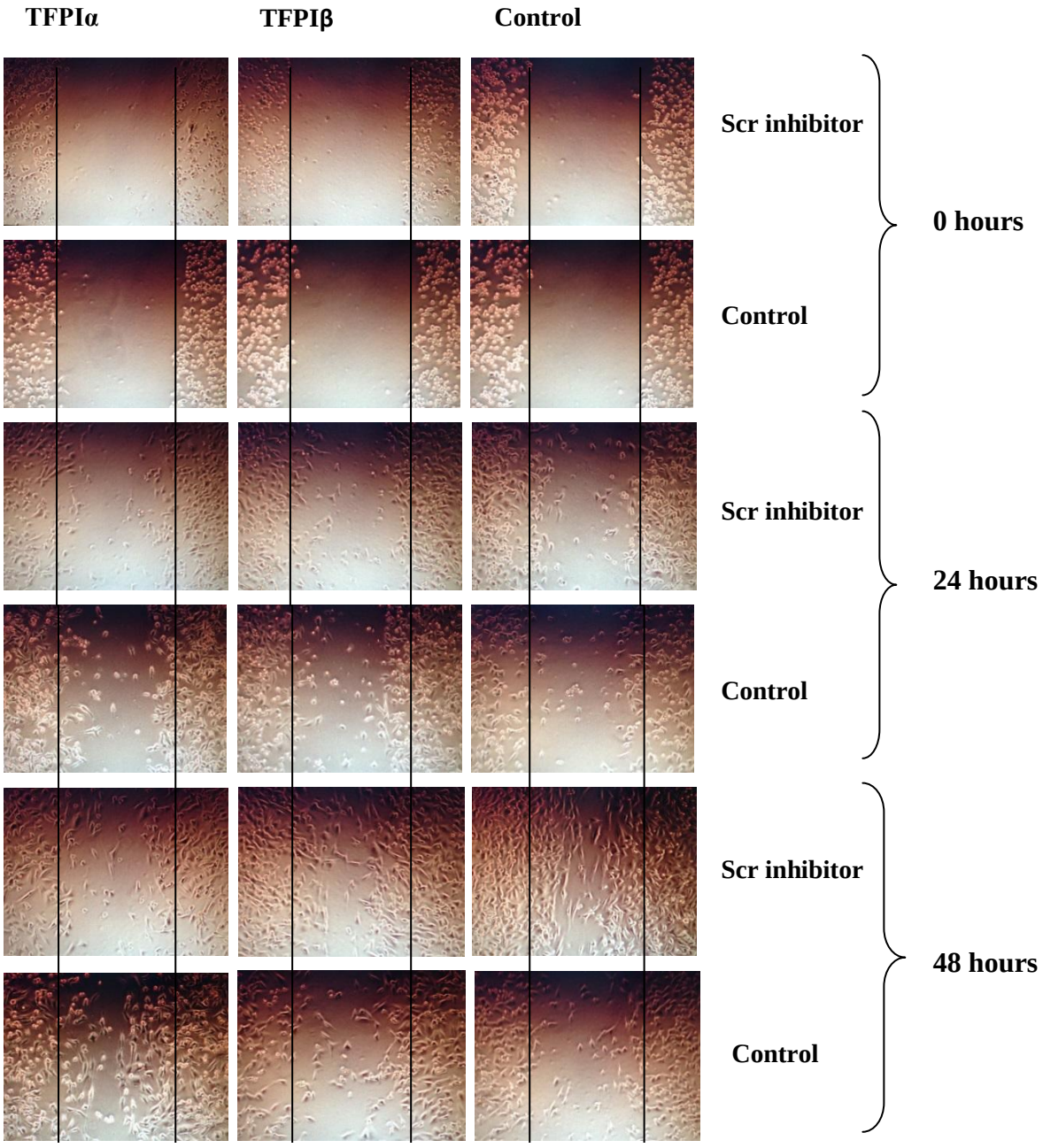

Figure 4.25 Scratch-wound assay in TFPIα and TFPIβ upregulated cells with Src inhibitor. MDA-MB-231 cells were transfected with TFPIα plasmid, TFPIβ plasmid or empty vector (control). Src inhibitor (5 μM) was incubated with the TFPIα and TFPIβ upregulated cells and control cells for 30 min before the wound was made. Cells incubated with DMSO served as a control. Images were taken after 0, 24 and 48 hours after the wound was made.

4.4.4 Levels of p-Src in cell lysates from TFPIα and TFPIβ upregulated cells

Levels of phosphorylated Src (p-Src) in cell lysates from TFPIα and TFPIβ upregulated cells after 0, 5, and 10 min of serum stimulation, were measured by Western blotting. At start there were no differences between the TFPIα and TFPIβ upregulated cells compared to the control cells (Figure 4.26). After 5 min and 10 min, both the TFPIα and the TFPIβ upregulated cells showed decreased the p-Src levels compared to the control cells. The decrease in p-Src levels was greatest after 10 min for TFPIα (30%), while for TFPIβ upregulated cells the decrease was greatest after 5 min (35%). Over all, after serum stimulation the levels of p-Src were lower in the TFPI upregulated cells compared to the control cells.

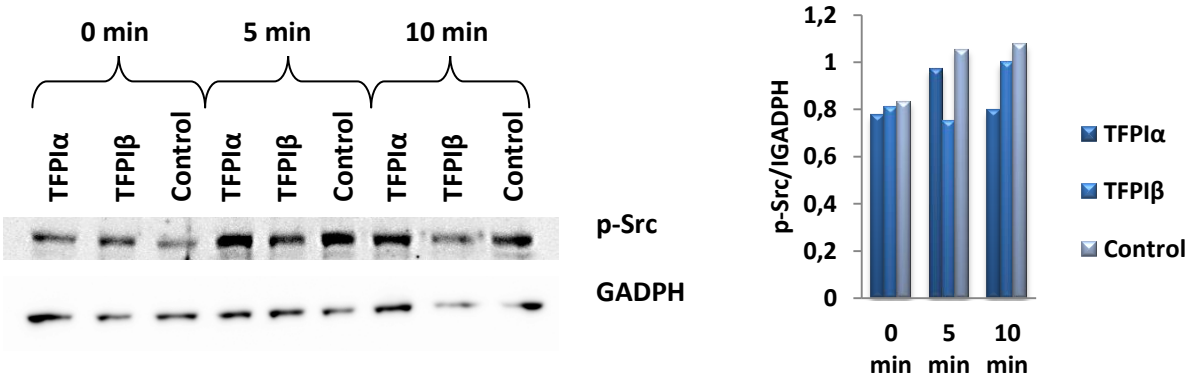

Figure 4.26 p-Src levels in cell lysates in TFPIα and TFPIβ upregulated MDA-MB-231 cells. Cells were starved for 5 hours before $1.0x10^6$ cells were stimulated with 10% FBS for 0, 5 and 10 minutes. p-Src levels were measured by Western blotting (left) and quantified and corrected with GADPH (right). Mean values from two Western blott are presented.

5 Discussion

There is increasing evidence that TFPI has anti-tumor effects, including anti-metastatic characteristics, in addition to its main function as an inhibitor of blood coagulation. Most previous studies of TFPI, have examined how overexpression of full length TFPIα or recombinant TFPIα (rTFPIα) affect cancer development, however, few have observed the effect of the TFPIα and TFPIβ isoform separately, and if there are any difference in biological function between the two. To investigate this further, transient breast cancer cell models with knockdown and overexpression of TFPIα and TFPIβ, separately, were established. These models were then used in experiments measuring how the manipulation of the TFPI levels affected growth, adhesion and migration properties of breast cancer cells.

5.1 Breast cancer cell lines

In this thesis, breast cancer cell lines were used to investigate TFPI's effect on cancer biology. In contrast to primary cells which have a limited lifetime when cultured *in vitro*, cell lines have been immortalized by for example injection of Epstein-Barr virus, and have therefore an infinite cell division potential (Kilger *et al.* 1998; Lea 2006). This advantage make it possible to study the biology of the cells that otherwise would be limited by short lifetime. Cell lines may also be frozen and thawed whenever they are needed. The risk of cross-contamination and for the cell lines to diverge from the original cells, due to long cultivation periods under different condition, exists. Therefore, it is important to use a recommended culture medium, and keep the cells at a constant temperature of 37°C and 5% CO_2 atmosphere. Furthermore, it is important that the cell handling is kept under sterile conditions. Since cell lines represent an isolated system, effects observed in cell models should be tested in animal models before the effects can be transferred to *in vivo* systems.

Two different breast cancer cell lines were used in this thesis; MDA-MB-231 and MDA-MB-436. The MDA-MB-231 cell line was already in house and has previously been used in experiments with stable downregulation of TFPI. Since the research group had already tested that both transient up- and downregulation of TFPI was possible in this cell line, the MDA-MB-231 cells were chosen for the functional experiments in this thesis. Attempts were also made to create stable cell lines with TFPIα or TFPIβ upregulated in the MDA-MB-231 cells, however, during the selection all the cells died. This has also previously been observed by the

research group in an earlier attempt to create a stable cell line with TFPI upregulated in the same cells. The reason why this occurred is not clear, but one explanation might be that MDA-MB-231, which already express high levels of TFPI do not tolerate an even higher level. To be able to compare effects in stable cell lines with up- or downregulated TFPI levels, a new cell line with the similar characteristics as MDA-MB-231 cells, but with lower TFPI expression was therefore searched for. Because of the heterogeneity of breast cancer tumors, similar characteristics in terms of hormone receptor status, tumor subtype and p53 mutation status was important for future comparison of effects in the two cell lines. The breast cancer cell line MDA-MB-436 was chosen as an appropriate candidate for establishment of stable cell lines with TFPIα or TFPIβ upregulated since this cell line had low endogenous expression of TFPI. Moreover, like the MDA-MB-231 cells, the MDA-MB-436 cells have a basal-like subtype, are triple negative, and have mutated p53.

For the establishment of the stable cell line with TFPIα or TFPIβ upregulated, the MDA-MB-436 cells were transfected with TFPIα or TFPIβ plasmid. After approximately three weeks of selection, the overexpression was checked at both the mRNA and the protein level. An increase in mRNA expression and in TFPI protein levels were measured in both TFPIα and TFPIβ overexpression cells. Thus, the attempt to create stable cell lines with TFPIα and TFPIβ overexpression was successful. Unfortunately, there was not enough time to perform functional experiments with this newly established stable cell line. The cells were frozen for later use.

5.2 Transient overexpression and knockdown cell models of TFPIα and TFPIβ

One of the aims in this study was to create a knockdown cell model for TFPIα and TFPIβ. Since the TFPIα isoform has not been successfully knocked down before, new siRNAs that exclusively knock down TFPIα were designed. siRNAs that target TFPIβ were already in house and earlier optimized by the research group. Even though the supplier guarantees an efficient knockdown using the siRNAs, the knockdown efficiency may be cell type specific and they may not work at all (Cullen 2006b). It is therefore crucial to screen the siRNAs to test their efficiencies before functional studies may be performed. The screening in this thesis was conducted in HEK293T cells and demonstrated that only three of the six tested siRNA oligonucleotides were efficient in knocking down TFPIα. In addition, it was also shown that the 27mer siRNAs (siRNA α3-α6) were more efficient than the, until now standard 21mer siRNAs (siRNA α1 and α2). This finding is in accordance with Kim *et al.* (2005) which tested

the efficiency of siRNAs with different length specific to a variety of genes. The reason why some siRNAs provide an efficient knockdown and others not, may be caused by the highly sequence-specific recognition process. Nucleotide mismatches between the siRNA sequence and the mRNA sequence may prevent the knockdown (Elbashir *et al.* 2001). siRNAs that differ by only one nucleotide may therefore show different knockdown efficiencies in the same cell line. Moreover, the same siRNA may also provide different knockdown efficiencies in different cell lines due to that some cells being more resistant to transfection than others (Cullen 2006a).

In order to obtain firm results it is preferred to use several siRNA that target the same gene. The three TFPIα specific siRNAs with the most efficient knockdown in the screening experiment were further optimized in the breast cancer cell line MDA-MB-231. Optimization is important for finding the lowest effective concentration of the siRNAs which results in an efficient knockdown. Too high siRNA concentrations may produce nonspecific off-target effects like activation of interferon response (Cullen 2006a), while too low siRNA concentrations will not provide efficient knockdown. The optimization performed in this study showed a dose-response effect; high siRNA concentrations resulted in high knockdown efficiencies, while low siRNA concentrations showed low knockdown efficiencies. Two different siRNA:Lipofectamine ratios were also tested; the 10:1 ratio showed a higher knockdown efficiency compared to the 20:1 ratio, which demonstrated that higher siRNA concentration not necessary provides higher knockdown efficiencies. The 20:1 ratio may have exceeded Lipofectamine's ability to enclose the siRNA and transfer them into the cells. Since the 10:1 ratio showed the highest knockdown efficiency, this ratio was chosen for the rest of the experiments. To test the specificity of the TFPIα specific siRNAs, the mRNA expression of the TFPIβ isoform was tested. Of the six TFPIα siRNAs tested, only one siRNA affected the expression of the TFPIβ isoform, and was therefore not used in further experiments. The siRNAs that target TFPIβ isoform were also tested to not influence the expression of TFPIα.

Functional experiments should be performed when the knockdown is most efficient, since the effect between the downregulated cells and the control cells can then easier be observed. To find the most efficient time point(s), a time dependent knockdown of TFPIα and TFPIβ was performed in the MDA-MB-231 cells. The separate knockdown of both the TFPIα and the TFPIβ isoform was relatively stable from 24 hours up to 120 hours after transfection, and there were only small differences in knockdown efficiencies between the two isoforms. Since

the cells divide continuously, we expected that the knockdown effect would disappear gradually by time, but this was not the case in this study. The highest knockdown efficiencies for TFPIα and TFPIβ were measured after 72 and 96 hours after transfection, (84% and 88%, respectively). The reason for this might be that the MDA-MB-231 cells grew slowly, as shown in two different growth experiments. The knockdown was also confirmed at the protein level using total TFPI ELISA. Due to the complex process of translating proteins in the cell, a delay in the knockdown at the protein level was expected. Indeed, the knockdown of TFPIα and TFPIβ protein was not observed before 48 hours after transfection. After 96 hours a surprising increase in total TFPI protein levels was observed in lysates from cells transfected with siRNA β7. This was most likely an outlier since the overall trend showed lower total TFPI for the knockdown cells compared to the control cells. However, the effect measured after 96 hours was not particularly convincing for cells transfected with siRNA β9 either, so it seems like an unidentified systematic failure may have happen at this time point during the experiment. The high TFPI protein level measured for the control at 120 hours was neither expected, the reason why this was observed is not clear. Given that the surprising results was due to a systematic failure, the knockdown efficiency was highest between 72 and 120 hours at both mRNA and protein level for TFPIα and TFPIβ, it was therefore decided to perform the functional studies with the TFPI downregulated cells at 96 hours after transfection. To compare the two isoforms of TFPI in this thesis were siRNA α3 and siRNA β7 used. The siRNAs that showed most efficient knockdown in this study are currently converted to shRNA and cloned into a shRNA vector, to establish stable cell lines with downregulated TFPIα.

An overexpression model was also established to compare effects observed with TFPI downregulated cells with TFPI upregulated cells. As for the TFPIα and TFPIβ downregulated cells, a time-dependent experiment between 6-72 hours was conducted for cells transfected with TFPIα or TFPIβ plasmid. The time dependent overexpression of TFPIα and TFPIβ showed an overall successful upregulation of TFPIα and TFPIβ. Overexpression of TFPIβ showed a much higher increase in mRNA expression compared to the increase of TFPIα expression, a 4000-fold increase compared to 600-fold increase, respectively. This was also observed in the MDA-MB-436 cells. The reason for this is not clear, but the quality of the plasmid preparation, contamination in the plasmid isolation or overestimation of the plasmid concentration could perhaps explain some of the observed difference in overexpression between the two isoforms. The overexpression of TFPIα and TFPIβ was also confirmed at the

protein level. Both isoforms showed an increase in TFPI protein levels, a 53-fold increase for the TFPIα upregulated cells and a 25-fold increase for the TFPIβ upregulated cell was measured at 72 hours after transfection. Since both isoforms showed a high overexpression at 72 hours after transfection, this time point was initially chosen for performing the functional studies. But because of increased cell death during the experiment, the functional studies were performed at 48 hours after transfection instead of the initially chosen time point.

5.3 TFPI's effect on growth

To investigate TFPI's role on growth of breast cancer cells, growth experiments when TFPIα or TFPIβ was up- or downregulated were conducted in the MDA-MB-231 cell line. Growth was examined both by measuring total protein in lysates and by cell counting at different time intervals after transfection. Cell counting measures the growth directly, while total protein quantification is a color reaction that measures the amount of total protein in cell lysates compared to a standard curve and may thus be used as an indirect growth measure. Cells with downregulated TFPIα or TFPIβ indicated a trend towards a reduced proliferation rate compared to the control cells, both when total protein levels was measured and the cells were counted. However, a significant difference was only observed after 48 and 72 hours for TFPIα downregulated cells and at 72 hours for TFPIβ downregulated cells when the total protein levels were considered. No significant differences were observed by cell counting. This observation is in line with the report by Stavik *et al.* (2010) where they measured growth in TFPI downregulated Sum102 cells by adding WST-1 to the cells. Stavik *et al.* (2011) also counted Sum102 cells directly as in this thesis, then an increase in growth was observed for the Sum102 cells with downregulated TFPI, but only when the cells were seeded at low concentrations. Since the growth experiment in this thesis was only performed once, methodological limitations like uneven seeding of the cells may have led to uncertain results. This result is therefore just an indication of how downregulated TFPI affects the growth of breast cancer cells. The experiments have to be repeated before anything can be concluded.

For the TFPIα and TFPIβ upregulated cells, no increase in growth was seen between 6 and 72 hours after transfection, even not for the control cells. This was observed both when measuring total protein and by cell counting, but it is worth mentioning that these two growth experiments were performed with cells from the same experimental setup. Many dead cells were also observed in the microscope during the experiment. Inhibition of cell growth might be a direct consequence of the transfection. Transfecting a plasmid into the cell may be

stressful for the cell, and the cell may end up dying, which is probably what happened in this particular experiment. Since the growth experiments with TFPI upregulated cells were not successful, no conclusion could be drawn concerning how upregulated TFPIα or TFPIβ levels influence the growth of the MDA-MB-231 breast cancer cells. The growth experiments (total protein quantification and cell counting) were only performed once, and should therefore be repeated to observe if the same result is provided or if the result in this thesis was just a coincidence. It might be that transiently transfected cells that are transfected right before the experiment is not optimal for growth measurements, so an experiment with stably transfected should be considered for future growth studies. An experiment with the use of WST-1 could also be tested in addition to the experiment already performed.

5.4 TFPI's effect on adhesion to collagen I

To observe how TFPIα and TFPIβ affect the breast cancer cells' ability to adhere, experiments with adhesion to collagen I with both TFPIα and TFPIβ up- and downregulated MDA-MB-231 cells were conducted. It was especially interesting to observe the effect of the TFPIα isoform since this has not been examined before. When TFPIα was upregulated, a slight decrease in adhesion to collagen I was observed, and in one out of the three experiments, a decrease of 40% was measured for the TFPIα upregulated cells. This may indicate a possible anti-tumor effect of the TFPIα isoform. A t-test was performed to measure if the decrease was significant, but the test was negative. However, the dataset contained only three data points, which are too few samples to obtain reliable results in a t-test. No differences were observed when the TFPIβ isoform was upregulated, this may be explained by the lower downregulation effect measured at the protein level for the TFPIβ isoform compared to the TFPIα isoform. Stavik *et al.* (2011) have previously measured breast cancer cells' ability to adhere to different extracellular matrix components, and reported a significant increase in adhesion to collagen I for total TFPI (α+β) or TFPIβ downregulated MDA-MB-231 cells. Since Stavik *et al.* measured increased adhesion to collagen I in downregulated cells, it makes sense that a decrease in TFPIα upregulated cells was measured in this thesis. In contrast, we did not observe any difference in adhesion to collagen I for TFPIβ upregulated cells. However, before anything can be concluded, the experiment should be repeated to obtain more reliable results.

For the TFPIα or TFPIβ downregulated cells, a significant decrease to collagen I was observed for both the isoforms. This result is in disagreement to what Stavik *et al.* (2011)

reported when they measured adhesion to collagen I with stable cell line with total TFPI (α+β) or TFPIβ downregulated. The most obvious explanation for this contradiction is the use of transiently transfected cells, as opposed to the stable cell lines Stavik *et al.* used in their study. By using transiently transfected cells instead of stably transfected cells, the cells are going through a rough transfection procedure with Lipofectamine just before the experiment which may have led to alterations in the cells' ability to adhere. In addition, the transiently transfected cells may give a high background caused by untransfected cells, and the cells are not so "fresh" (cultivated for a longer period) compared to stable cells. Furthermore, uneven coating, seeding and washing may also have contributed to these results. A methodological limitation in the adhesion experiment performed in this thesis is that WST-1 measure metabolic activity in the cells, and not directly the cell number. An additional adhesion method using cells labeled with a suitable fluorescent dye may therefore be a method worth trying. Then the cells could be counted before and after the adhesion to collagen I and a number of how many cells that actually adhered would be provided.

Adhesion may be mediated by different integrin molecules (Morgan *et al.* 2007). Integrins are transmembrane adhesion molecules involved in cancer metastasis, and are detected at several cancer cells (Varnera & Chereshb 1996). Integrins may activate multiple signaling pathway including signaling pathway which promote adhesion, growth and increased expression and secretion of matrix metalloproteins (Moschos & Kirkwood 2007). Increased levels of integrins may therefore lead to more aggressive tumors cells. To evaluate the involvement of integrins in the adhesion to collagen I of the TFPI manipulated MDA-MB-231 cells, Western blotting measuring the integrin α2 levels in the lysates was performed in this thesis. A significant decrease in integrin α2 levels was measured in TFPIα upregulated cells. Decreased adhesion to collagen I and decreased integrin α2 levels measured with TFPIα upregulated cells in this thesis may indicate an anti-tumor effect of TFPIα. This is in line with Stavik *et al*. (2011) which measured elevated levels of integrin α2 in total TFPI or TFPIβ downregulated MDA-MB-231 cells. In this thesis, no differences were observed in integrin α2 levels with TFPIβ upregulated cells which reflect the adhesion results.

For the TFPIα and TFPIβ downregulated cells, an increase in integrin α2 levels was observed, although not statistically significant. Based on this, an increase in adhesion would be expected for the TFPI downregulated cells, however, as described above that was not the case in this study. Since adhesion experiments with TFPIα or TFPIβ downregulated cells showed the

opposite of what have been observed before for TFPI knockdown cells, while the integrin α2 levels corresponded with previous findings (Stavik *et al.* 2011), it is likely that the inconsistent results are due to the methodological limitations including uneven seeding, coating and washing in the adhesion experiments.

5.5 TFPI's effect on migration

Cancer cells often have an increased ability to migrate so they can move and spread from one site of the body to another (Hanahan & Weinberg 2000). To examine how the two isoforms of TFPI affected migration of breast cancer cells, scratch-wound assays with TFPI up- and downregulated cells were performed. A decrease in migration measured with TFPI upregulated cells was observed compared to the control cells. The decrease was observed for both the TFPIα and the TFPIβ upregulated cells, but the differences were only significant for the TFPIα isoform. This result is in accordance with the findings by Stavik *et al.* (2011) which reported increased migration in stable total TFPI (α+β) or TFPIβ downregulated breast cancer cells. Based on these findings it was also expected to observe increased migration for the TFPI downregulated cells, however, this was not the case in this study where no differences in migration were observed for the TFPI downregulated cells.

The reason why the migration results with TFPI downregulation provided in this thesis were in disagreement with Stavik *et al*. may involve the use of transiently transfected cells compared to stable cell lines which Stavik *et al.* used. A pool of transiently transfected cell will always contain some untransfected cells, these cells may have contributed to the migration observed in the scratch-wound assay with the TFPI downregulated cells. Since these cells have avoided the manipulation, they will have the similar migration abilities as for the control cells, and potentially effects may be disguised by the untransfected cells. The use of stable cell lines which are a homogenous group of cells may perhaps provide a more clear-cut difference between the test and control and thereby clearer result. It would therefore be interesting to test the stable cell lines with downregulated TFPIα which are currently under progress in the laboratory and with the TFPIβ downregulted stable cell lines, to observe if experiments with these cells would provide a different result. Another limitation with the scratch-wound assay is that differences in migration may be a result of growth and not migration itself. Additional migration experiments like Boyden chamber assay should therefore be tested to provide more certain results.

The Src family kinases may activate signaling pathways leading to growth and migration of cells (Mitra & Schlaepfer 2006). To evaluate the involvement of Src in the TFPIα or TFPIβ upregulated cells, a stimulation experiment with serum was conducted. Analyzed by Western blotting, the p-Src levels seemed to increase by the time of stimulation, and the overall trend was slightly decreased levels of the p–Src in both TFPIα and TFPIβ upregulated cells, compared to the control cells. Stavik *et al.* (2011) reported increased p-Src levels in TFPI downregulated cells, which is in accordance with this result. Since decreased p-Src levels compared to the control cells was measured when both TFPIα and TFPIβ were upregulated, and reduced migration of the of the same cells was observed, it might indicate that Src signaling pathway is involved in effect of TFPI on the migration of the breast cancer cells. Less phosphorylated Src, leads to less activated FAK and integrin molecules, which may result in reduced migration.

To further examine if the signaling pathway activated by Src was involved in the migration of cells with upregulated TFPIα or TFPIβ, an experiment with Src inhibitor was performed. If TFPI's effect on migration involves the Src pathway, it was expected to observe a further decrease in migration for TFPIα and TFPIβ, and for the control cells when Src and thereby the signaling pathways activated by the FAK-Src complex was inhibited. The result provided in this thesis showed no clear answer of the involvement of Src. The wound made in the TFPIα upregulated control cells seemed to be slightly more closed than the TFPIα upregulated cells incubated with Src inhibitor, while the opposite was observed for the TFPIβ upregulated cells. However, the differences observed between the cells incubated with Src and the control cells were too small to drawn a conclusion. This experiment has to be repeated to be able to conclude if Src is involved in the migration of TFPI upregulated cells.

5.6 Statistics

Common for the experiments conducted in this thesis is the low number of repeated experiments and biological parallels, especially for the growth experiments which was only performed once. The statistics used should therefore be interpreted with caution, and is only provided as an estimate of the significance.

5.7 Conclusions

The experiments with cells overexpressing TFPIα and TFPIβ showing decreased adhesion and migration may indicate a possible anti-tumor effect of both of isoforms. If investigation further suggests that TFPI has an anti-tumor effect, TFPI may be useful in treatment not only for prevention of VTE, but also to reduce cancer progression, which may be independent of the coagulation system.

The specific conclusions of this thesis were:

- Four siRNA oligonucleotides that exclusively knock down the TFPIα isoform were designed, and three of the siRNAs showed an efficient knockdown of TFPIα without affecting the TFPIβ isoform. Two of the siRNAs were further used to optimize the TFPIα knockdown
- An transient knockdown and overexpression model for TFPIα and TFPIβ were successfully established and were further used in the functional studies
- Two different methods measuring growth indicated a slightly reduced growth of both TFPIα and TFPIβ downregulated cells, while no difference was observed for TFPIα or TFPIβ upregulated cells
- TFPIα upregulated cells showed a slight decrease in adhesion to collagen I together with decreased integrin α2 levels, while the TFPIβ upregulated cells showed no differences in adhesion to collagen I or in integrin α2 levels
- TFPIα and TFPIβ downreglated cells showed a decreased adhesion to collagen I, but elevated integrin α2 levels
- Cells with TFPIα and TFPIβ upregulated showed a decrease in migration, while no differences were observed for TFPIα or TFPIβ downregulated cells
- Src signaling pathways may be involved in the migration, since decreased p-Src levels were measured in the TFPIα and the TFPIβ upregulated cells
- Stable cell line with TFPIα and TFPIβ were successfully established in the breast cancer cell line MDA-MB-436
- Altogether, the experiments with TFPIα and TFPIβ upregulated cell look more promising than experiments performed with TFPIα and TFPIβ downregulated cells

5.8 Suggestions for further work

- Repeat both the total protein quantification and cell counting growth experiments for both TFPI downregulated- and upregulated cells
- Try an alternative growth experiment for the TFPI upregulated cells, for example using WST-1
- Try an alternative cell adhesion method, like fluorescent-based adhesion assay
- Try an alternative migration method, like using Boyden chambers
- Perform all the above mentioned experiments with the newly established cell line with TFPIα or TFPIβ upregulated and cell line with downregulated TFPIα that are currently created in the laboratory

References

Agostino, D., Cliffton, E. E. & Girolami, A. (1966). Effect of Prolonged Coumadin Treatment on Production of Pulmonary Metastasis in Rat. *Cancer*, 19 (2): 284-288.

Alberts, B., Johnson, A., Lewis, J., Raff, M., Roberts, K. & Walter, P. (2008). *Molecular Biology of the Cell*. 5th ed., vol. Fifth Edition: Garland Science. 1268 pp.

Amirkhosravi, A., Meyer, T., Chang, J. Y., Amaya, M., Siddiqui, F., Desai, H. & Francis, J. L. (2002). Tissue factor pathway inhibitor reduces experimental lung metastasis of B16 melanoma. *Thromb Haemost*, 87 (6): 930-936.

Blom, J. W., Doggen, C. J. M., Osanto, S. & Rosendaal, F. R. (2005). Malignancies, Prothrombotic Mutations, and the Risk of Venous Thrombosis. *JAMA*, 293 (6): 715-722.

Boccaccio, C. & Comoglio, P. M. (2005). A Functional Role for Hemostasis in Early Cancer Development. *Cancer Research*, 65: 8579-8582.

Boccaccio, C., Sabatino, G., Medico, E., Girolami, F., Follenzi, A., Reato, G., Sottile, A., Naldini, L. & Comoglio, P. M. (2005). The MET oncogene drives a genetic programme linking cancer to haemostasis. *Nature*, 434: 396-400.

Bortnera, C. D. & Cidlowskia, J. A. (1998). A necessary role for cell shrinkage in apoptosis. *Biochemical Pharmacology*, 56 (12): 1549–1559.

Breier, G., Grosser, M. & Rezaei, M. (2014). Endothelial cadherins in cancer. *Cell Tissue Res*, 355 (3): 523-7.

Broze, G. J. J. & Girard, T. J. (2013). Tissue Factor Pathway Inhibitor: Structure-Function. *Front Biosci*, 17: 262-280.

Burkhart, D. L. & Julien Sage, J. (2008). Cellular mechanisms of tumour suppression by the retinoblastoma gene. *Nature Reviews Cancer*, 8: 671-682.

Campisi, J. (2001). Cellular senescence as a tumor-suppressor mechanism. *Trends in CELL BIOLOGY*, 11 (11): 27-31.

Carmeliet, P. & Jain, R. K. (2000). Angiogenesis in cancer and other diseases. *Nature*, 407: 249-257.

Chew, H. K., Wun, T., Harvey, D., Zhou, H. & White, R. H. (2006). Incidence of Venous Thromboembolism and Its Effect on Survival Among Patients With Common Cancers. *JAMA Internal Medicine*, 166 (4): 458-464.

Cross, M. J. & Claesson-Welsh, L. (2001). FGF and VEGF function in angiogenesis: signalling pathways, biological responses and therapeutic inhibition. *TRENDS in Pharmacological Sciences* 22 (2): 201–207.

Cullen, B. R. (2006a). Enhancing and conforming the spesificity of RNAi experiments. *Nature Methods*, 3 (9): 677-681.

Cullen, B. R. (2006b). Induction of stable RNA interference in mammalian cells. *Gene Therapy*, 13: 503-508.

Darmoul, D., Gratio, V., Devaud, H., Peiretti, F. & Laburthe, M. (2004). Activation of Proteinase-Activated Receptor 1 Promotes Human Colon Cancer Cell Proliferation Through Epidermal Growth Factor Receptor Transactivation. *Mol Cancer Res*, 2: 514-522.

DeBerardinis, R. J., Lum, J. J., Hatzivassiliou, G. & Thompson, C. B. (2008). The Biology of Cancer: Metabolic Reprogramming Fuels Cell Growth and Proliferation. *Cell Metabolism*, 7 (1): 11-20.

Downward, J. (2004). Use of RNA interference libraries to investigate oncogenic signalling in mammalian cells. *Oncogene*, 23: 8376-8383.

Elbashir, S. M., Martinez, J., Patkaniowska, A., Lendeckel, W. & Tuschl, T. (2001). Functional anatomy of siRNAs for mediating efficient RNAi in Drosophila melanogaster embryo lysate. *The EMBO journal*, 20 (23): 6877–6888.

Enjyoji, K., Kamikubo, Y. & Kato, H. (1995). Effect of Heparin on the Inhibition of Factor Xa by Tissue Factor Pathway Inhibitor: A Segment, Gly212-Phe243, of the Third Kunitz Domain Is a Heparin-Binding Site. *Biochemistry*, 34 (17): 5725-5735.

Falanga, A., Marchetti, M. & Vignoli, A. (2013). Coagulation and cancer: biological and clinical aspects. *Journal of Thrombosis and Haemostasis*, 11: 223-233.

Felding-Habermann, B., O'Toole, T. E., Smith, J. W., Fransvea, E., Ruggeri, Z. M., Ginsberg, M. H., Hughes, P. E., Pampori, N., Shattil, S. J., saven, A., et al. (2001). Integrin activation controls metastasis in human breast cancer. *PNAS*, 98 (4): 1853-1858.

Ferlay, J., Soerjomataram, I., Ervik, M., Dikshit, R., Eser, S., Mathers, C., Rebelo, M., Parkin, D., Forman, D. & Bray, F. (2013). *Cancer Incidence and Mortality Worldwide*. World Cancer Researh Fund International: International Agency for Research on Cancer. Available at: http://www.wcrf.org/cancer_statistics/world_cancer_statistics.php.

Foulkes, W. D., Smith, I. E. & Reis-Filho, J. S. (2010). Triple-Negative Breast Cancer. *N Engl J Med*, 363: 1938-1948.

Furie, B. & Furie, B. C. (2006). Cancer-associated thrombosis. *Blood Cells, Molecules, and Disease*, 36: 177-181.

Giancotti, F. G. & Ruoslahti, E. (1999). Integrin Signaling. *Science*, 285 (5430): 1028-1033.

Gomez, K. & McVey, J. H. (2006). Tissue Factor Initiated Blood Coagulation. *Bioscience*, 11: 1349-1359.

Goustin, A. S., Leof, E. B., hipley, G. D. & Moses, H. L. (1986). Growth Factors and Cancer. *Cancer Research*, 46: 1015-1029.

Gupta, G. P. & Massagué, J. (2006). Cancer Metastasis: Building a Framework. *Cell*, 127 (4): 679–695.

Hamuro, T., Kamikubo, Y., Nakahara, Y., Miyamoto, S. & Funatsu, A. (1998). Human recombinant tissue factor pathway inhibitor induces apoptosis in cultured human endothelial cells. *FEBS Letters*, 421: 197-202.

Hanahan, D. & Weinberg, R., A. (2000). The hallmark of cancer. *Cell*, 100: 57-70.

Hanahan, D. & Weinberg, R. A. (2011). Hallmarks of Cancer: The Next Generation. *Cell*, 144 (5): 646-74.

Hembrough, T. A., Ruiz, J. F., Papathanassiu, A. E., Green, S. J. & Strickland, D. K. (2001). Tissue Factor Pathway Inhibitor Inhibits Endothelial Cell Proliferation via Association with the Very Low Density Lipoprotein Receptor. *The Journal Of Biological Chemistry*, 275 (15): 12241–12248.

Hembrough, T. A., Swartz, G. A., Papathanassiu, A., Vlasuk, G. P., Rote, W. E., Green, S. J. & Pribluda, V. S. (2003). Tissue Factor/Factor VIIa Inhibitors Block Angiogenesis and Tumor Growth Through a Nonhemostatic Mechanism. *Cancer Researh*, 63: 2997-3000.

Hudis, C. A. (2007). Trastuzumab — Mechanism of Action and Use in Clinical Practice. *The New England Journal of Medicine*, 357: 39-51.

Igney, F. H. & Krammer, P. H. (2002). Death and anti-death: tumour resistance to apoptosis. *Nature Reviews Cancer*, 2: 277-288.

International Agency for Research on Cancer. (2014). *IARC TP53 database*. Available at: http://p53.iarc.fr/CellLines.aspx (accessed: 14.04.14).

Invitrogen. (2009). *pcDNA™3.1/V5-His TOPO® TA Expression Kit -User Manual*.

Iversen, N., Lindahl, A.-K. & Abildgaard, U. (1998). Elevated TFPI in malignant disease: relation to cancer type and hypercoagulation. *British Journal of Haematology*, 102 (4): 889-895.

Jinek, M. & Doudna, J. A. (2009). A three-dimensional view of the molecular machinery of RNA interference. *Nature*, 457 (22): 405-412.

Kamikubo, Y., Nakahara, Y., Takemoto, S., Hamuro, T., Miyamoto, S. & Funatsu, A. (1997). Human recombinant tissue-factor pathway inhibitor prevents the proliferation of cultured human neonatal aortic smooth muscle cells. *FEBS Letters*, 407: 116-120.

Kasthuri, R. S., Glover, S. L., Boles, J. & Mackman, N. (2010). Tissue Factor and Tissue Factor Pathway Inhibitor as Key Regulators of Global Hemostasis: Measurement of Their Levels in Coagulation Assays. *Semin Thromb Hemost*, 36 (7): 764-771.

Kerr, J. F. R., Winterford, C. M. & Harmon, B. V. (1994). Apoptosis Its Significance in Cancer and Cancer Therapy *Cancer*, 73 (8): 2013–2026.

Kilger, E., Kieser, A., Baumann, M. & Hammerschmidt, W. (1998). Epstein–Barr virus-mediated B-cell proliferation is dependent upon latent membrane protein 1, which simulates an activated CD40 receptor. *The EMBO journal*, 17 (6): 1700-1709.

Kim, D.-H., Behlke, M. A., Rose, S. D., Chang, M.-S., Choi, S. & Rossi, J. J. (2005). Synthetic dsRNA Dicer substrates enhance RNAi potency and efficacy. *Nature*, 23 (2): 222-226.

Klug, W. S., Cummings, M. R. & Spencer, C. A. (2007). *Essentials of Genetics* vol. Sixth edition.

Kubista, M., Andradeb, J. M., Bengtssona, M., Forootand, A., Jonáke, J., Linda, K., Sindelkae, R., Sjöbacka, R., Sjögreend, B., Strömboma, L., et al. (2006). The real-time polymerase chain reaction. *Molecular Aspects of Medicine*, 27 (2-3): 95–125.

Lea, T. (2006). *Immunologi og immunologiske teknikker*, vol. 3: Fagbokforlaget.

Lee, A. E., Rogers, L. A., Longcroft, L. M. & Jeffery, R. E. (1990). Reduction of metastasis in a murine mammary tumour model by heparin and polyinosinic-polycytidylic acid. *Clin Exp Metastasis*, 8 (2): 165-171.

Lehmann, B. D., Bauer, J. A., Chen, X., Sanders, M. E., Chakravarthy, A. B., Shyr, Y. & Pietenpol, J. A. (2011). Identification of human triple-negative breast cancer subtypes and preclinical models for selection of targeted therapies. *The Journal of Clinical Investigation*, 121 (7): 2750-2767.

Lillicrap, D. (2013). Introduction to a series of reviews on cancer-associated thrombotic disease. *Blood*, 122: 1687-1688.

Lin, Y.-F., Zhang, N., Guo, H.-S., Kong, D.-S., Jiang, T., Liang, W., Zhao, Z.-H., Tang, Q.-Q. & Ma, D. (2007). Recombinant tissue factor pathway inhibitor induces apoptosis in cultured rat mesangial cells via its Kunitz-3 domain and C-terminal through inhibiting PI3-kinase/Akt pathway. *Apoptosis*, 12: 2163-2173.

Lindahl, A. K., Sandset, P. M., Abildgaard, U., Andersson, T. R. & Harbitz, T. B. (1989). High plasma levels of extrinsic pathway inhibitor and low levels of other coagulation inhibitors in advanced cancer. *Acta chirurgica Scandinavica*, 155 (8): 389-393.

Lindahl, A. K., Ødegaard, O. R., Sandset, P. M. & Harbitz, T. B. (1992). Coagulation inhibition and activation in pancreatic cancer. Changes during progress of disease. *Cancer*, 70 (8): 2067-2072.

Lindahl, A. K. (1996). Tissue factor pathway inhibitor: from unknown coagulation inhibitor to major antithrombotic principle. *Cardiovascular Research*, 33 (286–291).

Lukashev, M. E. & Werb, Z. (1998). ECM signalling: orchestrating cell behaviour and misbehaviour. *trends in CELL BIOLOGY*, 8 (11): 437–441.

Lund University. (2012). *GOBO - Gene set analysis - Cell lines*. Available at: http://co.bmc.lu.se/gobo/gsa_cellines.pl (accessed: 14.04.14).

Luo, B.-H. & Springer, T. A. (2006). Integrin structures and conformational signaling. *Current Opinion in Cell Biology*, 18 (5): 579–586.

Maroney, S. A., Ellery, P. E. & Mast, A. E. (2010). Alternatively Spliced Isoforms of Tissue Factor Pathway Inhibitor. *Thromb Res*, 126 (4): 1-7.

Mechtcheriakova, D., Wlachos, A., Holzmüller, H., Binder, B. R. & Hofer, E. (1999). Vascular Endothelial Cell Growth Factor–Induced Tissue Factor Expression in Endothelial Cells Is Mediated by EGR-1. *Blood*, 93: 3811-3823.

Mitra, S. K. & Schlaepfer, D. D. (2006). Integrin-regulated FAK–Src signaling in normal and cancer cells. *Cell Biology*, 18: 516-523.

Morgan, M. R., Humphries, M. J. & Bass, M. D. (2007). Synergistic control of cell adhesion by integrins and syndecans. *Nature Reviews Molecular Cell Biology*, 8: 957-969.

Moschos, S. & Kirkwood, J. M. (2007). Integrins and Cancer. Available at: (http://www.cancernetwork.com).

Moschos, S. J., Drogowski, L. M., Reppert, S. L. & Kirkwood, J. M. (2007). Integrins and cancer. *Oncology*, 21 (9): 13-20.

Nasha, G. F., Walsha, D. C. & Kakkar, A. K. (2001). The role of the coagulation system in tumour angiogenesis. *The Lancet Oncology*, 2 (10): 608-613.

Nasha, G. F., Turnera, L. F., Scullyb, M. F. & Kakkar, A. K. (2002). Platelets and cancer. *The Lancet Oncology*, 3 (7): 425-430.

Ndonwi, M., Tuley, E. A. & Broze Jr, G. J. (2010). The Kunitz-3 domain of TFPI-α is required for protein S–dependent enhancement of factor Xa inhibition. *Blood*, 116 (8): 1344–135.

Nieswandt, B., Hafner, M., Echtenacher, B. & Männel, D. N. (1999). Lysis of Tumor Cells by Natural Killer Cells in Mice Is Impeded by Platelets. *CANCER RESEARCH*, 59: 1295–1300.

Novotny, W. F., Palmier, M., Wun, T. C., Broze, G. J. & Miletich, J. P. (1991). Purification and Properties of Heparin-Releasable Lipoprotein-Associated Coagulation Inhibitor *Blood*, 78 (2): 394-400.

Olivier, M., Hollstein, M. & Hainaut, P. (2010). TP53 Mutations in Human Cancers: Origins, Consequences, and Clinical Use. *Cold Spring Harb Perspect Biol*, 2 (1): 1-17.

Pennacchietti, S., Michieli, P., Galluzzo, M., Mazzone, M., Giordano, S. & Comoglio, P. M. (2003). Hypoxia promotes invasive growth by transcriptional activation of the met protooncogene. *Cancer Cell*, 3: 347-361.

Prandoni, P., Falanga, A. & Piccioli, A. (2005). Cancer and venous thromboembolism. *Lancet Oncol*, 6: 401-10.

Provencal, M., Michaud, M., Beaulieu, E., Ratel, D., Rivard, G. E., Ginras, D. & Beliveau, R. (2008). Tissue factor pathway inhibitor (TFPI) interferes with endothelial cell migration by inhibition of both the Erk pathway and focal adhesion protein. *Thrombosis and Haemostasis*, 99 (3): 576-585.

Qiagen. (2014). *Transfection Protocols & Applications*. Available at: http://www.qiagen.com/knowledge-and-support/spotlight/protocols-and-applications-guide/transfection/ (accessed: 15.04.14).

Sambrook, J. & Russell, D. W. (2001). *Monecular Cloning A Laboratory Manual*, vol. 1: Cold Spring Harbor Laboratory Press.

Sánchez-Bailón, M. S., Calcabrini, A., Gómez-Domínguez, D., Morte, B., Forero, E. M., Gómez-López, G., Molinari, A., Wagner, K.-U. & Pérez, J. M. (2012). Src kinases catalytic activity regulates proliferation, migration and invasiveness of MDA-MB-231 breast cancer cells. *Cellular Signalling*, 24: 1276-1286.

Sandset, P. M., Abildgaard, U. & Larsen, M. L. (1988). Heparin induces release of extrinsic: Coagulation pathway inhibitor (EPI). *Thromb Res*, 50 (6): 803-813.

Schaffner, F. & Ruf, W. (2009). Tissue Factor and PAR2 Signaling in the Tumor Microenvironment. *Arteriosclerosis, Thrombosis, and Vascular Biology*, 29: 1999-2004.

Shay, J. W. & Bacchetti, S. (1997). A survey of telomerase activity in human cancer. *European Journal of Cancer*, 33 (5): 787–791.

Sledge, G. W. J. & Miller, K. D. (2003). Exploiting the hallmarks of cancer: the future conquest of breast cancer. *European Journal of Cancer*, 39: 1668-1675.

Smyth, M. J., Crowe, N. Y. & Godfrey, D. I. (2001). NK cells and NKT cells collaborate in host protection from methylcholanthrene-induced fibrosarcoma. *Int. Immunol*, 13 (4): 459-463.

Spanoa, D., Heckc, C., Antonellisa, P. D., Christoforic, G. & Zollo, M. (2012). Molecular networks that regulate cancer metastasis. *Seminars in Cancer Biology*, 22 (3): 234–249.

Stavik, B., Skretting, G., Sletten, M., Sandset, P. M. & Iversen, N. (2010). Overexpression of both TFPIα and TFPIβ induces apoptosis and expression of genes involved in the death receptor pathway in breast cancer cells. *Molecular carcinogenesis*, 49: 951-963.

Stavik, B., Skretting, G., Åsheim, H.-C., Tinholt, M., Zernichow, L., Sletten, M., Sandset, P. M. & Iversen, N. (2011). Downregulation of TFPI in breast cancer cells induces tyrosine phosphorylation signaling and increases metastatic growth by stimulating cell motility. *BMC Cancer*, 11 (357): 1-14.

Stavik, B., Skretting, G., Olstad, O. K., Sletten, M., Vigeland, M. D., Sandset, P. M. & Iversen, N. (2012). TFPI Alpha and Beta Regulate mRNAs and microRNAs Involved in Cancer Biology and in the Immune System in Breast Cancer Cells. *Plos One*, 7 (10): 1-12.

Stavik, B., Tinholt, M., Sletten, M., Skretting, G., Sandset, P. M. & Iversen, N. (2013). TFPIα and TFPIβ are expressed at the surface of breast cancer cells and inhibit TF-FVIIa activity. *Journal of Hematology and Oncology*, 6 (5): 1-14.

Stetler-Stevensona, W. G. & Yub, A. E. (2001). Proteases in invasion: matrix metalloproteinases. *Cancer Biology*, 11: 143-152.

Sørensen, H. T., Mellemkjær, L., Steffensen, F. H., Olsen, J. H. & Nielsen, G. L. (1998). The risk of a diagnosis of cancer after primary deep venous thrombosis or pulmonary embolism. *The New England Journal of Medicine*, 338 (17): 1169-1173.

Sørlie, T., Perou, C. M., Tibshirani, R., Aas, T., Geisler, S., Johnsen, H., Hastie, T., Eisen, M. B., van de Rijn, M., Jeffrey, S. S., et al. (2001). Gene expression patterns of breast carcinomas distinguish tumor subclasses with clinical implications. *PNAS*, 98 (19): 10869-10874.

Teng, M. W. L., Swann, J. B., Koebel, C. M., Schreiber, R. D. & Smyth, M. J. (2008). Immune-mediated dormancy: an equilibrium with cancer. *J Leukoc Biol*, 84: 988-993.

Tinholt, M., Stavik, B., Wiiger, M. T., Louch, W. E., Sletten, M., Skretting, G., Mælandsmo, G. M., Sandset, P. M. & Iversen, N. (2012). TFPI in targeted cancer therapy? . *Poster, presented at the conferance Personalized cancer care, Oslo September 2012*.

Ueno, T., Koike, M., Nakamura, S. & Tominaga, T. (2000). Tissue factor expression in breast cancer tissues: its correlation with prognosis and plasma concentration. *British Journal of Cancer*, 83 (2): 164–170.

van der Logt, C. P. E., Reitsma, P. H. & Bertina, R. B. (1991). Intron-Exon Organization of the Human Gene Coding for the Lipoprotein-Associated Coagulation Inhibitor: The Factor Xa Dependent Inhibitor of the Extrinsic Pathway of Coagulation. *Biochemistry*, 30 (6): 1571-7.

Varnera, J. A. & Chereshb, D. A. (1996). Integrins and cancer. *Cell biology*, 8 (5): 724.

Watson, J. D., Baker, T. A., Bell, S. P., Gann, A., Levine, M. & Losick, R. (2008). *Molecular Biology of the Gene*. 6th ed. 841 pp.

Wesselschmidt, R., Likert, K., Girard, T., Wun, T.-C. & Broze, G. J. J. (1992). Tissue factor pathway inhibitor: the carboxy-terminus is required for optimal inhibition of factor Xa. *Blood*, 79: 2004-2010.

Wood, J. P., Ellery, E. R. P., Maroney, S. A. & Mast, A. E. (2014). Biology of tissue factor pathway inhibitor. *Blood*.

Yashima, Y., Milchgrub, S., Gollahon, L. S., Maitra, A., Saboorian, M. H., Shay, J. W. & Gazdar, A. F. (1998). Telomerase enzyme activity and RNA expression during the multistage pathogenesis of breast carcinoma. *Clinical Cancer Research*, 4: 229-234.

Zhang, J., Piro, O., Lu, L. & Broze, G. J. J. (2003). Glycosyl Phosphatidylinositol Anchorage of Tissue Factor Pathway Inhibitor. *Circulation*, 108: 623-627.

Zwaal, R. F. A., Comfurius, P. & Bevers, E. M. (1998). Lipid–protein interactions in blood coagulation. *Biochimica et Biophysica Acta*, 1376 (3): 433–453.

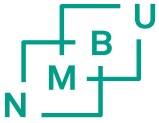

Norwegian University
of Life Sciences

Postboks 5003
NO-1432 Ås, Norway
+47 67 23 00 00
www.nmbu.no